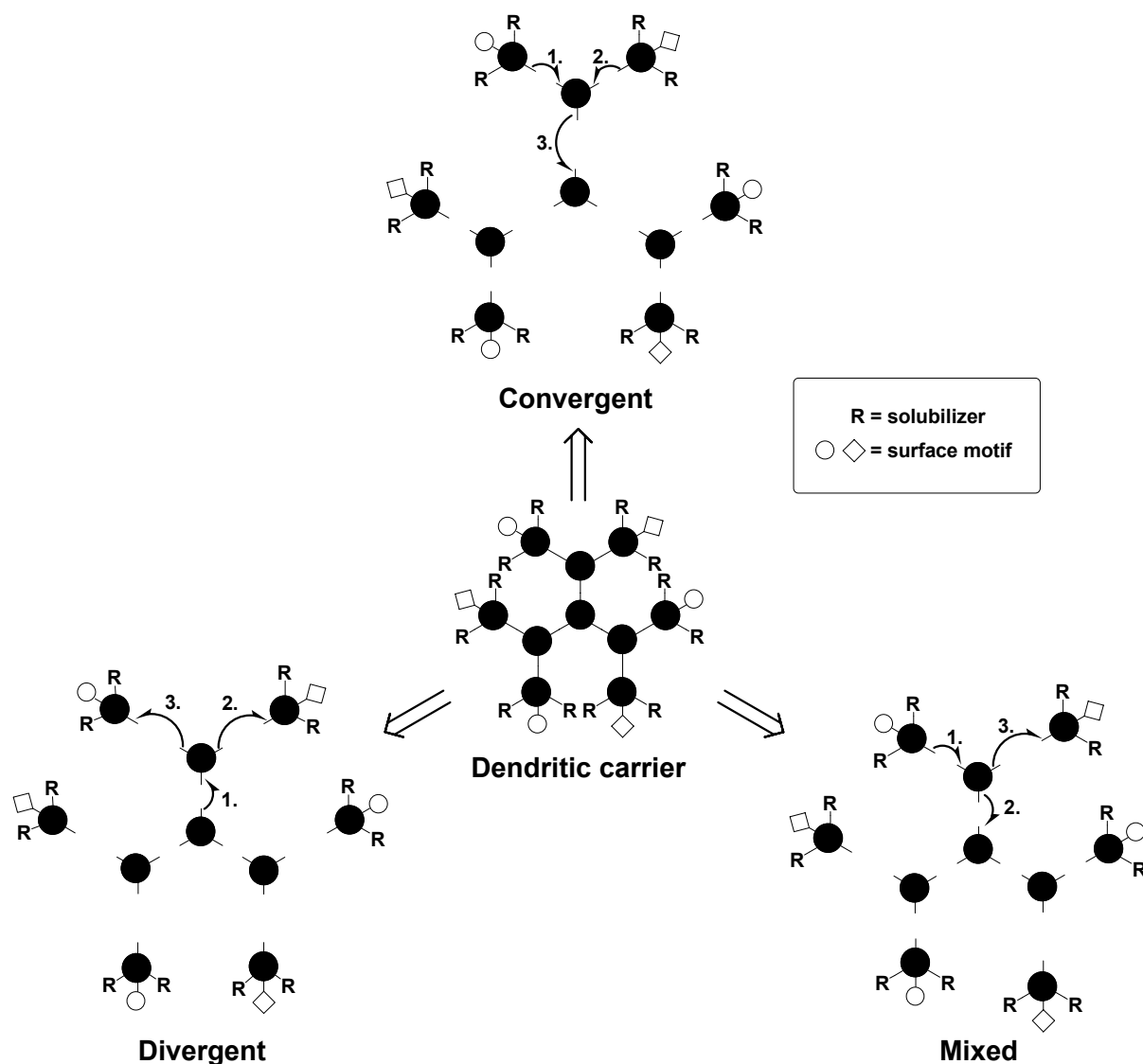


## 4 GENERAL PART

### 4.1 Retrosynthetic Strategy

The strategy for the construction of a suitable dendritic carrier for anticancer-therapeutics must consider its synthetic availability and the demands of its application. These prerequisites were already discussed in the introduction and the literature survey.

Since reliable pharmacokinetic and cytotoxic studies are always strictly related to the purity of a probe, it was necessary that the applied coupling protocols as well as the purification procedures worked effectively. All applied strategies to synthesize dendrimers are step-wise reactions (Scheme 8).



Scheme 8. Retrosynthetic pathways to the envisaged dendritic carrier.

The coupling protocols should work almost quantitatively, even when the reaction is sterically hindered. Since the purity of the compounds and the availability on a multi-gram-scale are equally important, each approach has certain advantages on the others.

Since many artificial ionic structures have a low biocompatibility, it is advantageous to employ OEGs or PEGs for solubility-reasons. The commercially available PEGs are not optimal candidates to solubilize a macromolecule in an aqueous phase, because the pharmacokinetics of polydisperse molecules may differ within a sample. *Tetra*-ethylene glycol and *penta*-ethylene glycol are the longest monodisperse ethylene glycol derivatives, which are affordable on a larger scale. However, these compounds are not always sufficiently long to enhance the solubility of large molecules in water. Dendritic scaffolds, which use PEGs, are also polydisperse. Their molecular weight distribution broadens with the number of attached PEGs and, therefore, their pharmacokinetics may differ significantly.

The synthesis of tailored dendrimers with different surface motifs can be accomplished employing *tris*-orthogonal  $AB_NB_M^*$ -branching units. Therefore, it is necessary that these building blocks are easily available on a larger scale. Some suitable examples were already known in our group (Fig. 14).<sup>162-164</sup> These compounds consist of two protected, selectively addressable amines for outward-, and one carboxyl-group at the focal point for inward functionalization.

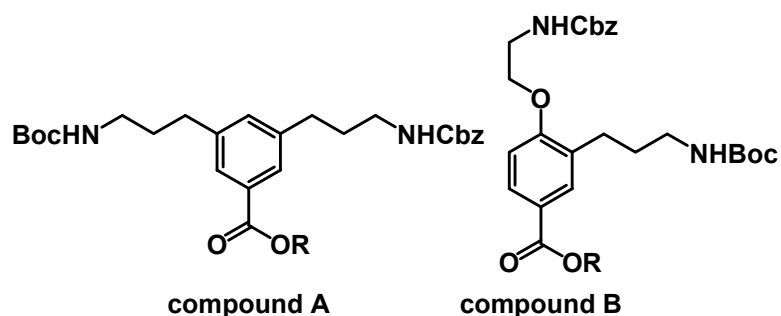


Fig. 14. Branching units with three orthogonally addressable functionalities.

Compound A resembles a standard  $AB_2$ -type branching unit, which is used in our group for the synthesis of dendrons and dendrimers. The efficiency of its deprotection and coupling protocols is already known for various systems. Unfortunately, both building blocks are only available on a several hundred milligram scale.

Since the commercially available ethylene glycol derivatives do not sufficiently match the properties of a dendritic drug carrier, it was necessary to find a different, better suitable candidate. Wegner and coworkers published a convenient synthesis of a symmetrical, secondary glycerol derivative, which carries two tri-ethylene glycol derivatives (compound C, Fig. 15).<sup>165</sup>

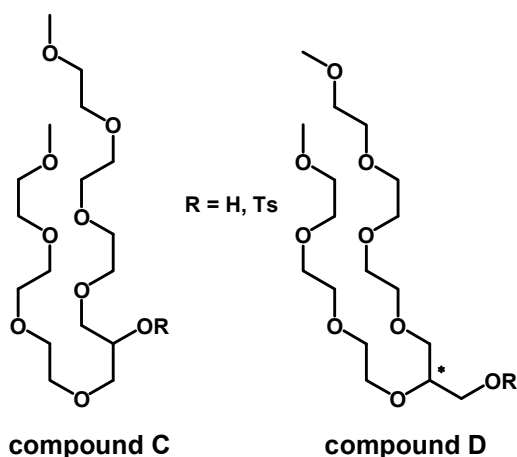
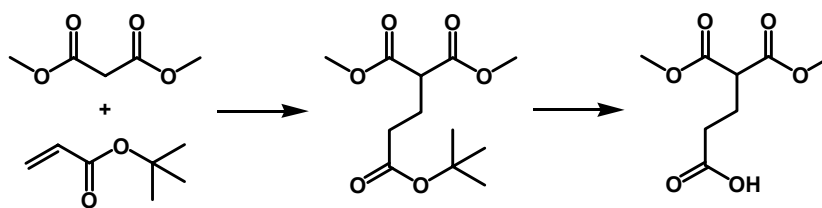


Fig. 15. OEGylated solubilizers.

A similar unsymmetrical, primary compound was synthesized in our group (compound D, Fig. 15).<sup>166</sup> Both structures dramatically improved the availability of PPPs in aqueous phase and were thus regarded suitable compounds for the present project.

The synthesis of defined dendrimer-platinum-conjugates requires bidentate chelates for complexation. Malonic acids and ethylene-diamine derivatives are suitable and well-known ligands with a valuable potential for platinum binding. However, malonic acid derivatives are superior to ethylene-diamines, because carboxylic acids can release platinum in intracellular compartments more easily by hydrolysis.

Katti and coworkers reported an effective approach towards the functionalization of malonic acids (Scheme 9).<sup>167</sup> They introduced an acrylic acid under Michael-conditions in very good yields. A selective activation and coupling of one of the three acids would allow coupling to an amine on the surface of a dendrimer. The surface decoration of a dendrimer with an ethylene-diamine moiety was already realized in our group by employing racemic diamino propionic acid derivatives.<sup>157, 168</sup>



Scheme 9. Malonic acid derivatives for further functionalization.<sup>167</sup>

Orthogonal branching units possess binding capacity for more than one functionality. The introduction of both, targeting function and fluorescence tag, should be possible. Since the stability of a delivery system is very important, the different building blocks are preferentially connected via amide-bonds. Although these connections may be cleaved by peptidases, they are much more stable than e.g. ester linkages which can be easily degraded by hydrolysis. Besides its pharmacological importance the intrinsic stability has a significant impact on the synthetic availability. Less stable linkages might break during reaction, work-up or purification on silica gel.

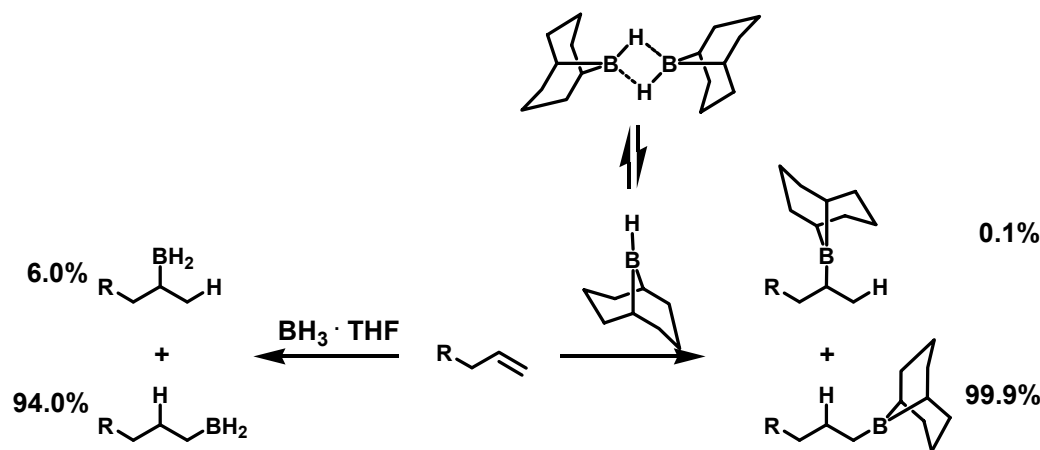
## 4.2 Coupling Chemistry

The formation of a dendrimer and its building blocks incorporates several coupling and activation protocols. Amide linkages have a high tolerance against other synthetic protocols and purification methods. Therefore, they were chosen to connect the individual building blocks. The synthesis of the orthogonally protected alkyl-aryl branching units afforded C(sp<sup>3</sup>)-C(sp<sup>2</sup>) bond formations. One of the most common tools for such connections is the Pd<sup>0</sup>-catalyzed Suzuki-Miyaura cross-coupling (SMCC) reaction. This method tolerates a large number of functional groups and is compatible with moisture. Since both coupling techniques usually proceed in very high yields, they are suitable for the large-scale synthesis of dendrimers and building blocks. However, a construction of a multifunctional carrier demands for orthogonal protection of individual synthons. The requirements for such tailored synthetic strategies are numerous, though a solution to these problems can be obtained from well-known protection and deprotection procedures. The SMCC and the amide-coupling are the most important protocols used in this thesis. Therefore, their mechanisms are discussed in detail. The other reactions/ methods will be briefly discussed where further explanations are necessary.

### 4.2.1 Suzuki-Miyaura Cross-Coupling

The SMCC is a variant of the well-known and widely used Suzuki cross-coupling (SCC) reaction. Whereas the regular Suzuki protocol makes exclusive use of boronic acids and borates connected to a  $sp^2$ -carbon, the SMCC utilizes alkyl-boranes and alkyl-borates connected to a  $sp^3$ -carbon.<sup>169-171</sup> Both mechanisms can be understood according to the general catalytic cycle for  $Pd^0$ -catalyzed cross-coupling reactions. They consist of oxidative insertion, transmetalation and reductive elimination.

Sonderquist and coworkers suggested a more detailed catalytic cycle of the SMCC, including the activation of the electron-poor borane prior to transmetalation.<sup>172</sup> These boranes are prepared by the *in situ* reaction of an olefin with primary or secondary boranes or a B-hydro borate. The regioselectivity of these *syn*-addition reactions can be optimized with bulky *bis*-alkyl-boranes (e.g. 9-BBN) to yield the product in which the olefine's less hindered side reacts most rapidly (Scheme 10). This regioselective addition is synergistically improved by an electronic effect. The electron-rich  $\alpha$ -carbon is the better nucleophile, because it has less H-atoms in its adjacent periphery than the  $\beta$ -carbon. Since boron will act as an electrophile in this reaction, it will more readily undergo addition to the partially negatively charged  $\alpha$ -carbon.



Scheme 10. Hydroboration of an olefin with different borans.

The most commonly used catalyst precursor for palladium-mediated reactions is  $Pd[PPh_3]_4$ , a saturated 18 e-complex (refer to Scheme 11 for illustration of the mechanism). The active, coordinatively unsaturated 14 e-catalyst **I** is formed in solution by the dissociation of two ligands from the precursor species.

The oxidative addition, **R-X** to **I**, is the rate-determining step in the catalytic cycle and the relative reactivity decreases in the order of X: I > OTf ~ Br >> Cl. Further activation of the oxidative addition is obtained for substrates with electron-withdrawing groups. Since *tri*-phenyl phosphine ligands have a big sterical demand, the remaining ligands in Pd[PPh<sub>3</sub>]<sub>2</sub> should reorganize to form a linear geometry. This forces the 16 e-complex **II** to a *trans*-configuration. The LUMO of **II** is the molecular orbital 2a<sub>1g</sub> which has very much the character of the atomic orbital d<sub>z<sup>2</sup></sub> of palladium. Consequently, any nucleophile has to attack the complex axially. **A** is the activated form of the hydroboration product, formed by the reaction of borane with one equivalent of base. This increase in nucleophilicity is necessary for the first phase in the transmetallation process. The substitution of the molecular fragment **X** by the activated borane **A** yields in distorted transition geometry. The pseudo-trigonal-pyramid then has to disintegrate to form another 16 e-complex, *trans*-**IIIa**, or *cis*-**IIIb** (left box in Scheme 11). Since the two remaining ligands still have the biggest sterical demand, *trans*-**IIIa** is the more reasonable transition state. The geometry of **IIIa/ b** can be understood as a pseudo-square-pyramidal hydroxo-μ<sub>2</sub>-bridged intermediate. A lone-pair of the hydroxyl occupies an equatorial position via a dative bond, and the α-methylene group occupies an axial position. This α-methylene is not yet a very good nucleophile. Therefore, the proposed pincer-like η<sup>2</sup>-intermediate will most probably benefit from an agnostic interaction of the polarized, covalent C-B-bond with the palladium. The second phase of transmetallation is the activation of the axial methylene group. A second equivalent of base attacks the boron to form **B**, which is then eliminated from its equatorial position. The release of the activated methylene group from the borate initiates its axial nucleophilic attack towards the palladium. The corresponding distorted trigonal pyramid has again two possibilities to relax into a square pyramidal geometry and to form either *trans*-**IVa** or *cis*-**IVb**. The final step in the catalytic cycle, the reductive elimination, needs a *cis*-geometry to proceed. The *trans-cis* rearrangement of the reasonable intermediate **IVa** can either proceed via ligand scrambling or via square planar interconversion (right box in Scheme 11).

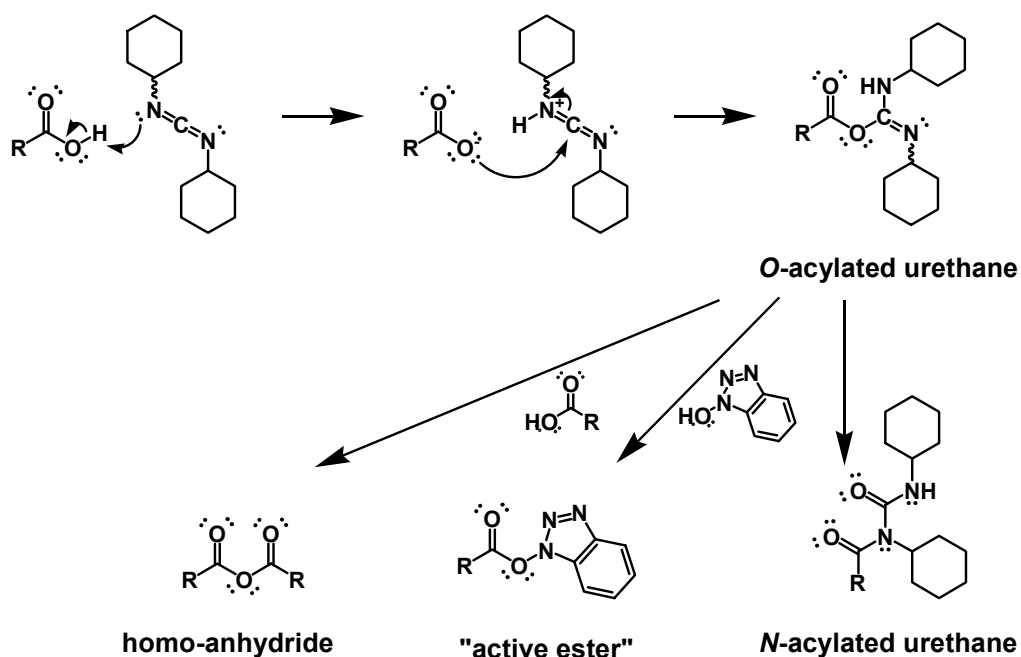


The geometrical reorganization by ligand scrambling can incorporate the association and exchange of ligands via a square-pyramidal transition-state, or the dissociation and reassociation of ligands via a trigonal transition-state. The tetrahedral interconversion can involve twisting of one pair of *cis*-ligands about an axis, or a shift of two pairs of *trans*-ligands into the opposite direction. The reductive elimination is not reversible. It recovers the activated catalytic species **I** for another cycle and generates a C-C-bond. All phases of the catalytic cycle very much depend on the electronic and sterical properties of the reagents, and the proposed mechanism may differ for a specific case.

### 4.2.2 Amide-Coupling

The reaction of a carboxylic acid with a primary or secondary amine does not generate an amide, but leads to the fast formation of an ammonium-carboxylate. This can be pyrolyzed to the corresponding amides (typically at 200-300°C). Since the number of side-reactions increases with temperature and many compounds do not possess sufficient thermal stability, these conditions are of no preparative value for the present work.

A more efficient procedure incorporates electron-withdrawing groups increasing the electrophilic character of the carbonyl group. Acid chlorides are commonly used carbonyl derivatives with such influence.



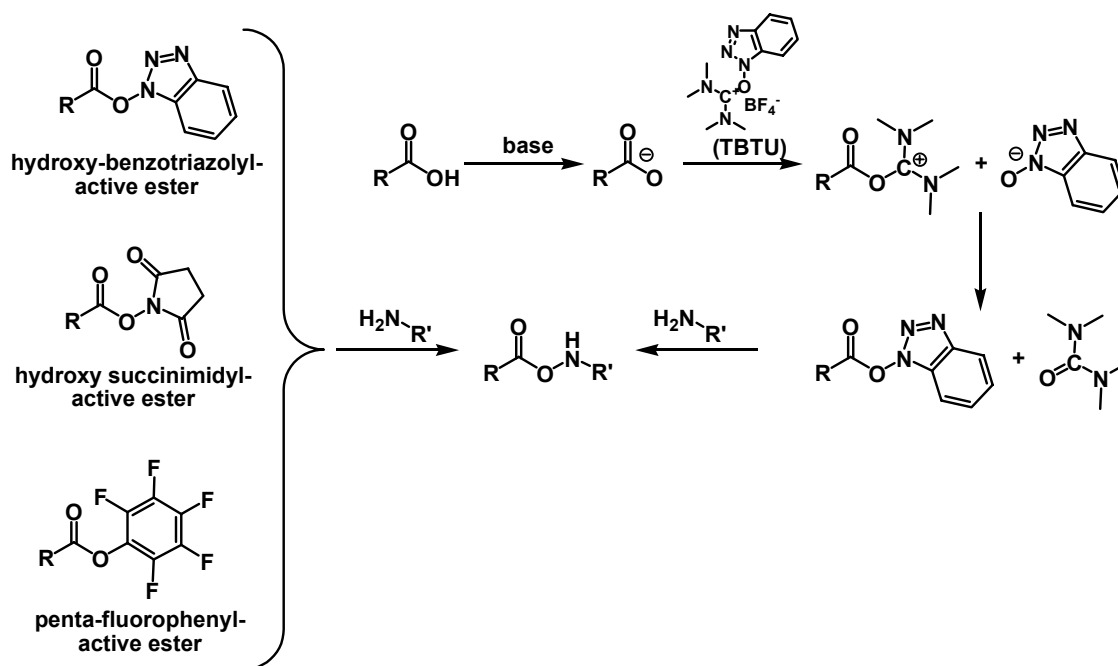
Scheme 12. Activation of a carboxylic acid.



However, it is not possible to generate an acid chloride on any substrate. Furthermore, this protocol can lead to racemization of the  $\alpha$ -carbon next to the carboxylic acid. Another approach uses coupling reagents, the most important of which are the carbodiimides. They serve to generate anhydrides or “active esters” (Scheme 12).

Homo-anhydrides cannot activate more than 50% of the carbonyl-groups because a “ring-opening” initiated by an amine would yield in an amide and a carboxylic acid. Mixed anhydrides arising from the reaction of an acid with, e.g. 2,4,6-trichlorobenzoyl chloride are more important. These compounds possess two different acyclic carbonyls, but nucleophiles chemoselectively react only with the originally provided acid. The reactive path to the other carbonyl (its LUMO) is sterically hindered by the *ortho*-chloro-substituents.

The preparative value of the “active ester” variant is much higher. It even increased with the interest in the development of solid- and liquid-phase peptide-synthesis. Since weak nucleophiles do not readily react with *O*-acylated *iso*-urethanes, the addition of a good nucleophile, e.g. hydroxyl-benzotriazole, hydroxyl-succinimide or *penta*-fluoro phenol, helps to avoid the formation of *N*-acetylated urethanes and stabilizes the reactive intermediate (Scheme 13).



Scheme 13. Amide-coupling with different “active esters”.

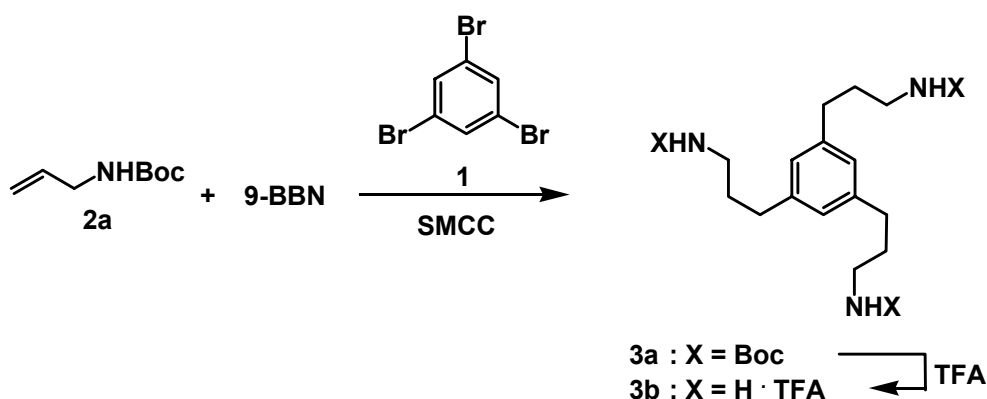
The *in situ* preparation of “active esters” enhances the coupling efficiency towards the desired nucleophile and prevents from the formation of *N*-acylated urethanes. An improved protocol utilizes *O*-hetarylated urethanes, e.g. TBTU and HBTU. These coupling reagents can quickly generate intermediates with a very high reactivity towards nucleophiles.

### 4.3 Synthesis of the Building Blocks

#### 4.3.1 Synthesis of Core Molecules

The core molecule is the central branching unit. A suitable candidate for such purposes should have several equivalent branches, as symmetrically arranged as possible. The number of branches of the core molecule is directly proportional to the total number of branches in a dendrimer and its molecular weight. Therefore, it should have as many branches as possible to arrive at a high molecular weight, even if it is just covered with a low generation dendron. The sterical stress for the very last couplings on a “hyper-core” may limit the yield and purity of a valence-saturated dendrimer. Consequently, the number of branches should be as high as possible and as small as necessary for the construction of a pure dendrimer with a high molecular weight. The synthesis of the core molecule on a gram-scale would be sufficient.

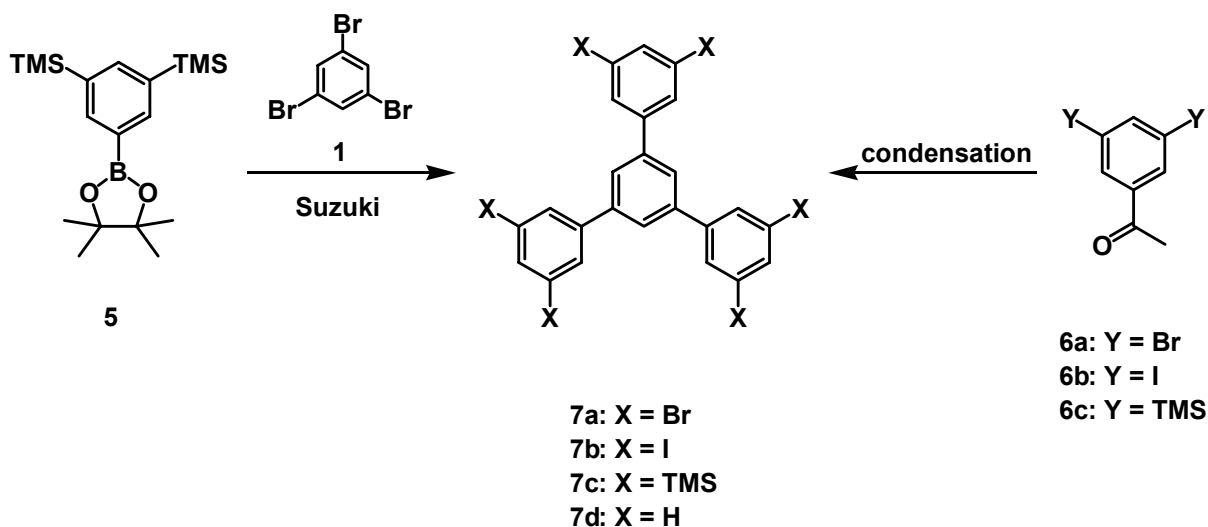
A suitable central branching unit (**3b**) with three valences was already synthesized in our group (Scheme 14).<sup>157, 168</sup> The molecule was readily available on a multi-gram scale via SMCC and the synthesis of dendrimers was successfully done in convergent and divergent protocols up to the second generation.



Scheme 14. Fuchs' core molecule.

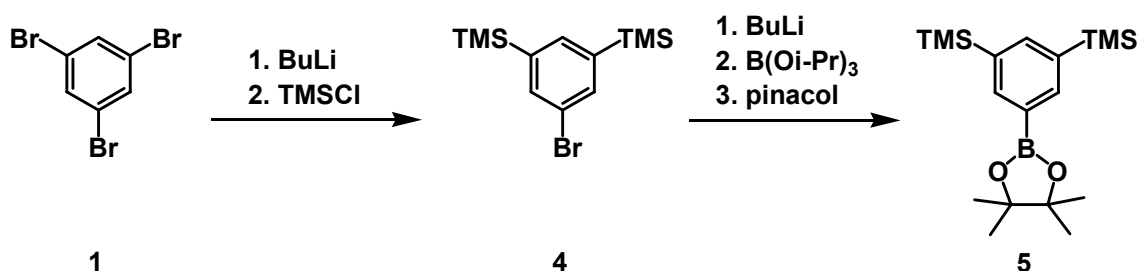
The high costs of 9-BBN and the palladium catalyst are the major disadvantage of SMCC. An analogue, obtained from the *tris*-alkylation of phluoroglucin, would be less expensive and should have comparable properties. It was not possible, however, to isolate the core precursor. Besides *mono*- and *bis*-alkylated species many other by-products were generated. These impurities were not fully characterized. The <sup>1</sup>H-NMR leads to the conclusion that the aryl-ring was alkylated.

Since a core molecule with twice as many connections than this one would nearly double the molecular weight of the corresponding dendrimer, it was reasonable to search for a *hexa*-functional analogue.<sup>V</sup> Miller and Nishide published the synthesis of the 1,3,5-triphenyl-benzene building blocks **7a/b**, which would allow for further functionalization via SMCC (Scheme 15).<sup>173, 174</sup>



Scheme 15. Synthesis of a *hexa*-functional core precursor.

The condensation reaction of **6a/b** did not work as sufficiently as described, and the isolated yields were below 6% for both cases. It was not possible to generate **7c** by the acid catalyzed condensation of **6c**. The TMS-groups were hydro-desilylated and the reaction yielded **7d**. An alternative approach towards the same molecules employs Suzuki cross coupling (SCC).

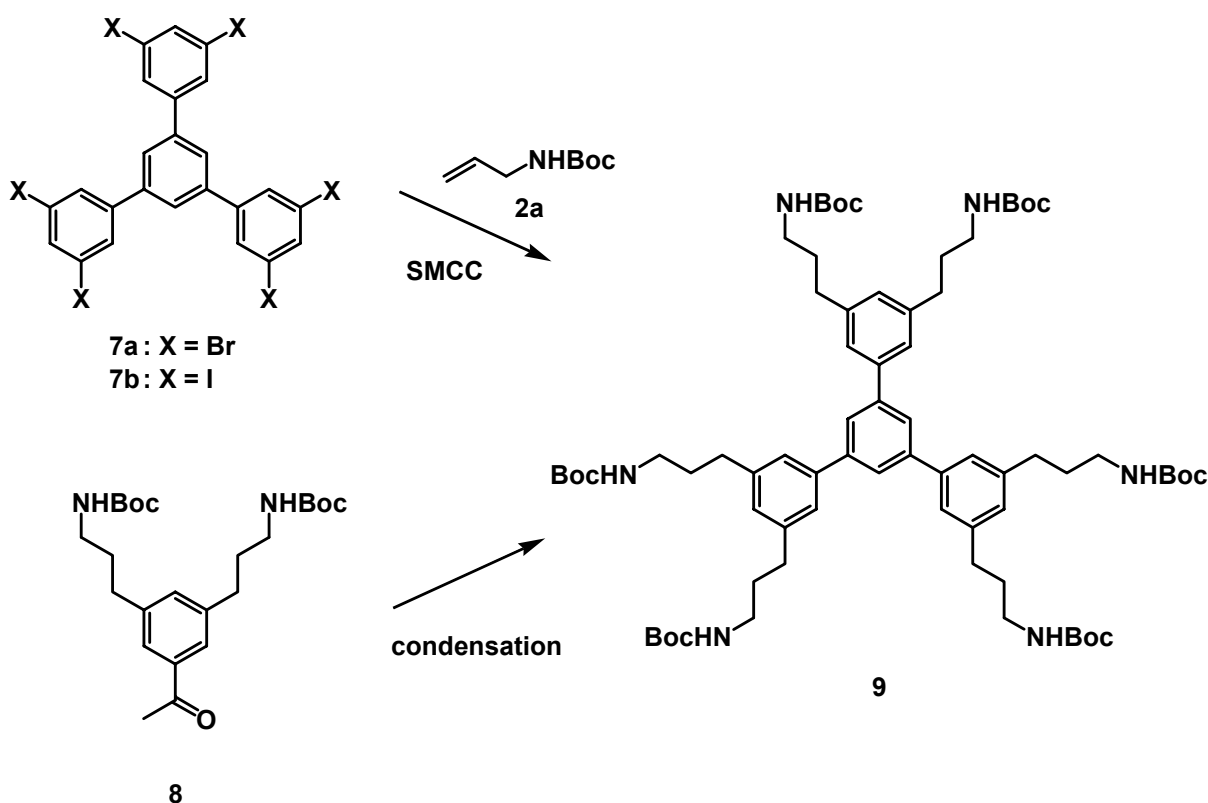


Scheme 16. Synthesis of a building block for an alternative core precursor.

**1** was *mono*-lithiated with one equivalent *n*-BuLi at  $-40^{\circ}\text{C}$  in diethylether. After scavenging of the generated aryl anion with a slight excess of trimethylsilyl chloride

<sup>V</sup> I am very grateful to Robert Meudtner who worked on the synthesis of the *hexa*-functional core molecule in his "Forschungspraktikum" and supported this part of my research.

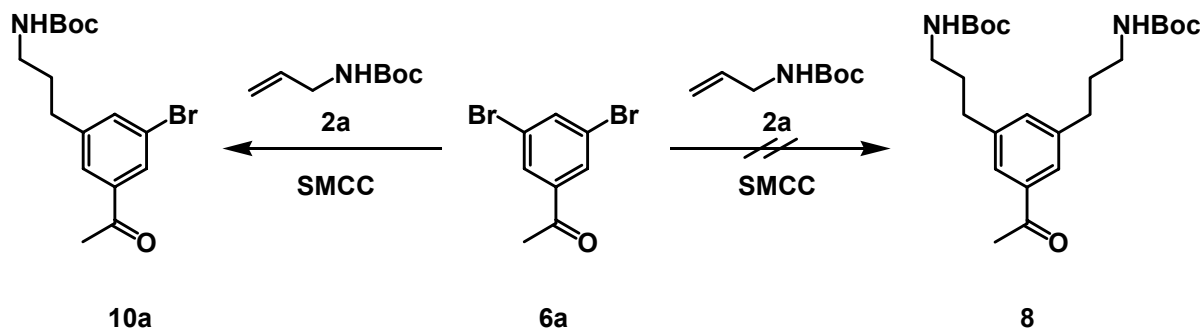
the second TMS-group was introduced in the same way to yield **4**.<sup>175, 176</sup> In another lithiation step, the remaining bromo functionality was substituted by a boronic ester functionality to give **5**. **7c** was obtained in good isolated yields (89%) after SCC of **5** with **1**. Indeed, it was not possible to replace all TMS-groups by iodo-desilylation with ICl. Even the improved protocols published by Bo did not serve to make the *hexa*-iodo-functionalized core precursor **7b** accessible.<sup>177</sup> However, **7a/b** were available on a small scale via the first route. The experiments to couple six protected allyl amines in a SMCC protocol did not succeed sufficiently. It was not possible to separate the preferred core molecule from a mixture of incomplete reacted compounds. The available amounts of **7a/b** did not allow a full screening for the optimization of the coupling efficiency. Therefore, this approach towards a *hexa*-functional core moiety was not investigated further.



Scheme 17. Synthesis of a *hexa*-functional core molecule.

Another idea for the synthesis of the desired core molecule was again based on the cyclo-trimerization of acetophenones. Since it was not possible to satisfactorily run six SMCCs on one molecule, it seemed reasonable to change the synthetic strategy. The SMCC works very well for alkyl 3,5-dibromo benzoates **11a**. However, the same protocols for the reaction of **6a** with **2a/b** did not yield **8**. Surprisingly, only *mono*-

coupled **10a/b** was obtained in rather low yields. A screening of the reaction conditions, including the use of a large excess of borane, different solvents, different bases, different temperatures, increased amounts of catalyst and the use of other Pd<sup>0</sup>-catalysts did not help to improve this reaction.

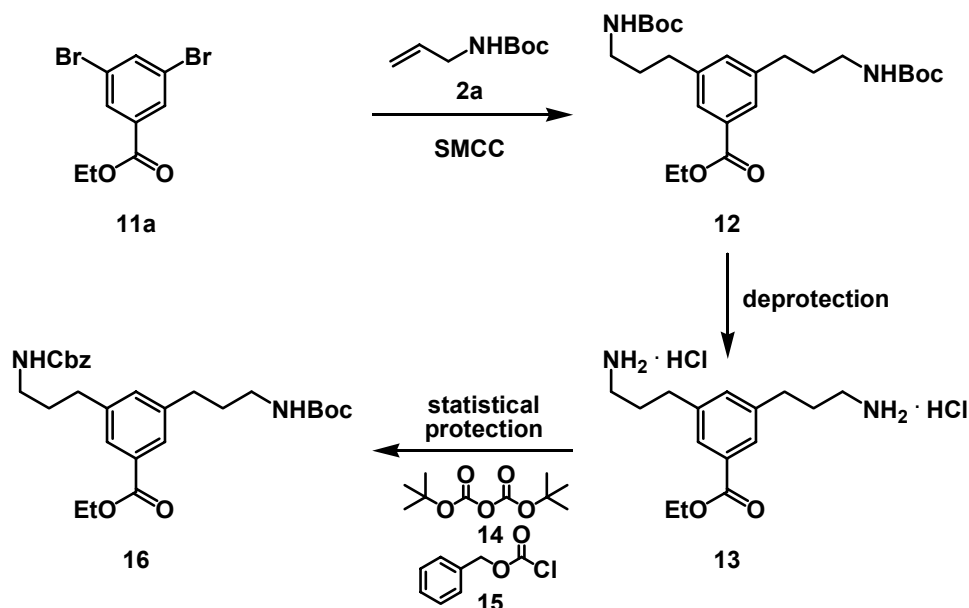


Scheme 18. Synthesis of a core precursor.

It was not even possible to generate the product of the oxidative addition of **10a/b**. One explanation is derived from the electronic situation of the molecule. The oxidative addition needs a rather electron-poor substrate to proceed. Acetophenone in **6a** is less electron-withdrawing than the ester in **11a** and the first coupling substitutes a -I-bromo-substituent to a +I-alkyl-substituent. Therefore, the electron-deficiency of the aromatic system decreases and another oxidative addition is not possible. Since these building blocks were not available, it was not possible to generate the shown *hexa*-functional core molecule via this approach.

### 4.3.2 Synthesis of Orthogonal Branching Units

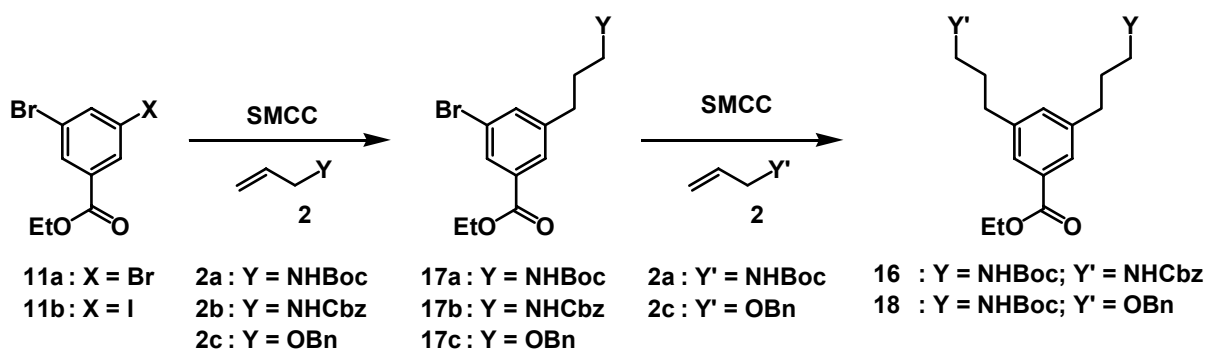
The synthesis of *tris*-orthogonal AB<sub>N</sub>B<sub>M</sub><sup>\*</sup>-branching units that were known in our group (Fig. 14, p. 31) had certain disadvantages. It was not possible to run these reactions in good yields on a larger scale. In Vetter's approach the introduction of an alkylamine by SMCC was the limiting step. Koch's method (Scheme 19) was restricted by the, more or less, statistical protection of **13** with **14** and **15**.<sup>164</sup> Even the best yields for the last step were always below 50% and purification was tedious, because the by-products almost had the same polarity. For very high purity of **16** it was actually necessary to deprotect and reprotect the *N*-Boc group with intermediate purification and additional purification at the end. Vetter and Koch improved this protocol to some extent by splitting the procedure into two SMCC reactions.<sup>163</sup> They functionalized **11a** first with only one equivalent **2a** and then covered the remaining bromine with an *N*-Cbz-protected propylamine **2b** to yield **16**.



Scheme 19. Koch's synthesis of a *tris*-orthogonally protected dendron.

Their conditions, however, were not optimized and the yields rather low. Since the reactivity of the Pd-catalyst in the oxidative addition of SMCC increases towards iodo-substituents, it was reasonable to examine if the mixed halogenated derivative **11b** can serve to improve the efficiency of this reaction.

**11b** was easily obtained by esterification of the corresponding, commercially available acid. An extract of the screening of the *mono*-coupling experiments is shown in Table 1. The Pd-catalyst was always freshly prepared, because the quality of the catalyst has a large influence on the efficiency of the reaction. In conclusion of the data obtained, several aspects, e.g. catalyst amount, batch size, base, solvent or reaction time, had an influence on the reactivity. The most important characteristic for this screening, however, was the reaction temperature. The isolated yields of the *mono*-coupled products **17a-c** increased with the temperature, but for batches above 50°C the undesired *bis*-coupled by-products were obtained and lowered the yields.



Scheme 20. Step-wise synthesis of a *tris*-orthogonally protected dendron.

In parallel, the necessary reaction time decreased. The best results (Table 1) were achieved at 50°C using one equivalent of the corresponding borane **2b/c** after two days of reaction time. These entries did not show the by-products above mentioned. Yields were improved by increasing the amount of the borane, but since the 9-BBN is very expensive, this modification is not reasonable.

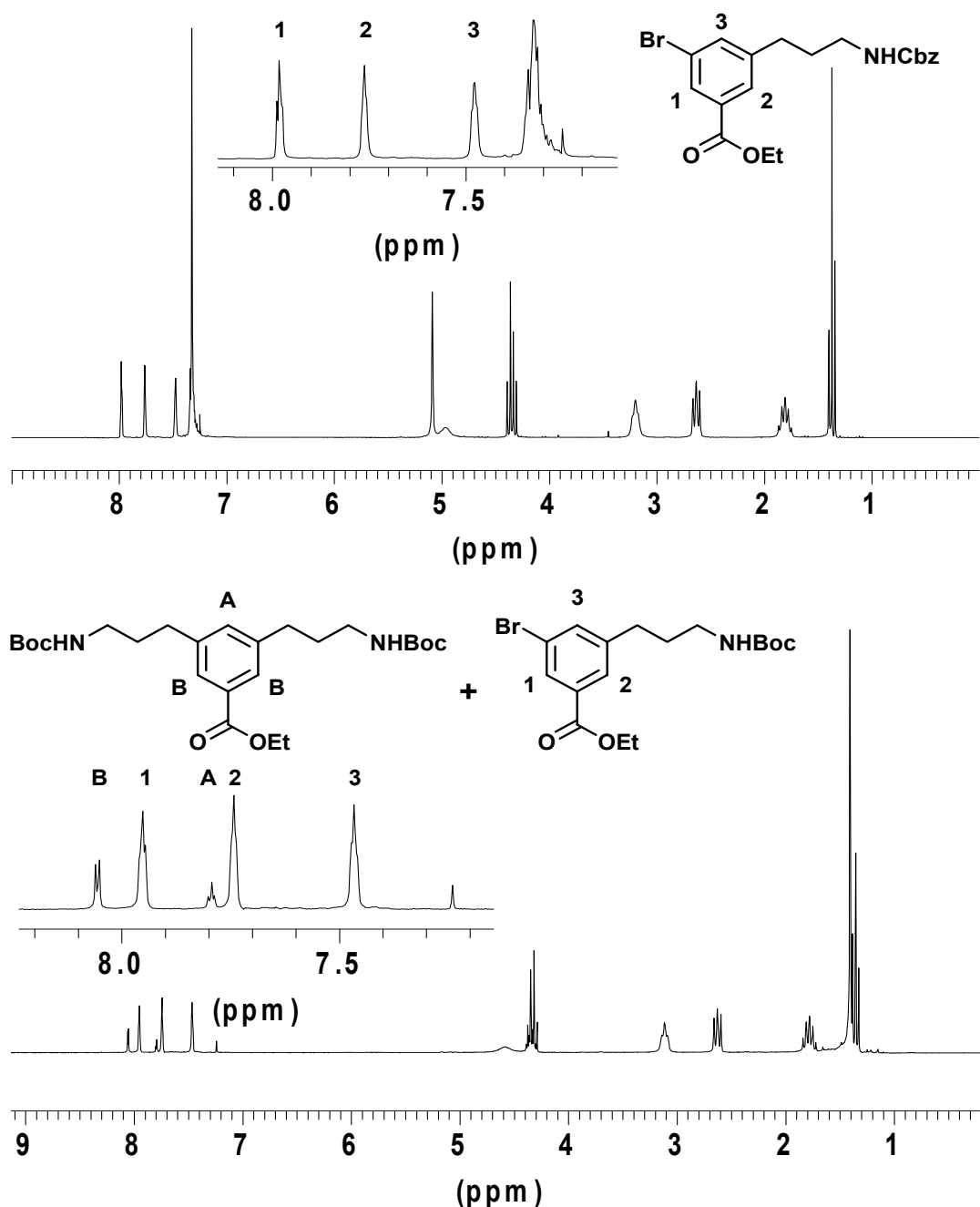


Fig. 16.  $^1\text{H-NMR}$  spectra of mono-coupling experiments with SMCC (250MHz,  $\text{CDCl}_3$ ).



Remarkably, it was not possible for all boranes to control the efficiency through the reaction temperature. Comparable studies on **2a** showed completely different results. The *bis*-coupled by-products **12** were even obtained at room temperature. This higher reactivity is not a trivial problem and a reasonable explanation is still needed.

entry	equiv. / borane	product	T [°C]	time [h]	isolated yield [%]
1	1 / <b>2b</b>	<b>17b</b>	25	120	75
2	1 / <b>2b</b>	<b>17b</b>	50	48	83
3	1 / <b>2b</b>	<b>17b</b>	Reflux	48	77
4	2 / <b>2b</b>	<b>17b</b>	25	120	85
5	2 / <b>2b</b>	<b>17b</b>	50	48	95
6	1 / <b>2c</b>	<b>17c</b>	25	120	70
7	1 / <b>2c</b>	<b>17c</b>	50	48	80
8	1 / <b>2c</b>	<b>17c</b>	Reflux	48	69
9	2 / <b>2c</b>	<b>17c</b>	25	120	75
10	2 / <b>2c</b>	<b>17c</b>	50	48	92

Table 1. Reaction-screening of SMCC starting from **11b**.

According to the mass spectra, the isolated *mono*-coupled products did not contain iodine. Since the *bis*-coupled by-products were not obtained below 50°C, it was realistic to get similar results for the reaction screening of **11a**.

entry	equiv. / borane	product	T [°C]	time [h]	isolated yield [%]
1	1 / <b>2b</b>	<b>17b</b>	25	120	40
2	1 / <b>2b</b>	<b>17b</b>	50	48	73
3	1 / <b>2c</b>	<b>17c</b>	25	120	32
4	1 / <b>2c</b>	<b>17c</b>	50	48	68

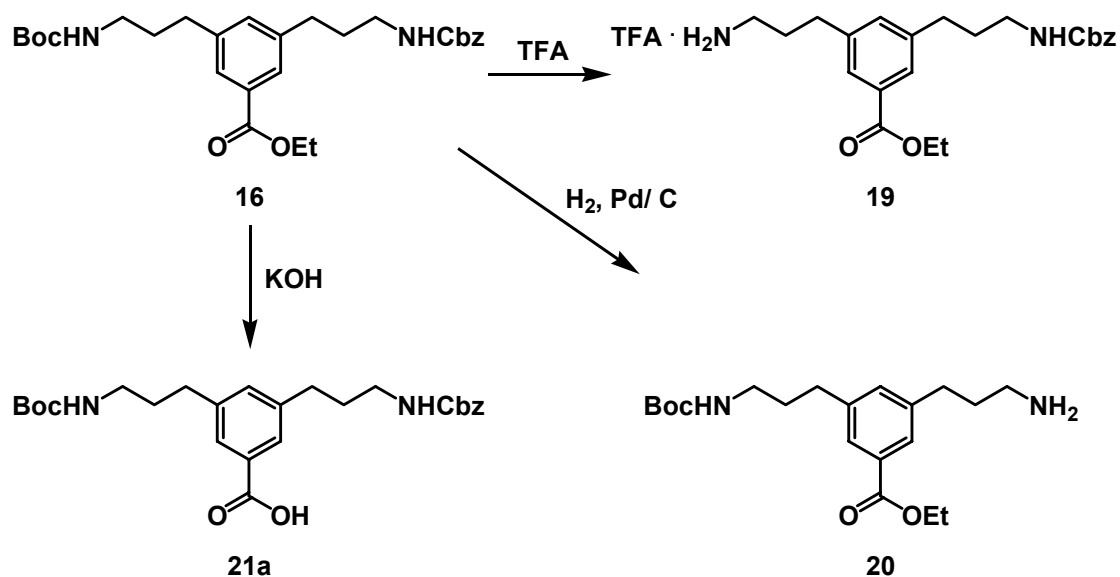
Table 2. Reaction-screening of SMCC starting from **11a**.

The results for this screening are summarized in Table 2. Again, the best results were achieved at 50°C. The isolated yields slightly decreased, but again only *mono*-coupled products were obtained below this temperature. The yields for larger batches decreased, but this was almost compensated by increasing the amount of catalyst (5-7 mol%). It was possible to run these reactions on a 20 gram scale of **11a** to yield **17b** in 67% and **17c** in 60%, respectively. **16/ 18** were then easily accessible in excellent yields by reemploying SMCC at higher temperatures (reflux in toluene/

water mixtures). Since **11a** is available on a 100 gram scale and much cheaper than **11b**, this discovery was the key to large amounts of very pure *tris*-orthogonally protected dendrons.

Another significant advantage of this approach on the statistical procedure is its ability to generate dendrons with three different protective groups, covering three different functionalities. **18** carries an alcohol, an amine and a carboxylic acid. This kind of branching unit offers the possibility to synthesize partially degradable dendrons and dendrimers with labile ester linkages and stable amide linkages.

Typical deprotection procedures can be shown for **16**. The best deprotection protocol for an *N*-Boc-group employed TFA in methylene chloride at room temperature and gave **19**. The reaction usually proceeded within several minutes and was easy to monitor by TLC. The excess of TFA was removed after several co-evaporations with methylene chloride. This protocol partially cleaved the *N*-Cbz-protective group, but worked much better than other procedures as e.g. hydrochloric acid in THF. All by-products, including the *bis*-deprotected dendrons, were removed with column chromatography.



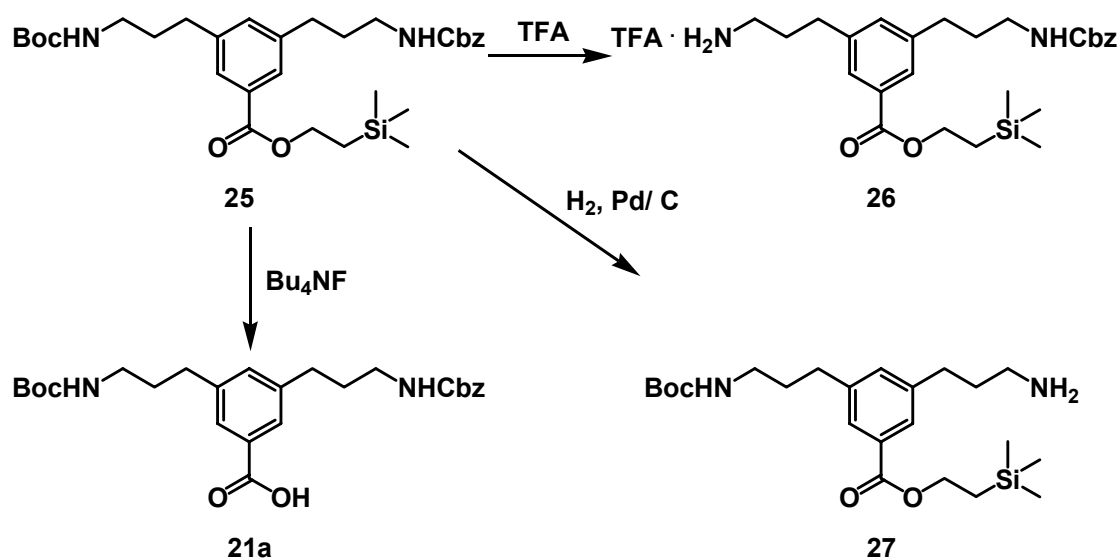
Scheme 21. Synthon-wise deprotection of **16**.

The selective deprotection of the *N*-Cbz-group of **16** was accomplished by catalytic hydrogenation at room temperature with palladium on charcoal as catalyst. A hydrogen atmosphere was sufficient for the deprotection, but the reaction proceeded faster under hydrogen pressure (usually 3 bar). The solvent was much more important. The best solvents for this kind of substrates were ethanol/ ethyl acetate



deprotected and covered via amide linkages. The *N*-Boc group was again easy to remove with TFA and did not affect the allyl ester. The *N*-Cbz-group was partially cleaved, but **23** was accessible after purification with column chromatography. On the other hand, it was not possible to selectively deprotect the *N*-Cbz-group. The catalytic hydrogenation deprotected the *N*-Cbz-group and did not affect the *N*-Boc group, but the allyl ester was always converted to a propyl ester and gave **24**.

Therefore another strategy was necessary, and **21a** was protected as trimethylsilylethanoyl (TMSE) ester **25**. This esterification was catalyzed with DCC/DPTS and gave **25** in 87% yield.<sup>178</sup>



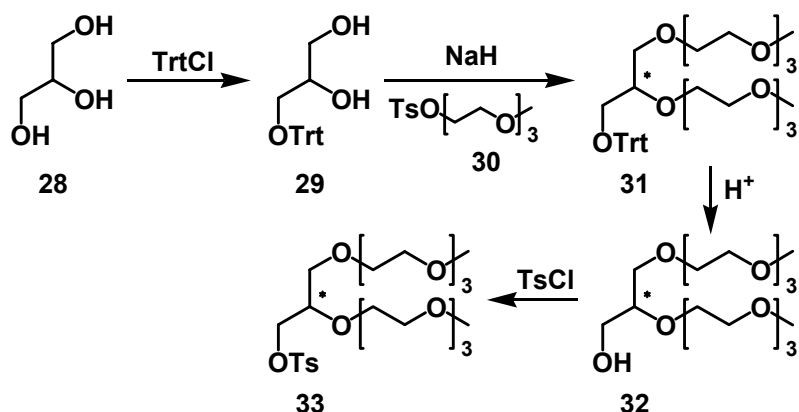
Scheme 23. Synthon-wise deprotection of **25**.

The deprotection of the *N*-Cbz group succeeded by catalytic hydrogenation and gave **27**. Neither the TMSE ester nor the *N*-Boc group were affected. The TMSE ester was cleaved with Bu<sub>4</sub>NF and **21a** was gained. No other functionality was addressed in this protocol. However, the deprotection of the *N*-Boc group with TFA in methylene chloride gave **26**, but the TMSE ester was also partially deprotected. It was possible to separate **26** by column chromatography, but the isolated yields were rather low (less than 40%). Although this strategy proved to be suitable for the desired pattern, its synthetic value was rather low.

#### 4.3.3 Synthesis of Branched, Monodisperse OEG-based Solubilizers

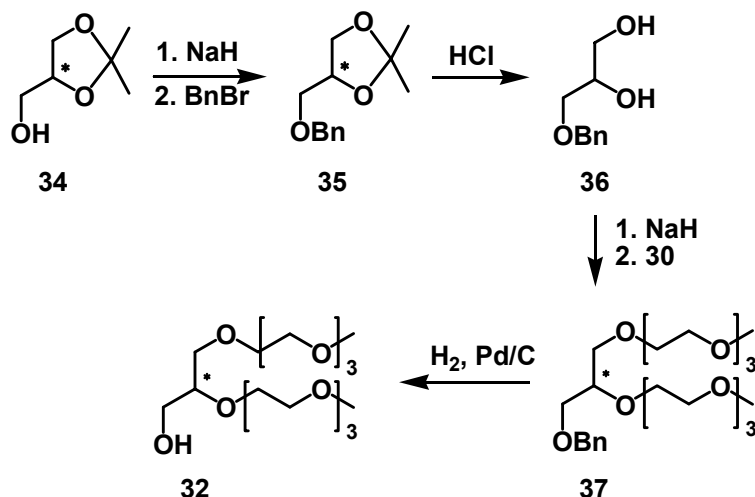
It was already discussed above that commercially available OEGs and PEGs have certain disadvantages. These led to the synthesis of branched, monodisperse

analogues. Kutzner developed a non-symmetrical glycerol derivative by employing Williamson's etherification method (Scheme 24).<sup>166</sup>



Scheme 24. Synthesis of a branched OEG based on glycerine according to Kutzner.

**32** was available on a scale of several grams, but the synthesis, and especially the deprotection of **31** with HCl, took too much time (1 week). This deprotection was improved by catalytic hydrogenation. The trityl-group can be seen as a substituted benzyl ester. Its cleavage proceeded within 12 hours in a hydrogen atmosphere at 50°C in ethanol. However, the removal of the trityl group decreased the molecular weight by more than 40%. Since **32** and **33** had to be purified by column chromatography, the practical value of this sequence was rather low.

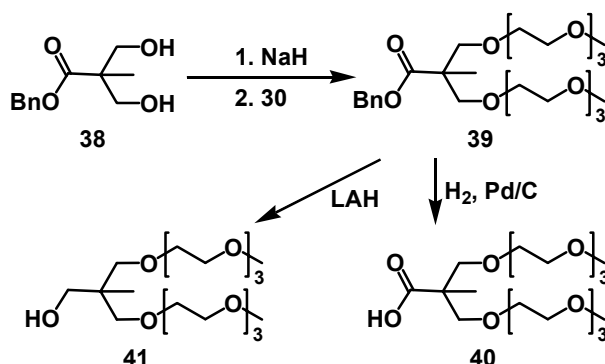


Scheme 25. Improved synthesis of **32**.

**32** was obtained by a different, more convenient approach (Scheme 25) in which the trityl ether was replaced by a benzyl ether. Prior to alkylation with benzyl bromide, **34** was deprotonated with NaH in THF and gave **35**, which was purified by vacuum distillation. Its ketale was quantitatively removed with hydrochloric acid, and **36** was

obtained after distillation. The etherification of **36** with **30** was carried out according to Kutzner's procedure for the synthesis of **31** and gave **37** in comparably high yields. After purification with column chromatography the deprotection of the benzylic ether proceeded quantitatively by catalytic hydrogenation with palladium on charcoal within 12 hours and gave **32**. After filtration the solvent was removed under reduced pressure. Further purification was not necessary. This synthetic sequence made **32** available on a scale of 20 to 30 grams within one week.

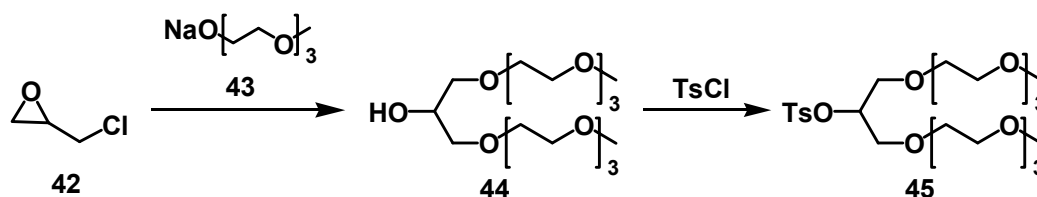
The synthesis of this racemic OEG still involved four synthetic steps. A different approach towards a suitable solubilizer was based on **38** and offered the opportunity to synthesize symmetrically equipped compounds with diverse functionalities (Scheme 26).



Scheme 26. Symmetrical, branched OEG.

The etherification reaction of **38** with **30** to give **39** was not considered to differ very much from the one employed for the synthesis of **31** and **37**. However, the yields dramatically decreased and it was very tedious to separate the *mono*-alkylated by-product from the *bis*-alkylated product.

**45** is the symmetrical analogue of **33**. Its synthesis was reported by Wegner and coworkers. The ring-opening of **42** was initiated with the *in situ* prepared **43** and gave **44**.<sup>165</sup>



Scheme 27. Synthesis of a symmetrical, branched OEG based on glycerin according to Wegner.

The purification of **44** was tedious. The original manuscript reports a vacuum distillation (bp: 180–185°C at  $8 \cdot 10^{-3}$  mbar), which was difficult to repeat. The obtained yellowish oil needed further purification with column chromatography to yield a very pure and colorless oil. In the end, **44** was available within 3 days on a 40 gram scale in relatively low yields (42%). However, the synthetic value of this one-step reaction was still much higher than that of the unsymmetrical analogue **32**.

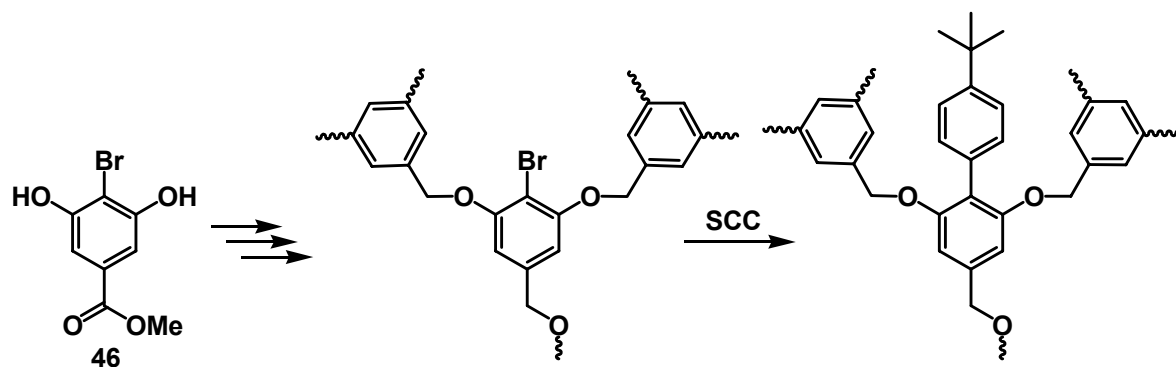
**32** and **44** were converted in excellent yields to the corresponding tosylates **33** and **45**. The best result for the formation of these sulfonic esters was achieved by using pyridinium tosylate in pyridine at 0°C.<sup>179</sup>

#### 4.3.4 Synthesis of Modifiable, Water-Soluble Molecules for Tailored Surface Functionalization

The dendritic scaffold of poly(amidoamin)s itself has a very low solubility in water, but these macromolecules can be solubilized in aqueous phase via quaternization of their peripheral groups. The bioavailability of such structures can be increased by surface derivatization with OEGs. Since the peripheral groups were supposed to covalently bind a drug motif, it was impossible to simply cover the periphery of a dendrimer with a solubilizer. Therefore, it was of great value to synthesize a molecule for surface coverage. This was supposed to enhance the solubility of the carrier and still offered the opportunity for further functionalization. Another important aspect was the linkage of such “caps” to a dendron or dendrimer. An aryl-alkyl amide linkage, generated by the reaction of a benzoate with an alkyl amine, was intended to be advantageous for the stability of the conjugate, because these amides were not degraded by several peptidases.<sup>VII</sup> Two suitable synthetic concepts were taken from literature and adapted for the design of such “caps”.

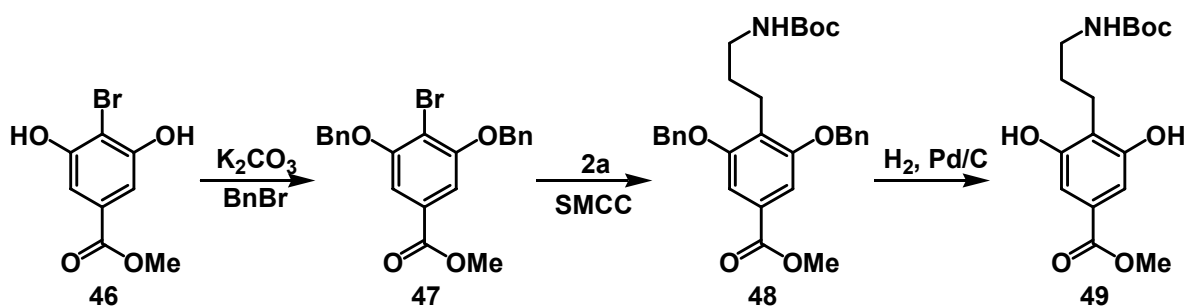
---

<sup>VII</sup> personal note of T. Kapp who is a member of the cooperating group of Prof. R. Gust, Institut für Pharmazie, Freie Universität Berlin, Berlin, Germany.



Scheme 28. Generation-specific functionalization of a dendrimer with SCC.

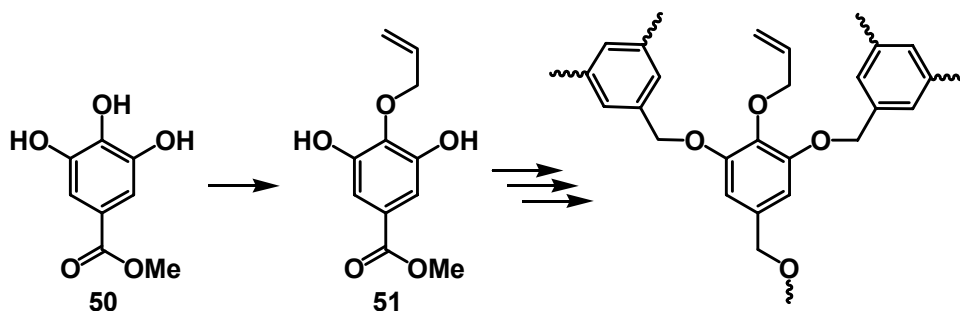
The first approach towards the synthesis of a “cap” was based on the work of Bo, who originally used this concept for the generation-specific functionalization of dendrimers.<sup>39</sup> **46** offers the possibility to *bis*-alkylate both of its phenols, to generate a C-C-bond via SCC on its aryl-bromide and to address the ester functionality by saponification.



Scheme 29. Concept for the synthesis of a “cap” employing SMCC.

**47** was easily obtained by *bis*-benzylation of **46**. However, the average yield for the SMCC of **47** with **2a** or any borane was below 5%. This was very surprising, because the yields for comparable SCC reactions on dendrimers were almost quantitative. The reaction on dendrimers had to face more sterical stress and, in particular, the oxidative addition had to proceed on a system with higher electron density (benzyl ether in the original work vs. benzoate in model-compound **47**). However, the bulky boranes, derived from 9-BBN, may have a decreased transmetalation ability. A full reaction screening, including the variation of several catalysts, bases and solvents, was done, but, unfortunately, without any influence on the yield of **48**. The catalytic hydrogenation of **48** quantitatively gave **49**, but this method had no synthetic value since the yields for **48** were not improved.

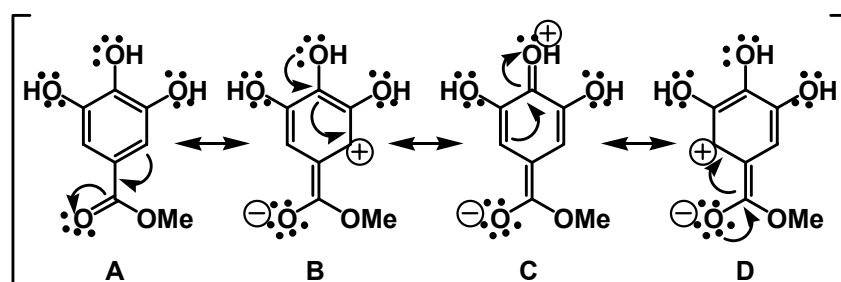




Scheme 30. Generation-specific functionalization of a dendrimer via selective alkylation reactions.

The second approach was based on the work of Freeman, whose concept was very closely related to that of Bo, but used etherification protocols instead of SCC.<sup>38</sup>

The selective 4-*O*-alkylation of **50** can be explained by its resonance-structures. The ester is an electron-withdrawing group and has an  $-I$ - and an  $-M$ -effect. The “en-acetalate” resonance-structure, reasonable though charge-separating, assigns two electrons from the carbonyl bond to the carbonyl oxygen. The electron deficit of the carbonyl carbon can be equilibrated by assimilation of an aromatic electron-pair.

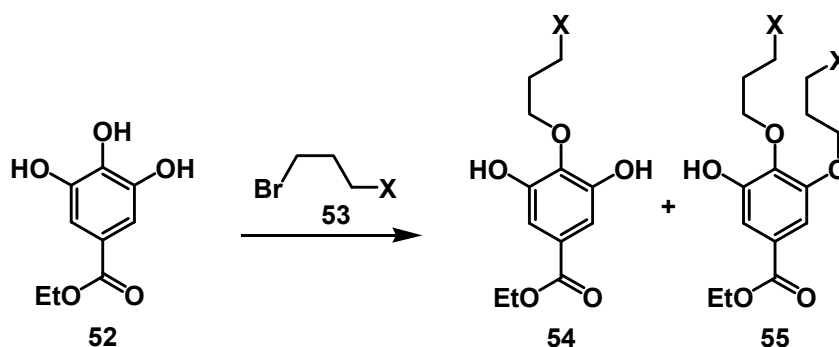


Scheme 31. Resonance-structures of **50**.

In consequence, the positive charge can be defined in the *ortho*-positions and the *para*-position to the ester. The resonance-structure for the *para*-position can incorporate an electron-pair from the phenol to give a quasi-quinoidic structure, in which the positive charge can be assigned to the oxygen. Since the positive charge is not located in the *meta*-positions, it is not possible to formally describe a comparable resonance-structure for the other phenols. Therefore, the oxygen in the *para*-position will polarize the bond to its proton more than the others. The acidity of this proton increases and a weaker base is sufficient for its deprotonation. Generally,  $K_2CO_3$  is used for the deprotonation of phenols. In this particular case  $NaHCO_3$  or  $KHCO_3$  were able to deprotonate the *para*-position, whereas the *meta*-positions

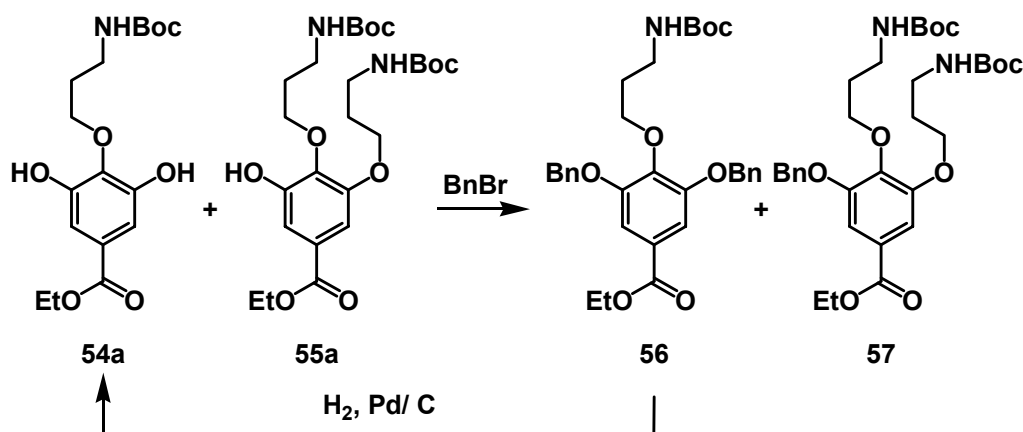
remained unaffected. This indicated that the pKa of the *para*-phenol has about the same value as that of the proton of a benzoic acid.

The selectivity towards *para*-alkylation was used for the introduction of protected binding-sites, which allow for further functionalization. **52** was selectively alkylated with substituted 3-bromo propanes **53** in the presence of KHCO<sub>3</sub> at room temperature and gave **54**.



Scheme 32. Alkylation of **52**.

Usually, equimolar amounts of **52** and **53** were used. However, sometimes *bis*-alkylated by-products **55** were obtained, and it was impossible to separate these mixtures. Therefore, these batches were benzylated and gave a mixture of **56** and **57**. Now, the separation of this mixture was possible with standard column chromatography. Catalytic hydrogenation of **56** with Pd/ C in a polar protic solvent yielded pure **54a**.



Scheme 33. Accessibility of **54** from mixed batches with *bis*-alkylated by-products.

In consequence, **52** was successfully used in slight excess (1.2 equivalents) to avoid the extra steps. In order to get more control over the selectivity, less reactive alkyl

chlorides were used. These etherifications did not succeed at low temperatures and an increase in temperature yielded again a statistical mixture of **54** and **55**.

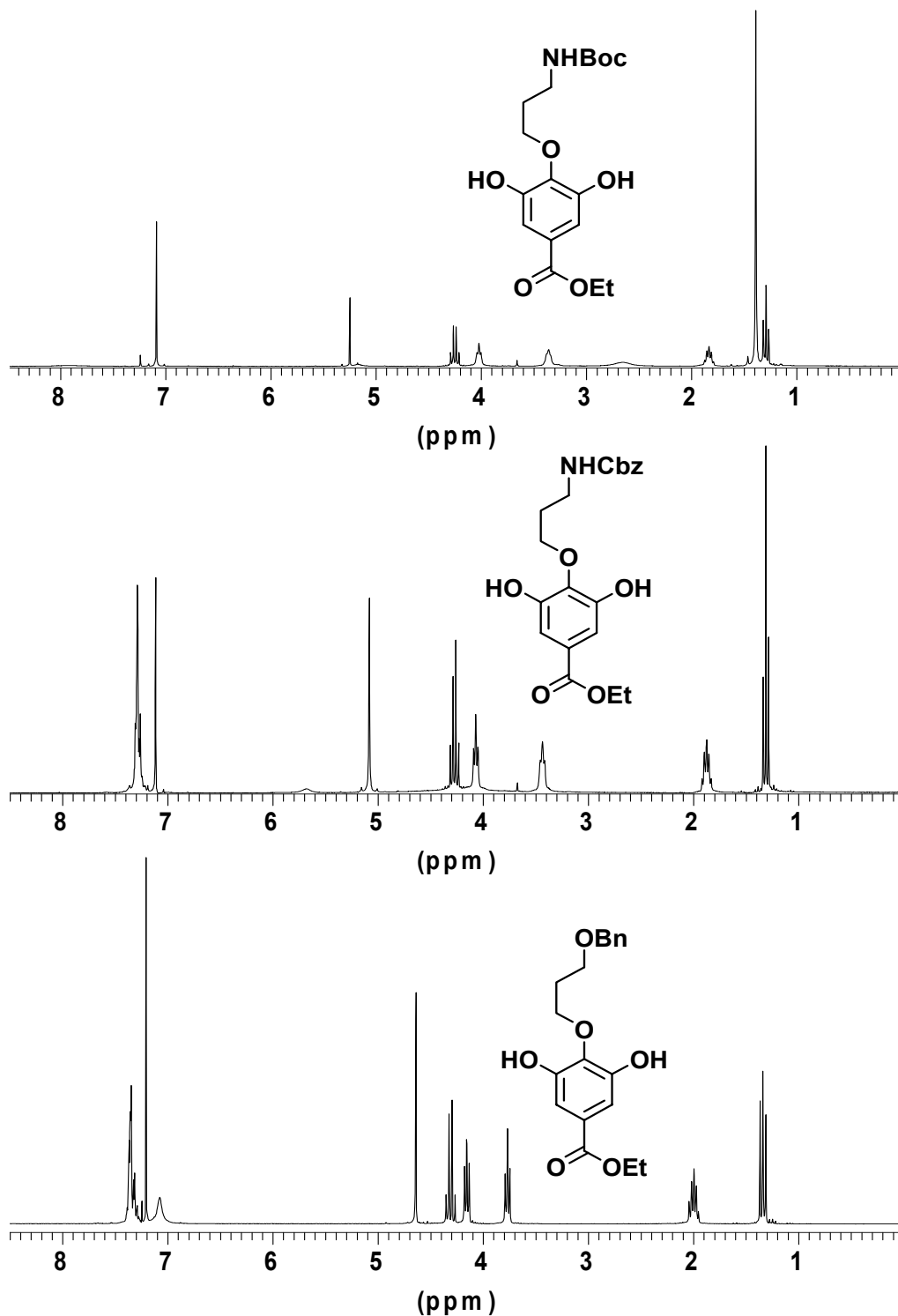
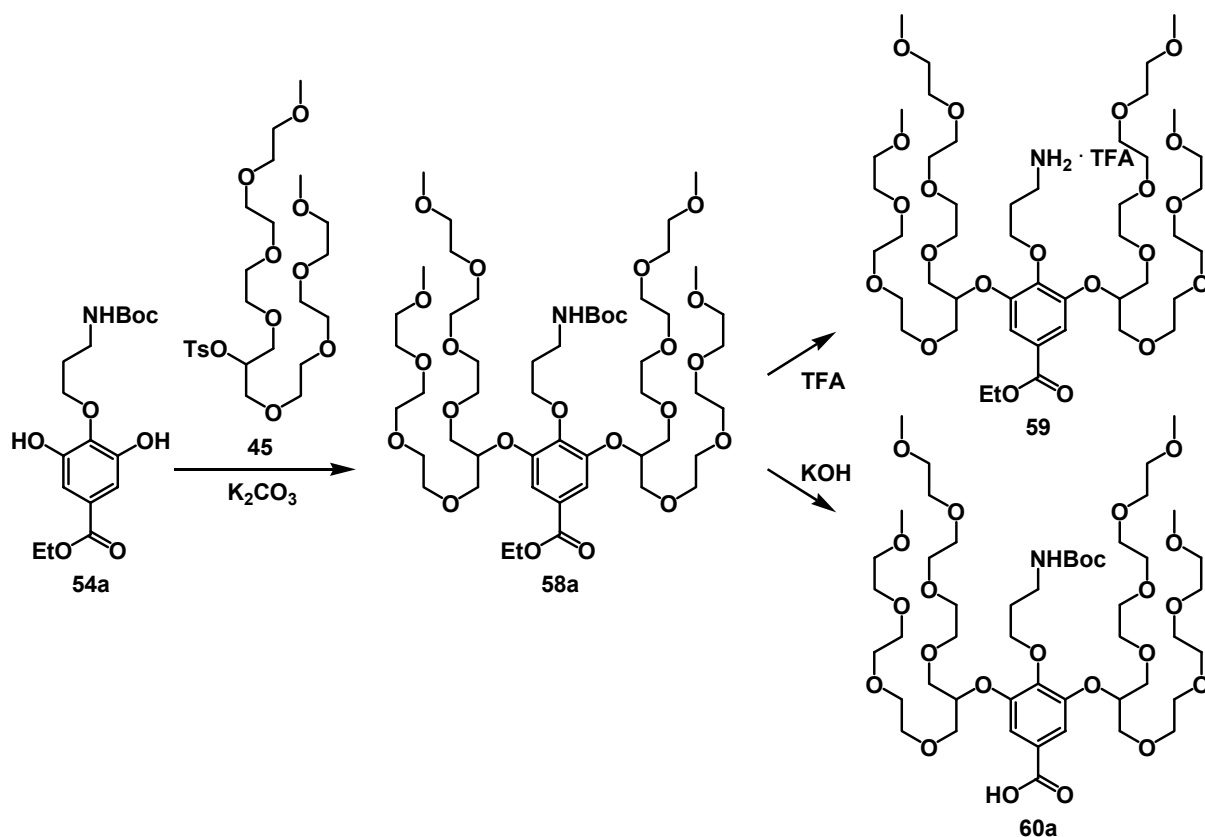


Fig. 17. <sup>1</sup>H-NMR spectra of mono-coupled products from etherification of **52** (250MHz, CDCl<sub>3</sub>).

Since the symmetric glycerol derivative **45** was available on a larger scale, it was preferentially reacted with compounds **54a/b/c** in a second etherification step. These

reactions were carried out in DMF, using  $K_2CO_3$  for deprotonation at  $80^\circ C$ . Reasonable yields for **58a/b/c** of 58-65% indicate a coupling efficiency of 75-80% per coupling.<sup>180</sup>



Scheme 34. Synthesis of "caps" employing selective etherifications.

At higher temperatures, the by-product resulting from the elimination reaction of **45** decreased the yields for **58**. Alternatively, Mitsunobu protocols were applied for the reaction of **54** with alcohol **44**, but the removal of the *tri*-phenyl phosphine oxide impurities was tedious. Model reactions with primary tosylates, e.g. with **30** and **33**, did not show significantly better yields.

The use of the secondary glycerol derivative had some advantages over its primary analogue. Besides the availability on a larger scale, its  $^1H$ -NMR resonance for the tertiary proton 1 (Fig. 18) was a nice diagnostic tool. The chemical shift of this rather isolated pentet (stemming from the coupling with four equivalent methylene protons) in the  $^1H$ -NMR was typically around  $\delta = 4.6$  ppm. It was conveniently used as an integrative reference for reaction control and for determination of the purity.

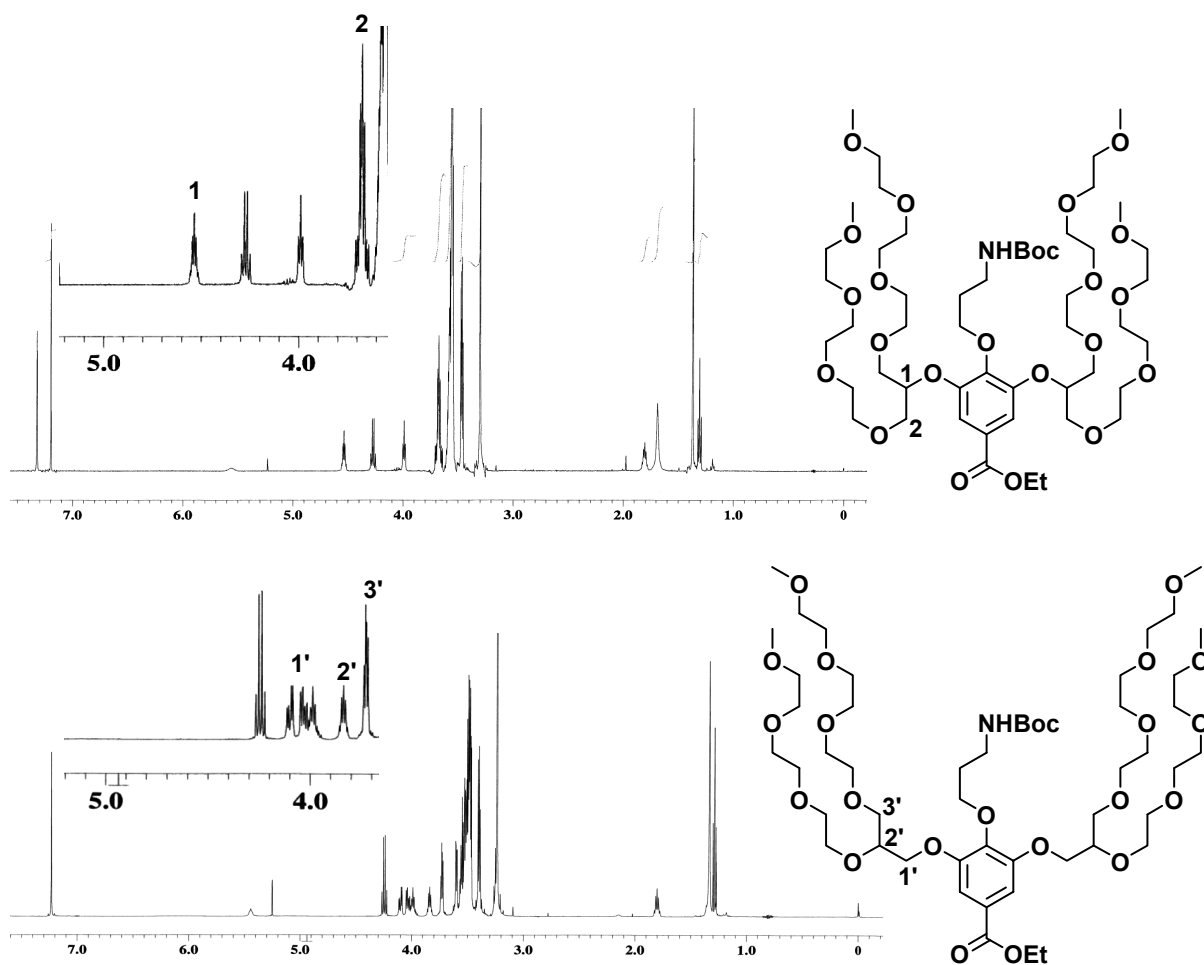
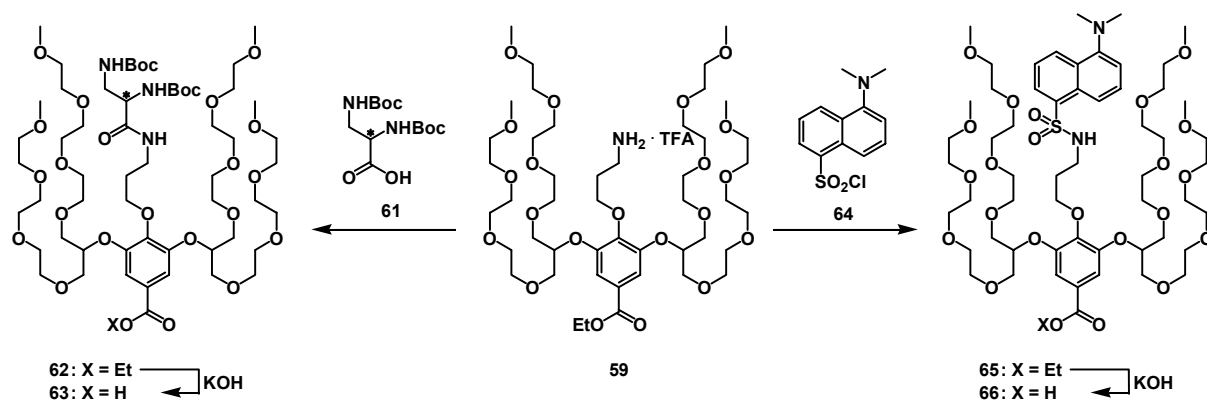


Fig. 18. Comparison of “caps” with symmetrical and unsymmetrical solubilizer.

The primary glycerol derivative has an unsymmetrical carbon and its proton coupling pattern was much more difficult. These multiplet-proton resonances were shifted to a higher field ( $\delta = 3.5\text{--}4.1$  ppm), interfered with other resonances, and did not possess expedient diagnostic information.

“Caps” **58** were available on a 7 gram scale and made a variety of compounds with different substitution patterns accessible. The orthogonal protective groups allowed for selective deprotection protocols and further functionalization. The most important compound for the synthesis of other “caps” was **58a**. Its *N*-Boc group was quantitatively deprotected with TFA in methylene chloride and gave **59**. The free benzoic acids **60** were gained from the saponification of **58** with KOH in ethanol. It was possible but not necessary to purify compounds **59** and **60** with column chromatography.



Scheme 35. Synthesis of “caps” with a fluorescence tag or an ethylene-diamine moiety.

The racemic *N*-Boc-protected diamino-propionic acid **61** depicts an ethylene-diamine moiety and was assembled with **59** under standard amide coupling conditions to give **62** (Scheme 35).<sup>157, 168</sup>

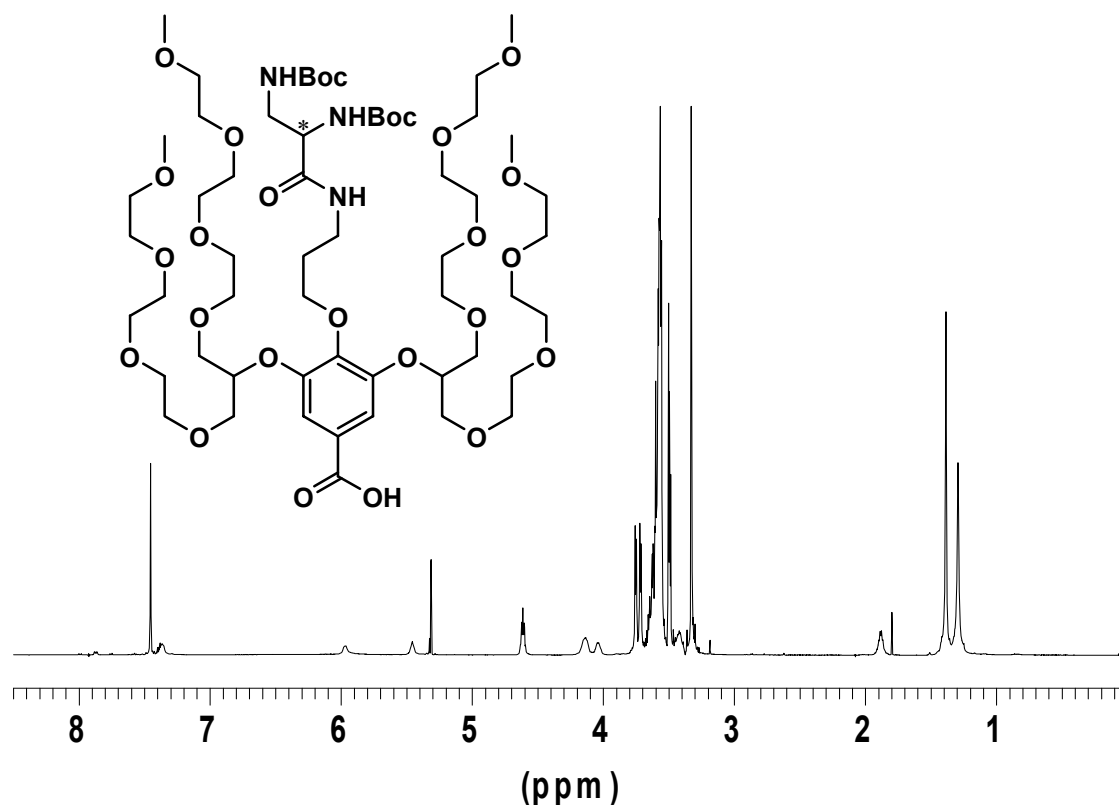


Fig. 19. <sup>1</sup>H-NMR spectrum of **63** (500 MHz, CD<sub>2</sub>Cl<sub>2</sub>).

Interestingly, this coupling succeeded with TBTU as active ester reagent. It was not possible to substitute the rather expensive *O*-hetarylated urethanes with other active ester reagents such as HOBt/ EDC or Hsu/ DCC. The free benzoic acid **63** was generated in excellent yields from **62** with KOH at room temperature in ethanol.

Dansyl chloride **64** was intended to work as a fluorescence tag. It was connected to **59** and gave **65** (Scheme 35). **66** was quantitatively obtained after saponification of **65** with KOH. The compounds with the fluorescence dansyl-label were stored and reacted in the dark to avoid oxidative degradation.

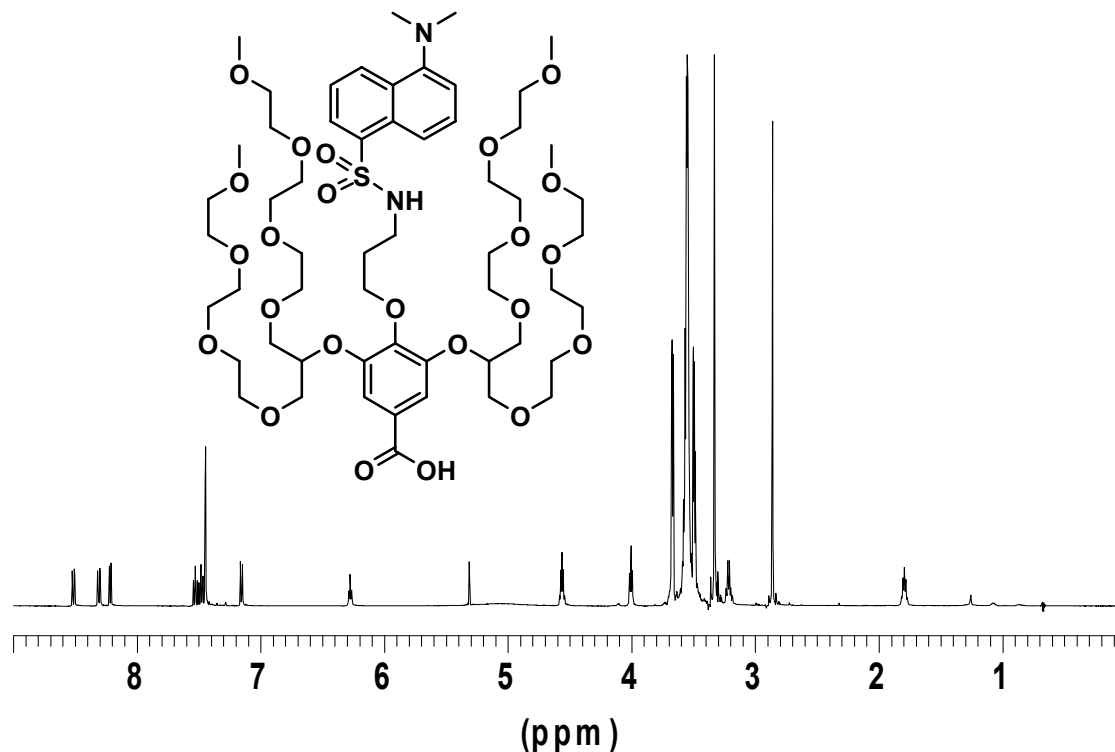
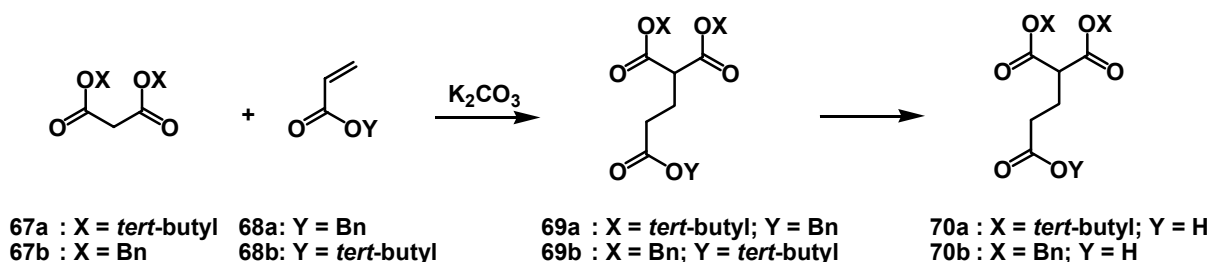


Fig. 20.  $^1\text{H-NMR}$  spectrum of **66** (500 MHz,  $\text{CD}_2\text{Cl}_2$ ).

The synthesis of “caps” with protected malonic acids was more difficult. *O*/ *O*-chelating malonic acids offering another free acid for assembly with a “cap” by an amide linkage, were not commercially available and had to be synthesized.<sup>167</sup>



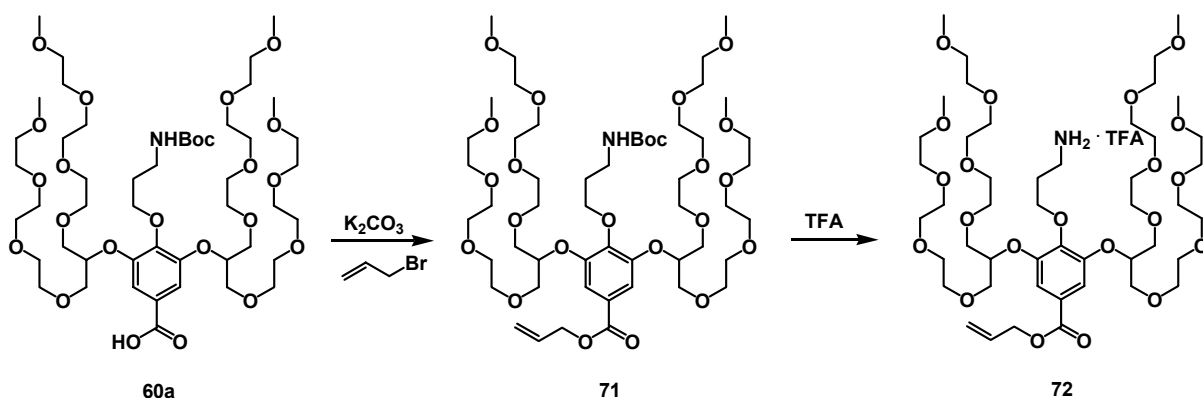
Scheme 36. Synthesis of protected malonic acid derivatives for the functionalization of “caps”.

Removing the protective groups of the malonic acid was neither supposed to affect the dendritic backbone, nor to lead to the acid’s decarboxylation. On the other hand, these protective groups had to be stable under coupling conditions and had to be

orthogonal towards other deprotection protocols. The best candidates to avoid decarboxylation were those malonic acids that were protected as *tert*-butyl or benzyl esters.

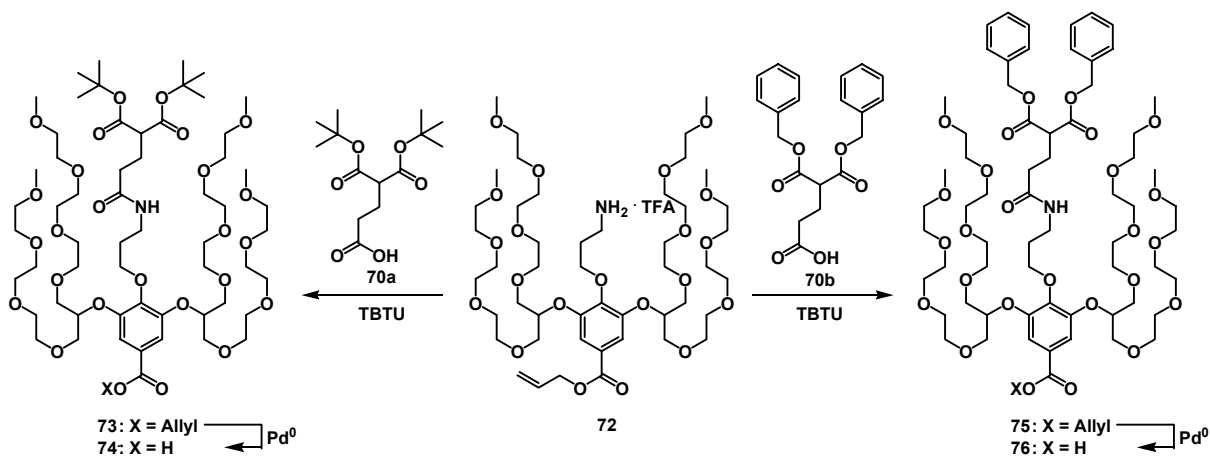
The *mono*-deprotected *tris*-acids **70** were generated from the protected malonic acids **67** and orthogonally protected acrylic acids **68** under Michael addition conditions (Scheme 36). This reaction always yielded a mixture of *mono*- and *bis*-alkylated malonates and their separation was tedious. It was possible to isolate pure **70a/b** after the deprotected raw mixture of **69** was purified with column chromatography.

As protected malonic acid derivatives were affected under saponification conditions with KOH, it was necessary to introduce a different, selectively addressable protective group for the benzoic acid of the “cap” (Scheme 37).



Scheme 37. Synthesis of “caps” with allyl benzoates.

The alkylation of the potassium salt of **60a** with an excess of allyl bromide gave **71**. Removal of its *N*-Boc-group was performed with TFA in methylene chloride and gave **72** without further purification.



Scheme 38. Synthesis of “caps” with a malonic acid moiety.



The protected *O*/*O*-chelating synthons **70a/b** were assembled with **72** under standard amide coupling conditions and gave **73** or **75** in excellent yields (Scheme 38).

The best results for these couplings were obtained with TBTU as active ester reagent. The same products were accessible in lower yields with other active ester reagents (HOBt/EDC or H<sub>Su</sub>/DCC).

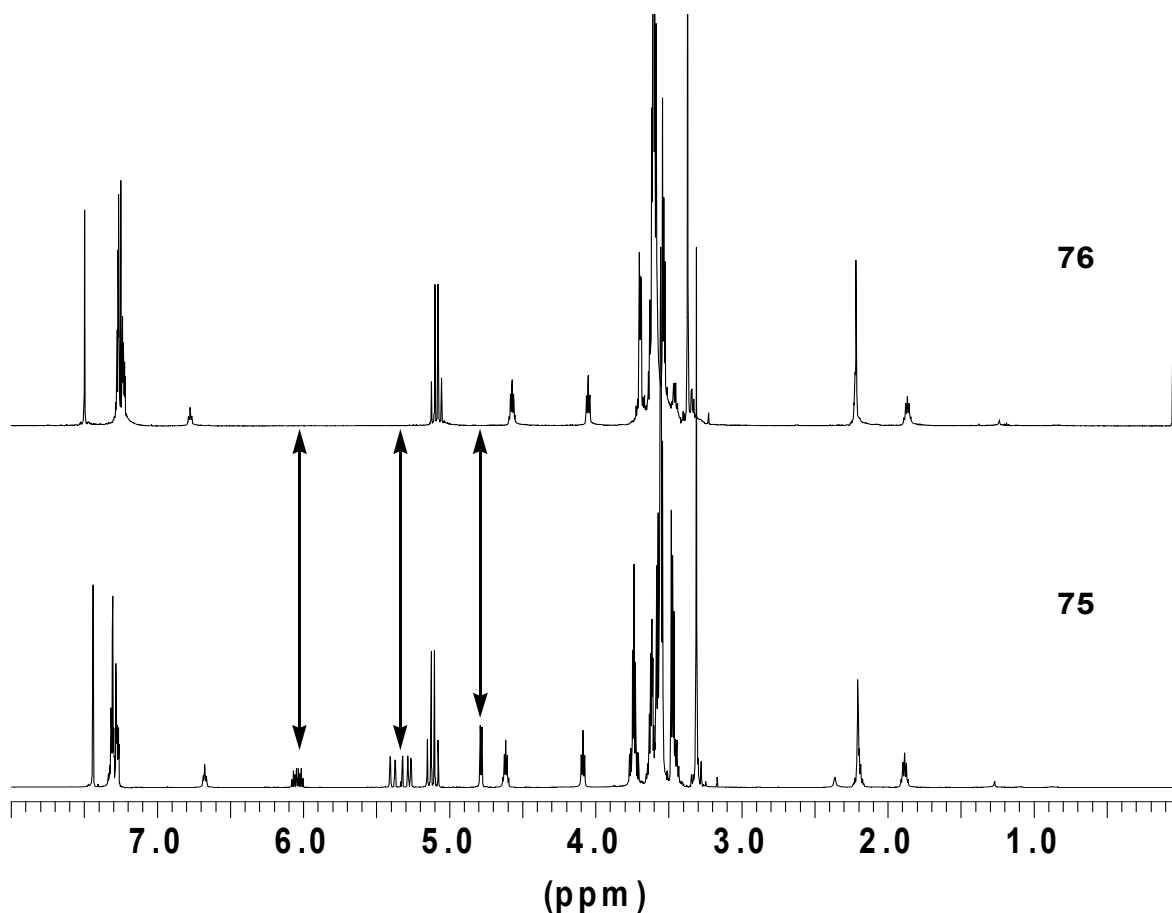
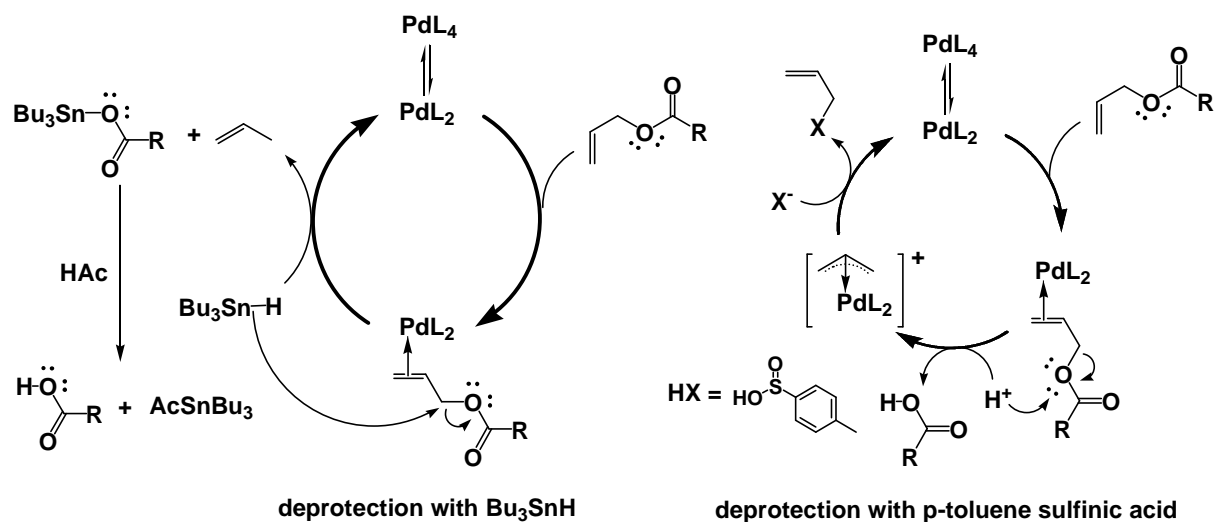


Fig. 21. Comparison of the <sup>1</sup>H-NMR spectra of **75** and **76** (500 MHz, for **75**: CD<sub>2</sub>Cl<sub>2</sub>, for **76**: CDCl<sub>3</sub>).

The deprotection of these esters was rather difficult. Several literature protocols did not drive the reaction to completion. The deprotection of these allyl esters was much more difficult than expected. Several well-known palladium catalyzed deprotection protocols, e.g. Pd[PPh<sub>3</sub>]<sub>4</sub> and others/ morpholine or pyrrolidine, PdCl<sub>2</sub>[PPh<sub>3</sub>]<sub>2</sub>/ dimedone, Pd[OAc]<sub>2</sub>/ PPh<sub>3</sub>/ TEA, were tested and either failed completely or worked unsatisfactorily. At this stage of the synthesis the complete deprotection reaction was very important, because the separation of the acids from the esters was tedious.

Another approach towards this deprotection problem employed  $\text{Pd}[\text{PPh}_3]_4$  and  $\text{Bu}_3\text{SnH}$ .<sup>181, 182</sup> The allyl benzoate was cleaved, but tributyl stannyl benzoates were generated exclusively. Their conversion into the acid succeeded, but it was impossible to completely remove the tin impurities.

The best results for the deprotection procedure were obtained according to the method reported by Nagakura and coworkers.<sup>183</sup> The allyl benzoates and  $\text{Pd}[\text{PPh}_3]_4$  were dissolved in methylene chloride, and a solution of *para*-toluene sulfonic acid in methanol was added. The reaction proceeded within 15-20 minutes at room temperature and gave the corresponding benzoic acids **74** and **76** in an almost quantitative yield after purification with column chromatography.

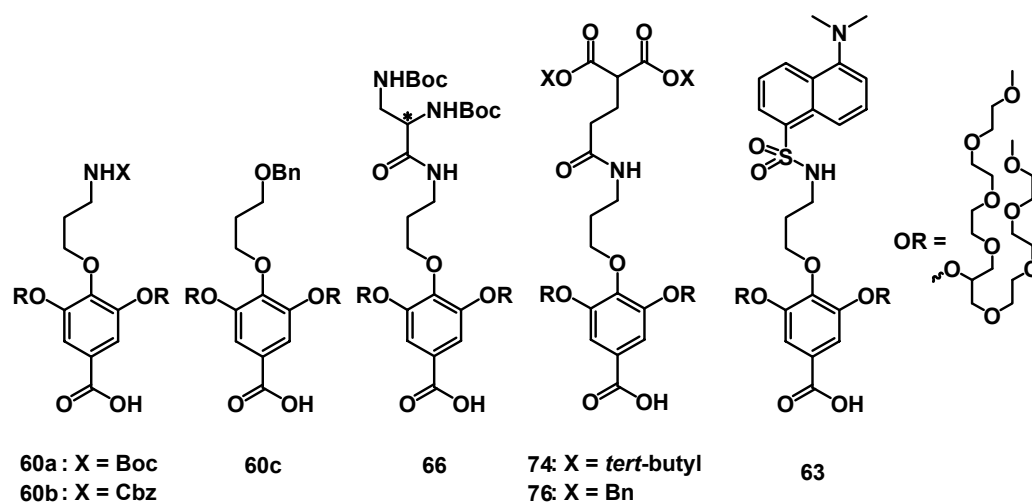


Scheme 39. Mechanisms for the deprotection of allyl esters.

The mechanisms of the two most effective deprotection procedures are somewhat different (Scheme 39). The active catalytic palladium species derived from  $\text{Pd}[\text{PPh}_3]_4$  is the 14 e-complex  $\text{Pd}[\text{PPh}_3]_2$ . The allyl ester forms a complex with the active palladium species. The p-orbital of the double bond of this quasi-ethylene ligand interacts with a molecular orbital of the palladium complex, typically with  $1a_1$  and  $3a_1$ , and gives electron-density for a weak s-donation. The interaction of the allylic  $p^*$ -orbital with the molecular  $b_2$ -orbital stabilizes the complex via a strong back-donation. The hydro-stannolysis protocol offers a hydride which can attack the  $\alpha$ -methylene group as a nucleophile. Propene is released and the active palladium species is recovered for the next catalytic cycle. The carboxylate combines with the stannyl-residue and forms the corresponding stannyl ester. The free acid is obtained by transesterification with a stronger acid.

The other deprotection protocol initially forms the same palladium-allyl-complex. A proton, provided by the sulfonic acid, is captured by the lone-pair of an oxygen in the carboxylate. The free acid is released and a cationic  $\eta^3$ -allyl-palladium complex is formed. The sulfinate intercepts the allyl-cation and recycles the active palladium species.

Scheme 40 shows all “caps” with symmetrical glycerol derivatives that were accessible via the selective alkylation of **52**. These compounds are highly water soluble and carry functionalities of pharmaceutical interest. Their free binding-site, the benzoic acids, can be linked to dendrimers and dendrons, either as stable amides or as degradable esters. The versatility of the synthetic concept offers the possibility of further tailored functionalization.



Scheme 40. Accessible “caps”.

## 4.4 Synthesis of Dendrons and Dendrimers

### 4.4.1 Synthesis of “Capped” G<sub>0</sub>-Dendrimers

Water soluble G<sub>0</sub>-dendrimers were synthesized by the assembly of functionalized “caps” with a core moiety by employing amide coupling chemistry.

In order to form three amide linkages, the *tri*-functional core was reacted with a slight excess of “cap” or dendron per branch. In contrast to the amido coupling protocol for alkanolic acids with primary alkylamines, benzoic acids reacted much more efficiently with HOBt/ EDC as active ester reagent. The couplings with *O*-hetarylated urethanes as active ester reagents did not work out well. The *in situ* formation of the active ester did not require low temperatures. The reaction performed at room temperature and was easy to monitor by TLC.

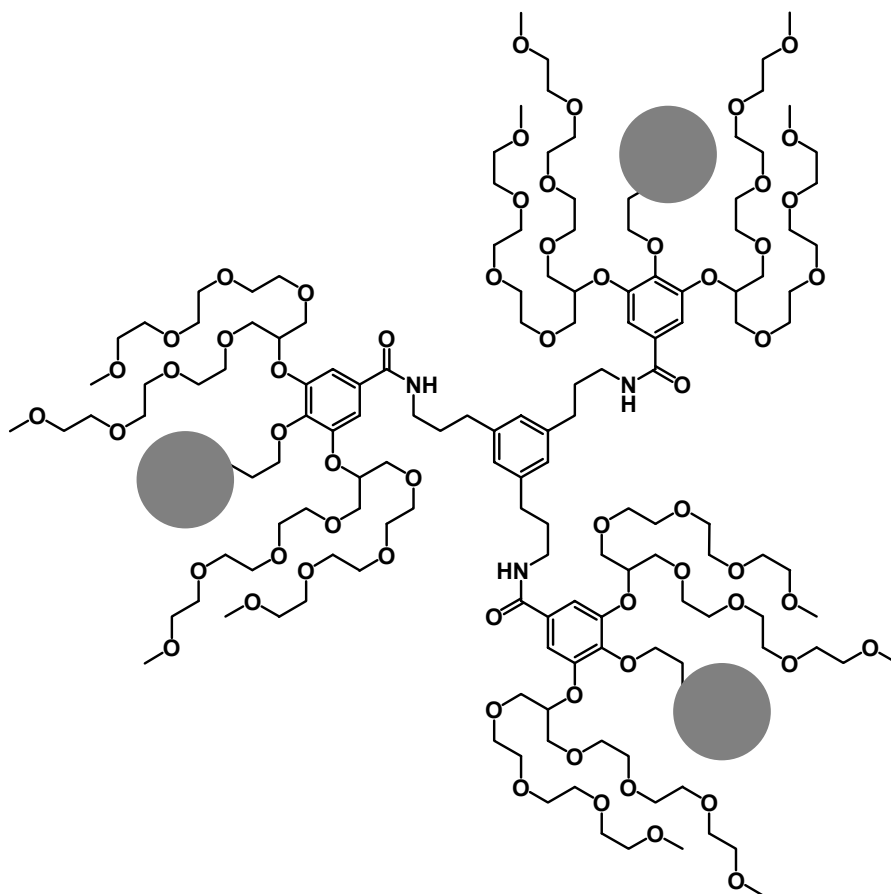


Fig. 22. PEGylated G<sub>0</sub>-dendrimer with a derivable surface motif.

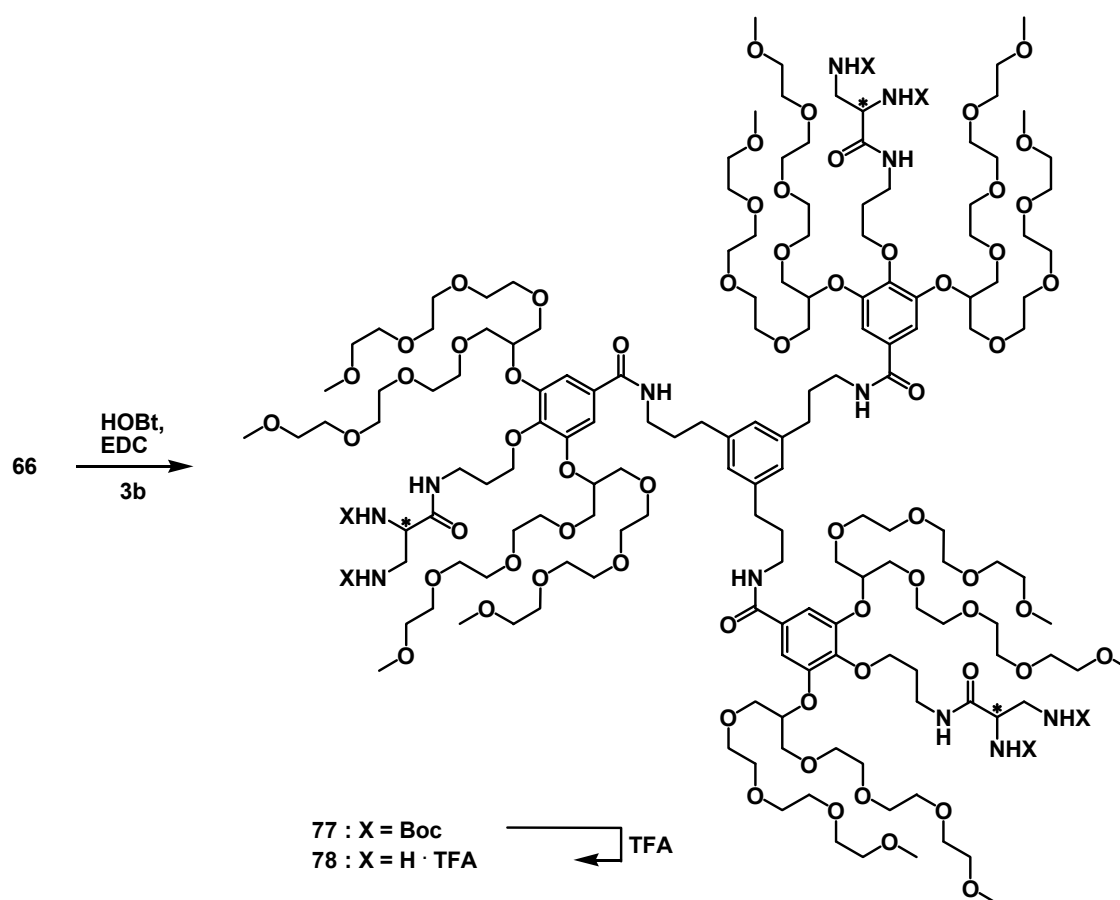
An excess of TEA was used to deprotonate the *tris*-hydrochloride **3b** and made the free amino groups available. To avoid side-reactions, the amido coupling reaction

was initiated at low temperatures, typically at  $-40^{\circ}$ , and was allowed to gently warm to room temperature. It was also possible to monitor these coupling reactions by TLC.

#### 4.4.1.1 G<sub>0</sub>-Dendrimers with *bi*-Dentate Ligands

Dendrimers which provide chelating ligands for conjugation of carboplatin- or cisplatin-analogues were accessible by reacting **66**, **74** and **76** with **3b**.

**66** contained an *N*-Boc protected ethylene-diamine moiety and was reacted with **3b**. The core molecule was homogeneously dissolved in methylene chloride/ methanol mixtures prior to addition.



Scheme 41. Synthesis of a G<sub>0</sub>-dendrimer with an ethylene-diamine moiety.

After purification by standard column chromatography the pure dendrimer **77** was obtained in excellent yields. The excess of active ester was recovered as the corresponding methyl ester. This was reconverted by saponification with aqueous 1M KOH and gave **66**. The dendrimer was characterized by  $^1\text{H}$ - and  $^{13}\text{C}$ -NMR and MALDI-TOF MS. Some proton resonances were covered by the very intensive resonances of the OEG-protons. It was, however, possible to assign all resonances

in the  $^1\text{H}$ -NMR-spectra with the information provided by 2D-homo- and hetero-nuclear correlated NMR-spectroscopy (COSY, HMBC and HMQC). All 31 carbon resonances were detected by  $^{13}\text{C}$ -NMR, but it was not possible to assign all of them.

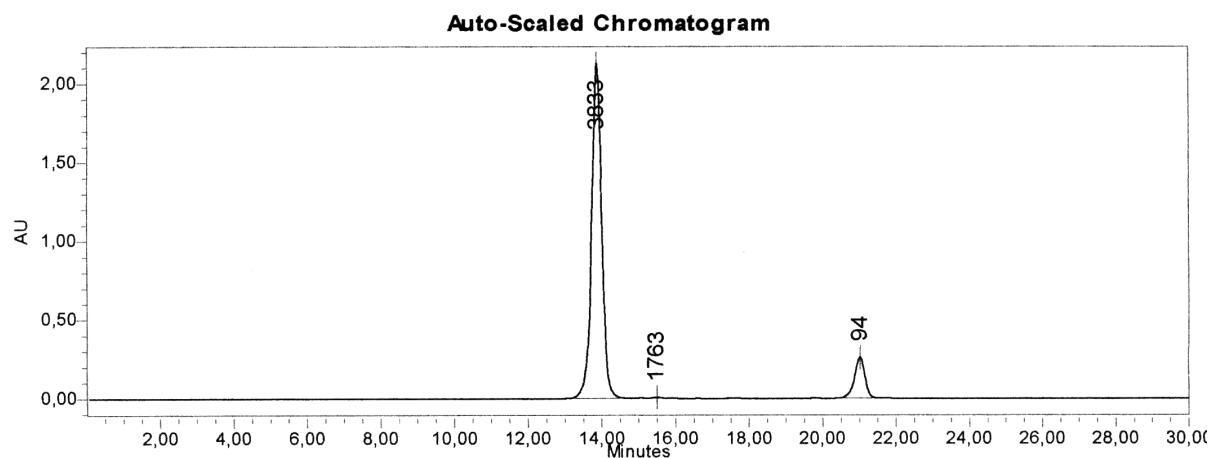


Fig. 23. GPC-chromatogram of **77** (indicating 99% purity; ref. at 21 minutes: toluene).

The monoisotopic peak of the sodium salt and its isotopic pattern were determined by MALDI-TOF MS in reflective mode. The purity of the compound was determined with analytical GPC.

The acid labile *N*-Boc-carbamates were deprotected with a large excess of TFA in methylene chloride at room temperature and gave **78** (as *hexakis*-hydro-trifluoro acetate). Completion of the procedure was monitored with  $^1\text{H}$ -NMR spectroscopy. The deprotected dendrimer was again characterized by  $^1\text{H}$ - and  $^{13}\text{C}$ -NMR (assignment by 2D- correlated spectroscopy) and MALDI-TOF MS. The comparison of the  $^1\text{H}$ -NMR spectra of **59** and **60** clearly indicated that the resonance for the *N*-Boc groups disappeared after treatment with TFA.

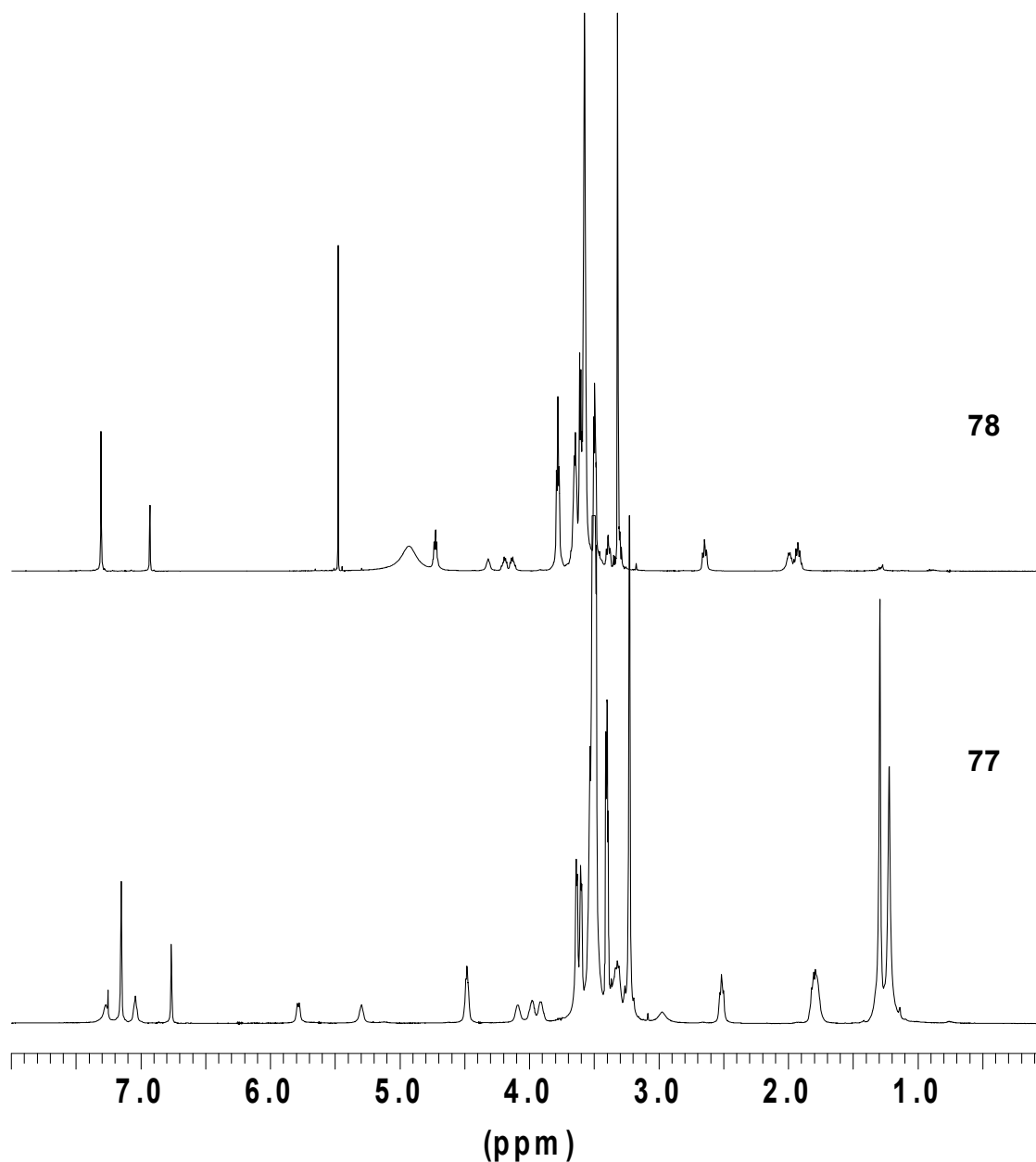
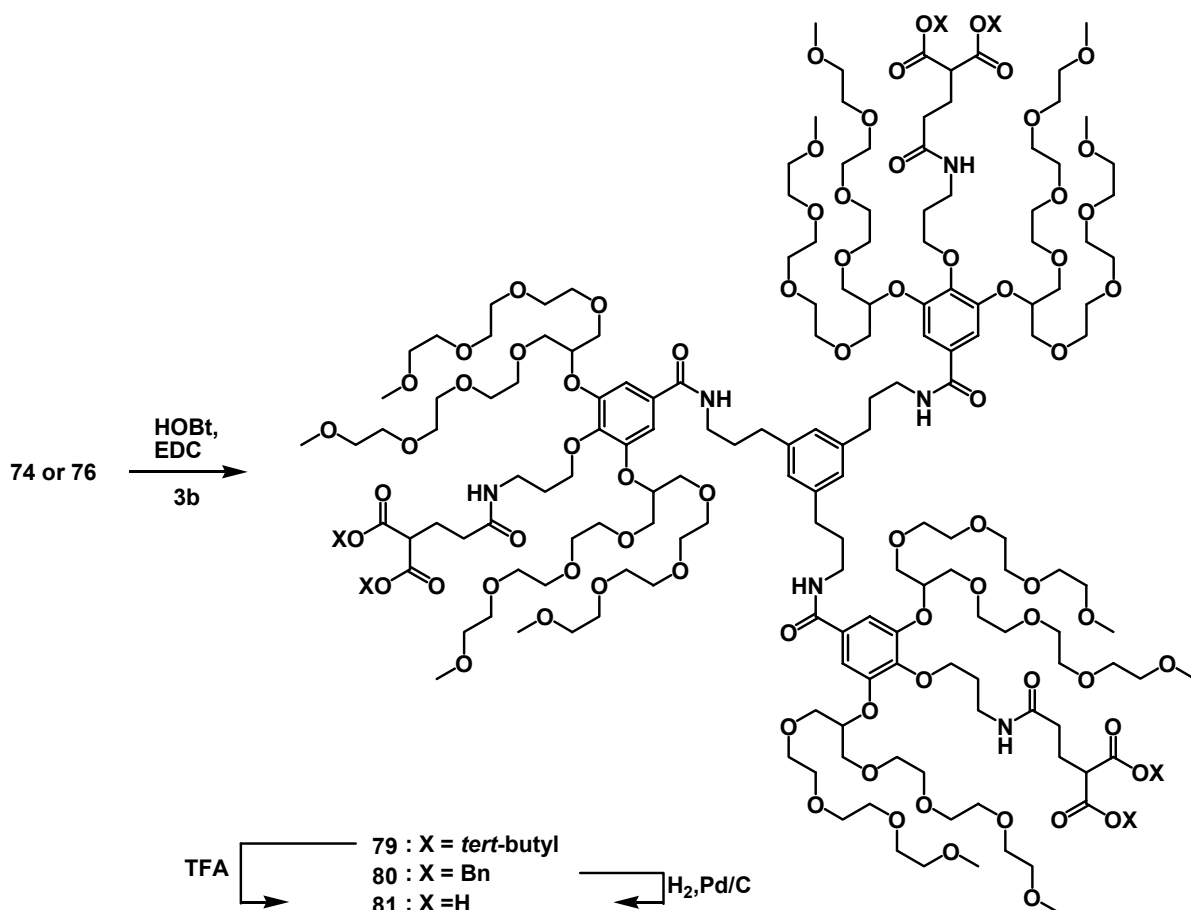


Fig. 24. <sup>1</sup>H-NMR spectra of *N*-Boc protected **77** and deprotected **78** (500 MHz, for **77**: CDCl<sub>3</sub>; for **78**: CD<sub>2</sub>Cl<sub>2</sub> + d<sup>4</sup>-MeOH).

**74** and **76** provided protected malonic acid derivatives and were assembled with **3b**. The coupling procedure was very similar to the one described for the synthesis of **77**, but this time the core molecule was suspended in methylene chloride and not homogeneously dissolved by the addition of methanol.



Scheme 42. Synthesis of G<sub>0</sub>-dendrimers with malonic acid moieties.

The reason for these slightly different reaction conditions is very simple. Generally, it was more difficult to separate the dendrimers and the free acids than to separate their corresponding methyl esters with column chromatography. Besides easier purification, it was also possible to recover the excess of active ester as methyl esters and to reconvert them by saponification. The methyl esters of **74/ 76** were not selectively addressable in the presence of the protected malonates and it would not have been possible to recover them. Therefore, the reaction was quenched with aqueous 1M NaHCO<sub>3</sub>. It was possible to recover the multi-step compounds **74/ 76**, this modification made purification more difficult. The dendrimers **79** and **80** were again characterized with standard techniques. The assignment of the obtained resonances in the <sup>1</sup>H-NMR-spectrum was again based on 2D- homo- and hetero-nuclear correlated NMR-spectroscopy (COSY, HMBC and HMQC). The expected number of carbon resonances was confirmed by <sup>13</sup>C-NMR spectroscopy. The molecular weight was determined by MALDI-TOF MS in linear mode and matched the calculated value. The MALDI-TOF measurements in the linear mode did not



succeed and, therefore, it was not possible to determine the isotopic pattern. Analytical GPC proved the purity of the compounds.

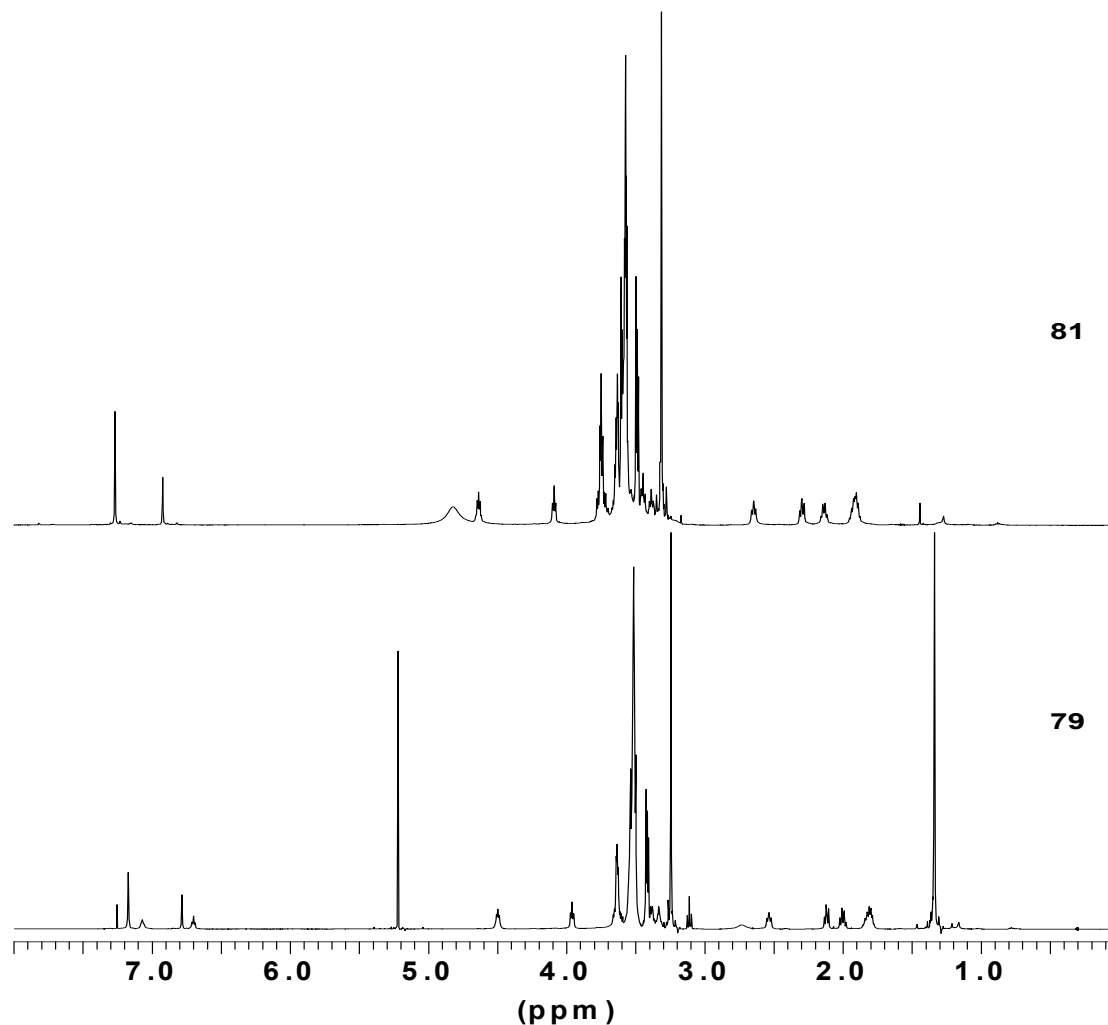
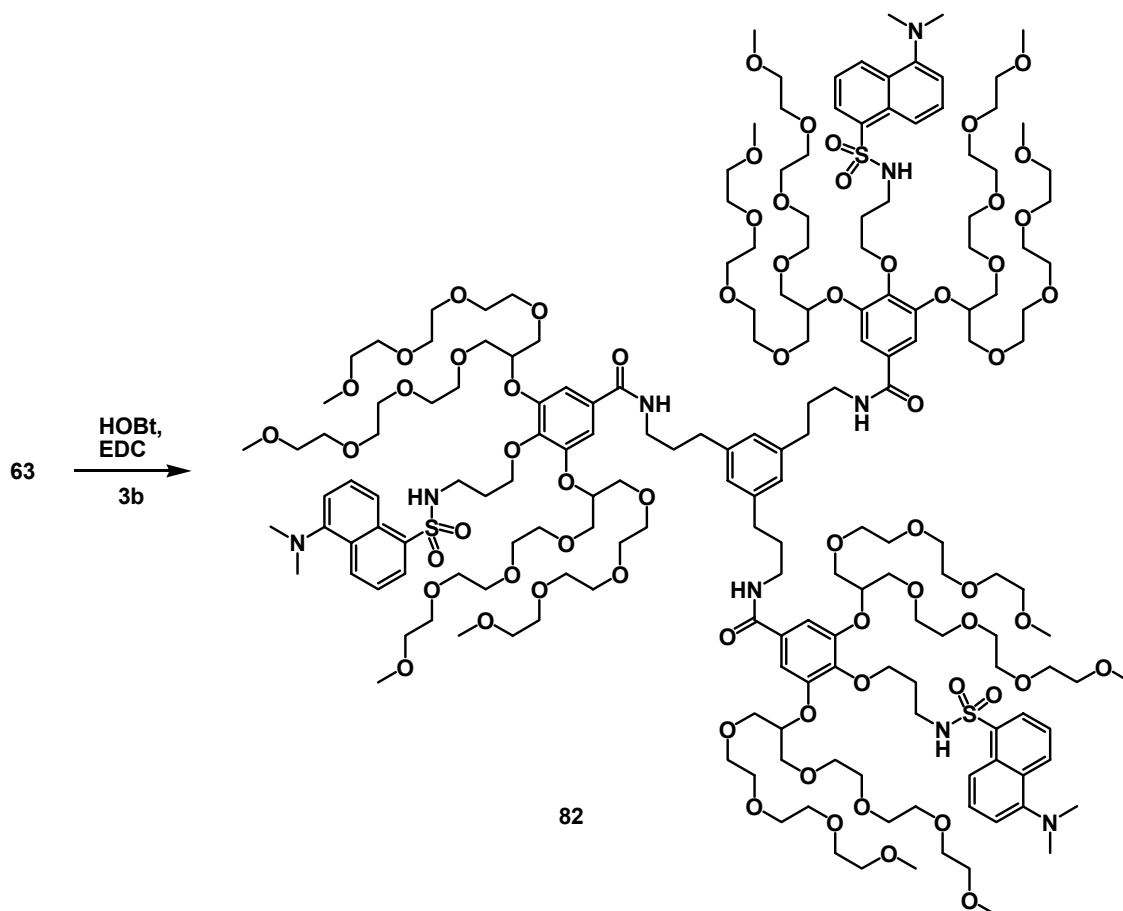


Fig. 25.  $^1\text{H}$ -NMR spectra of *tert*-butyl protected **79** and deprotected **81** (500 MHz, for **79**:  $\text{CDCl}_3 + \text{CD}_2\text{Cl}_2$ ; for **81**:  $\text{d}^4\text{-MeOH}$ ).

The *tert*-butyl malonates of **79** were deprotected with a large excess of TFA in methylene chloride at room temperature and gave pure **81** without further purification. Catalytic hydrogenation of **80** with Pd/ C in methanol proceeded within several hours and also gave pure **81** without further purification. Both deprotection procedures showed equal spectroscopic and spectrometric data.  $^1\text{H}$ - and  $^{13}\text{C}$ -NMR-spectra indicated that all protective groups were cleaved without any decarboxylation. The MALDI-TOF MS showed decarboxylated by-products, but this was not an evidence for the undesired decarboxylation, because the ionization- or acceleration-process of the measurement itself can initiate the evolution of  $\text{CO}_2$ .

## 4.4.1.2 G0-Dendrimers with a Fluorescence Tag

A dendrimer that contains a fluorescence tag was accessible by the assembly of **63** with **3b**. The fluorescence dansyl-label was already successfully used by Fuchs to study the cellular uptake of her polycationic carriers.



Scheme 43. Synthesis of G0-dendrimers with a fluorescence tag.

The coupling procedure was the same as described for the synthesis of **77** and gave pure **82** in 92% yield after purification with standard column chromatography. The compound was characterized with standard methods. The purity of **82** can be seen from its  $^1\text{H-NMR}$  spectrum and its analytical GPC.

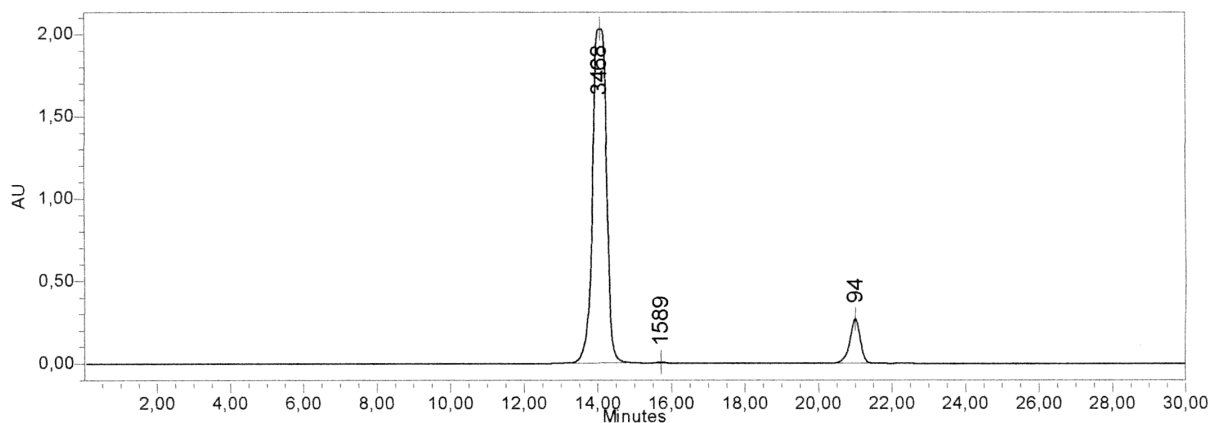


Fig. 26. GPC-chromatogram of **82** (indicating 99% purity; ref. at 21 minutes: toluene).

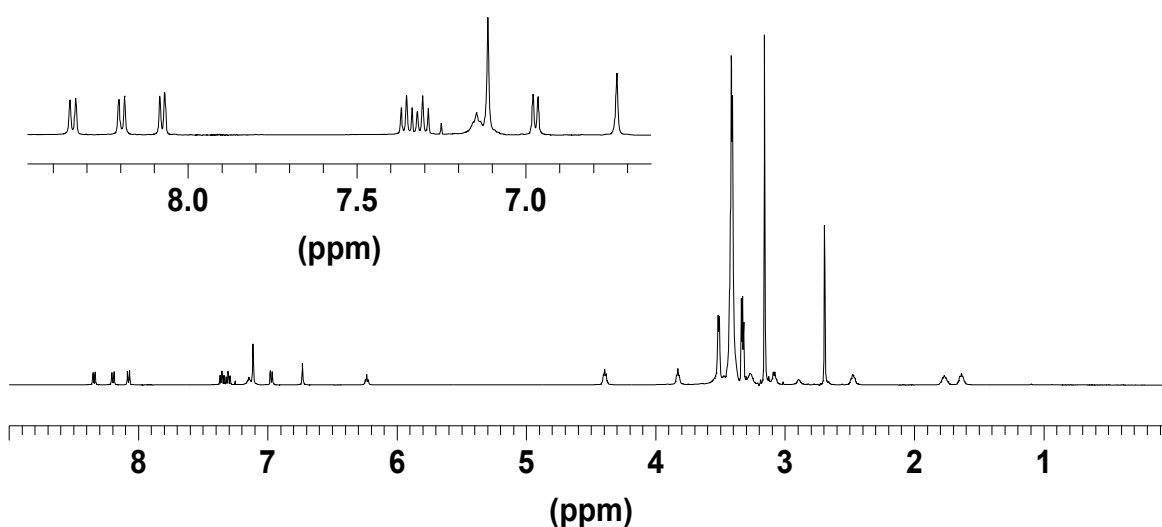
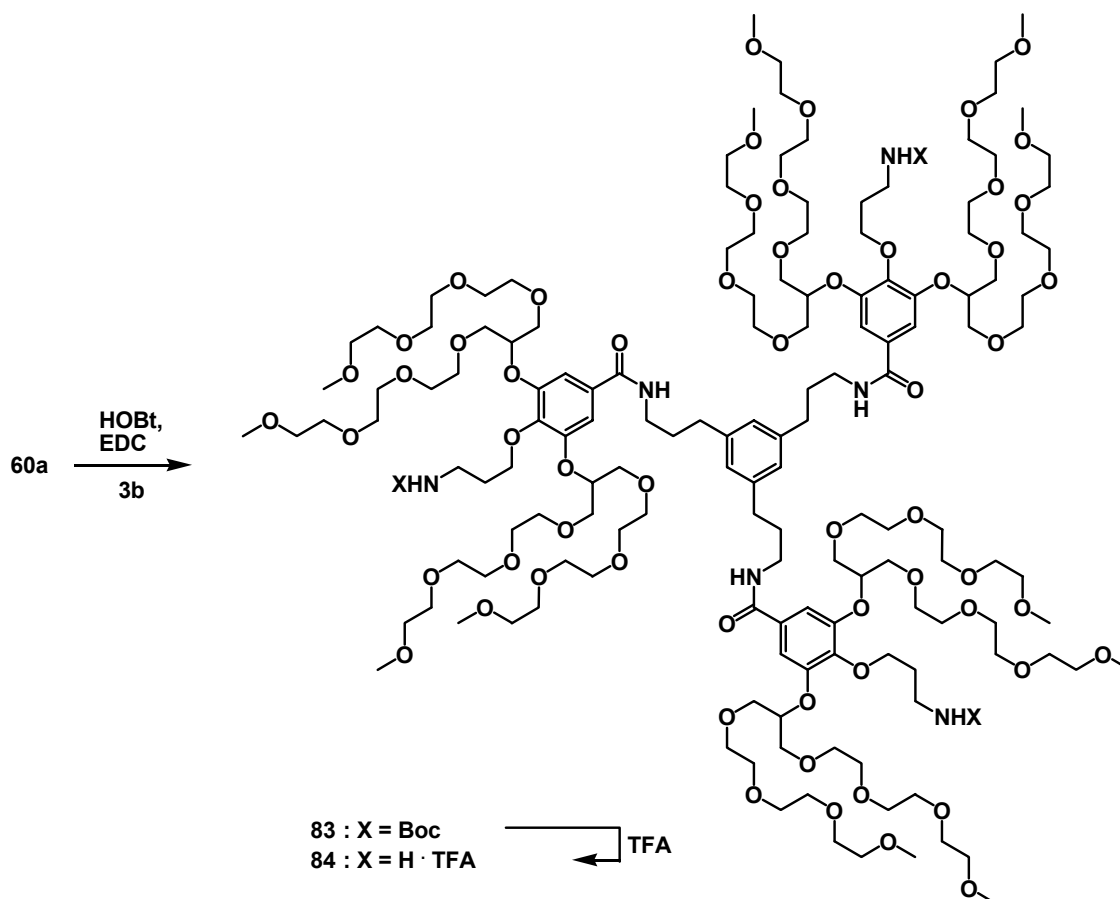


Fig. 27.  $^1\text{H-NMR}$  spectra of **82** (500 MHz,  $\text{CDCl}_3$ ).

#### 4.4.1.3 G0-Dendrimers with a Targeting Moiety

Folic acid offers binding-sites to form amide linkages and is a well-known and suitable candidate for active tumor targeting. Aronov optimized its amide coupling protocols for conjugates with linear PEGs. Based on these procedures, the assembly of a *tri*-functional G0-dendrimer with folic acid was intended to serve as a model for studying the coupling procedure and its efficiency.

**60a** provided an *N*-Boc protected propylamine and was reacted with **3b**. Purification with standard column chromatography gave **83** in 95% yield.



Scheme 44. Synthesis of G<sub>0</sub>-dendrimers for the assembly with folic acid.

**83** was fully characterized with NMR-techniques, MALDI-TOF MS and analytical GPC.

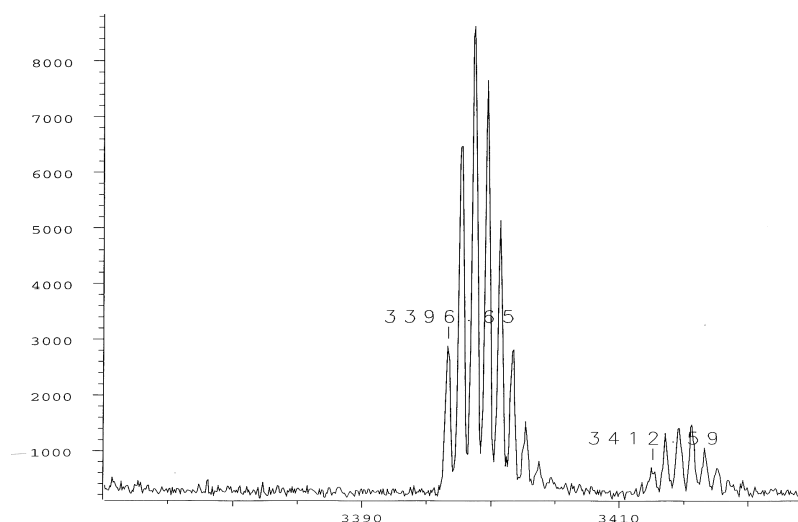


Fig. 28. MALDI-TOF mass spectrum (reflective mode) of **83**.

The *N*-Boc-carbamates were removed with a large excess of TFA in methylene chloride and gave **84** (as *tris*-hydro-trifluoro acetate). The deprotection was

monitored with  $^1\text{H-NMR}$ . The efficiency of the deprotection is demonstrated by the complete disappearance of the signal for the 27 protons of the *N*-Boc group of dendrimer **84** at  $\delta = 1.40$  ppm (Fig. 29).

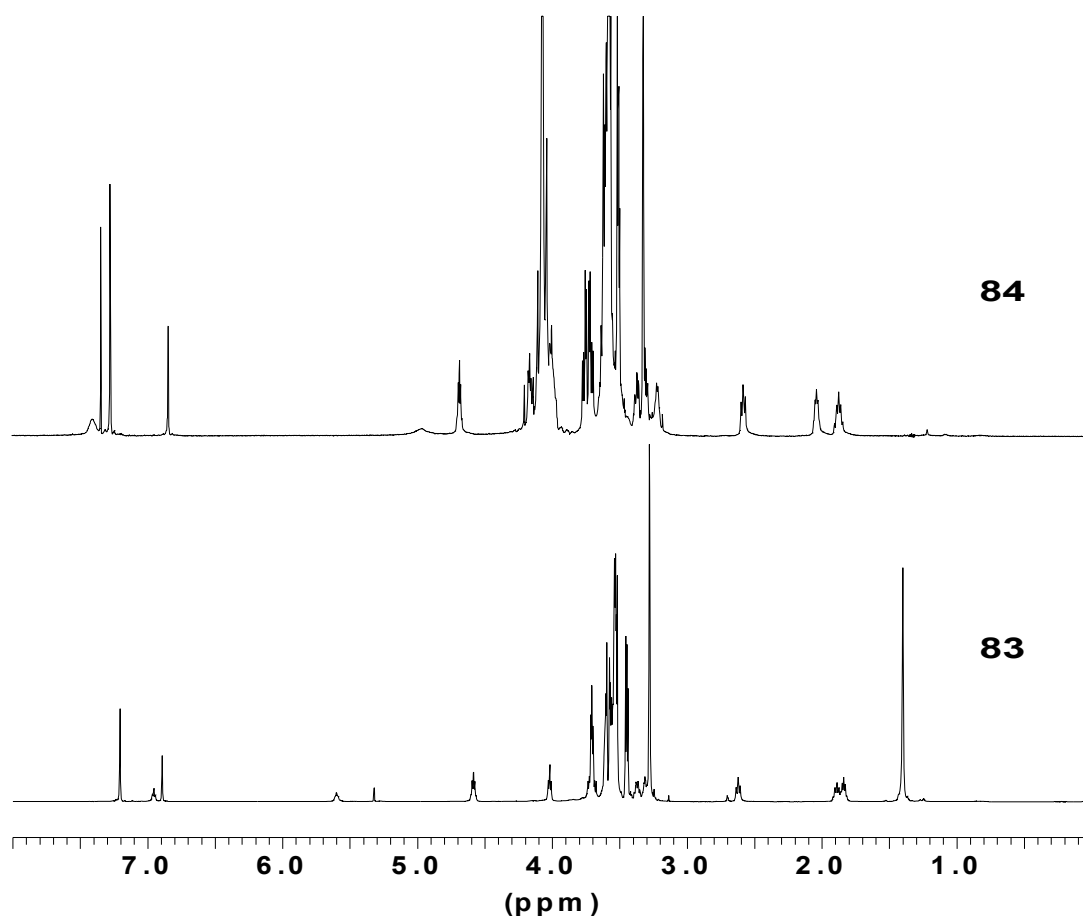
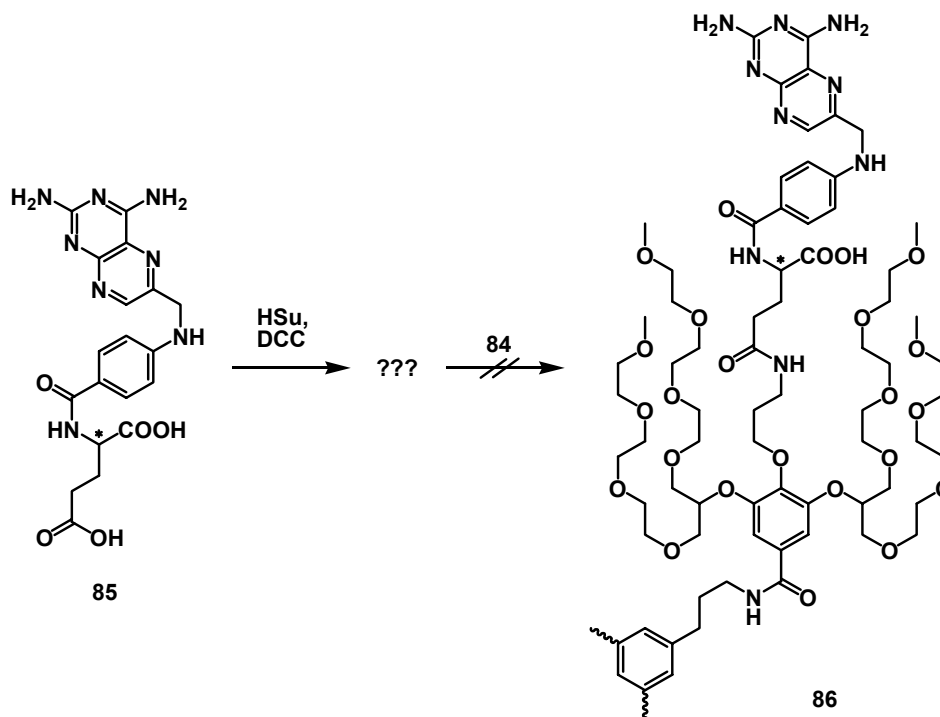


Fig. 29.  $^1\text{H-NMR}$  spectra of *N*-Boc protected **83** and deprotected **84** (500 MHz, for **83**:  $\text{CD}_2\text{Cl}_2$ ; for **84**:  $\text{d}^4$ -methanol &  $\text{CDCl}_3$ ).

The reaction of **85** with Hsu/ DCC in DMSO was supposed to generate the corresponding hydroxyl-succinimidyl ester.<sup>59-61, 145</sup> Since the solubility of the active ester was very low, neither its purification nor the determination of its relative amount in the raw material was possible.

A full reaction screening was done. Reaction temperature and dilution conditions varied. Different active esters were used and the excess of active ester on **84** was dramatically increased, but it was impossible to constructively influence the product distribution. The interpretation of the screening was based on MALDI-TOF MS. The obtained spectra were all very much alike and indicated the presence of *mono*- and *bis*-reacted by-products and the absence of **86**. This led to the conclusion that the

intramolecular reaction of the  $\alpha$ -carboxyl-group of a *mono*- or *bis*-reacted by-product is faster than the intermolecular reaction with another active ester.



Scheme 45. Synthesis of a G<sub>0</sub>-dendrimer with a targeting moiety.

The raw sample was partly soluble in THF and analyzed by GPC. The chromatogram led to the conclusion that at least two high-molecular weight fractions were obtained.

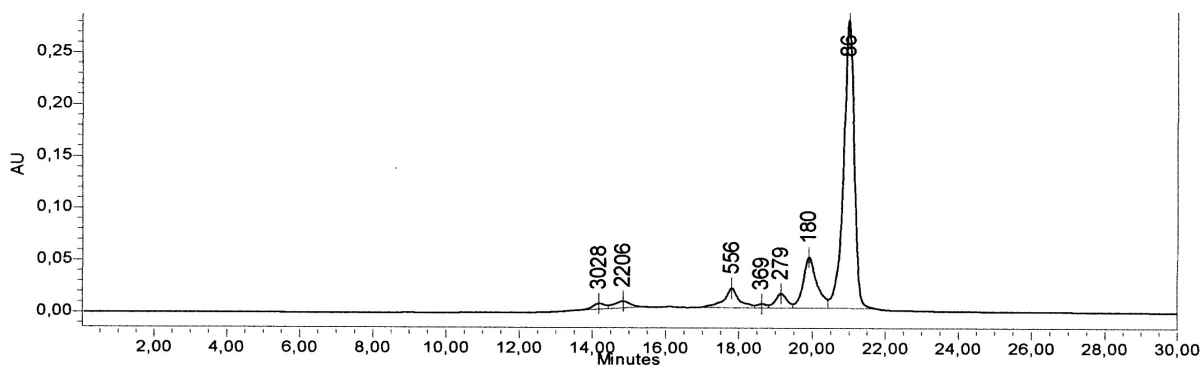


Fig. 30. GPC-chromatogram of the THF-soluble fraction of the raw **86**.

#### 4.4.2 Synthesis of “Capped” G<sub>1</sub>-Dendrons

Well-defined, non-ionic and water soluble G<sub>1</sub>-dendrimers, which display two contrasting surface-motifs, were accessible by functionalization of *tris*-orthogonal AB<sub>N</sub>B<sub>M</sub><sup>\*</sup>-branching units with “caps”. The synthetic principle here based on amide coupling chemistry and deprotection protocols. The reaction conditions were in

accordance with those described for the synthesis of G0-dendrimers and the best coupling results were obtained by the use of HOBt/ EDC as active ester reagent.

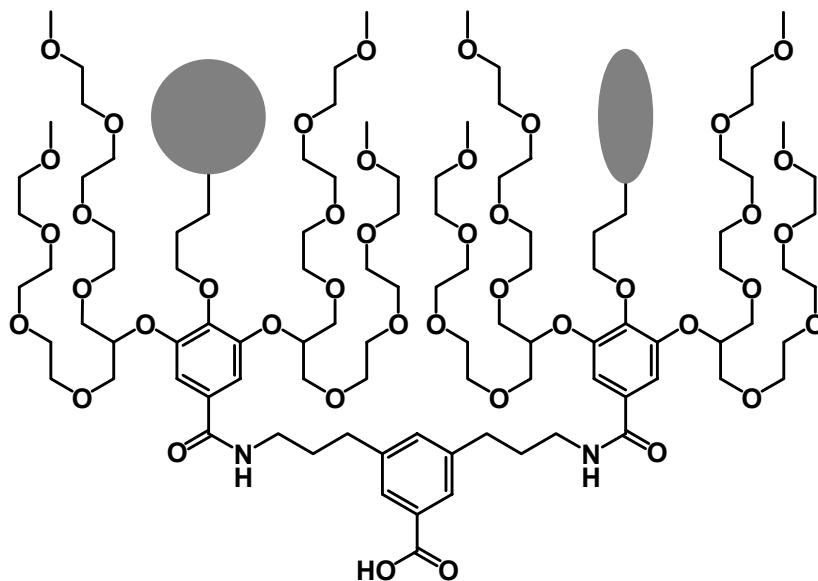


Fig. 31. G1-dendron with contrasting surface-motifs.

The synthesis of these “capped” G1-dendrons started from the mono-deprotected *tris*-orthogonal branching unit **19**. The synthesis of the G0-dendrimers required an excess of the active ester component to avoid unreacted by-products. However, the synthesis of half-covered dendrons demanded for a modification, because it was tedious to separate the mono-“capped” dendrons from the remaining excess of “caps” or the corresponding methyl esters with column chromatography or preparative GPC (Fig. 32).

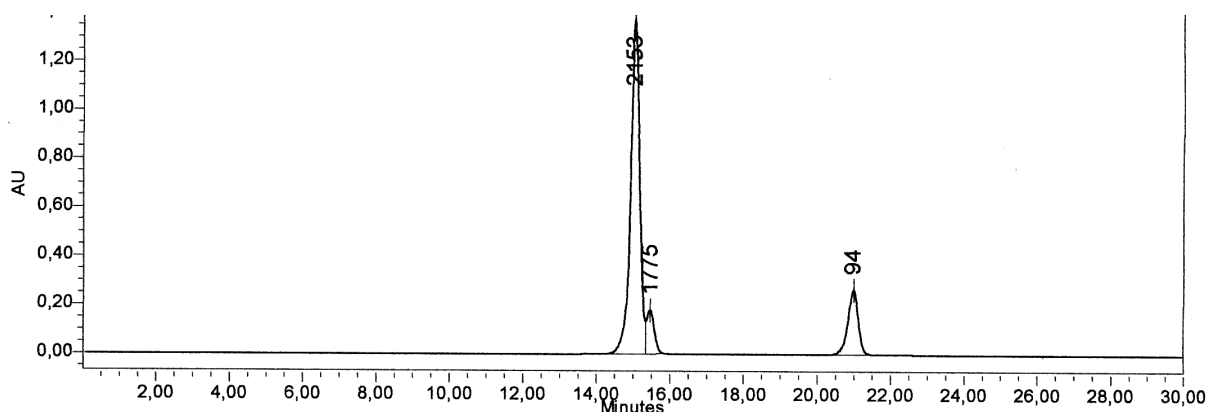


Fig. 32. GPC-chromatogram of the amido coupling with an excess of acid; synthesis of **87**.

The reaction of active ester with an excess of dendron **19** succeeded and gave pure mono-“capped” dendrons after purification with column chromatography (Fig. 33).

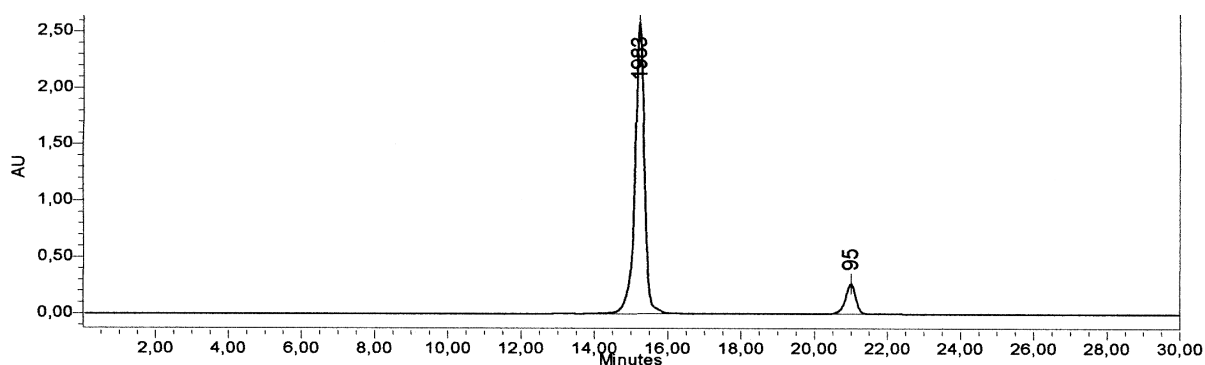
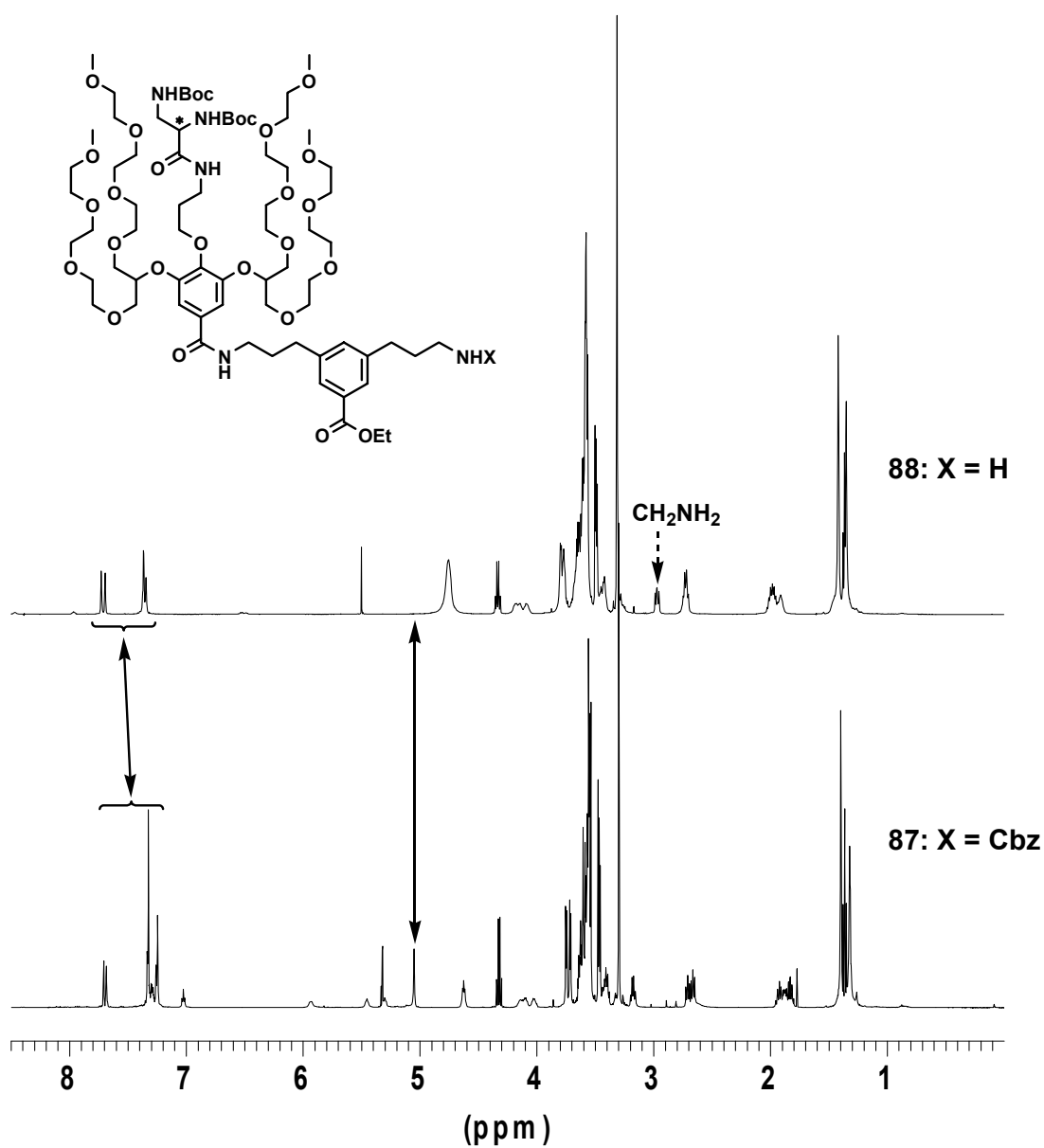


Fig. 33. GPC-chromatogram of the amido coupling with an excess of amine; synthesis of **89** (indicating 99% purity; ref. at 21 minutes: toluene).

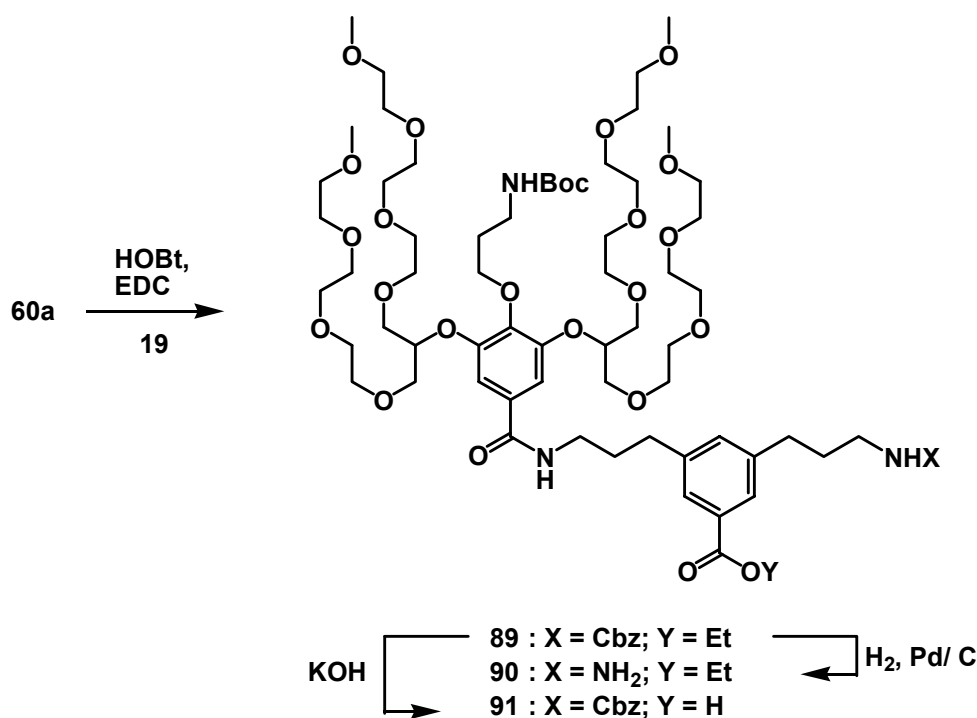


Scheme 46.  $^1\text{H}$ -NMR spectra of *N*-Cbz protected **87** and deprotected **88** (500 MHz, for **87**:  $\text{CD}_2\text{Cl}_2$ ; for **84**:  $\text{d}^4$ -methanol).



Dendron **87** contains a protected ethylene-diamine moiety and offered an *N*-Cbz protected amine for further functionalization.

**87** was converted to **88** by catalytic hydrogenation with Pd/ C. This deprotection proceeded within one hour in a hydrogen atmosphere. Since no other by-products were obtained, it was not necessary to purify **88** after filtration of the catalyst and removal of the solvent under high vacuum.

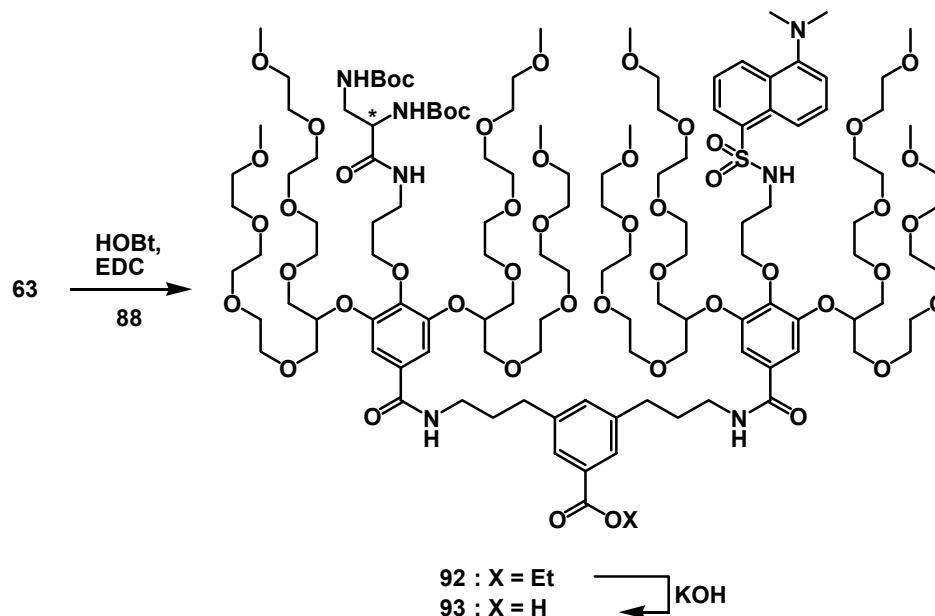


Scheme 47. Synthesis of dendron **89**.

The same coupling strategy was applied for the synthesis of dendron **89**. “Cap” **60a** was reacted with an excess of dendron **19**. After column chromatography **89** was isolated in almost quantitative yield. Cleavage of the *N*-Cbz protected amino synthon with catalytic hydrogenation gave dendron **90**. **89** was also converted by saponification with aqueous 1M KOH to give **91**. This compound was used for the synthesis of G1-dendrimers in a quasi mixed approach. Both deprotection protocols performed quantitatively, and further purification was not required.

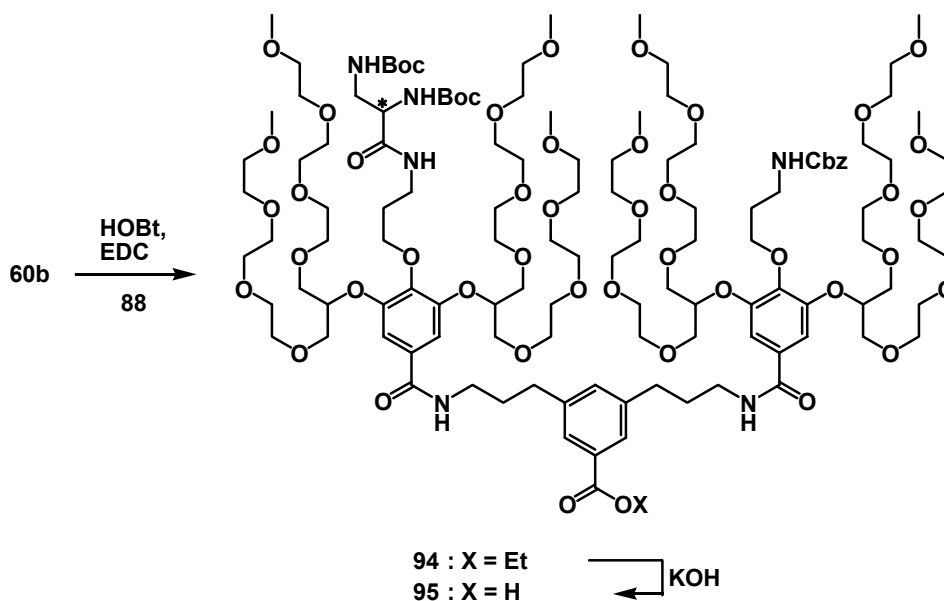
The free amine of the *mono*-capped dendrons **88** and **90** was used for the assembly with another “cap”. These *bis*-“capped” dendrons were obtained with standard amide coupling chemistry and employed HOBt/ EDC as active ester reagents. For separation reasons, the active esters were used in small excess.

**88** was used to synthesize dendrons, which additionally carried a fluorescence tag or an orthogonally protected amino-synthon. “Cap” **63** carried a dansylated fluorescence tag and its reaction with **88** gave **92** in 90% yield after separation with column chromatography.



Scheme 48. Synthesis of a “capped” G1-dendron with a fluorescence tag and an ethylene-diamine moiety.

The excess of **63** was recovered as methyl ester and reconverted to the acid by saponification.



Scheme 49. Synthesis of a “capped” G1-dendron with a protected binding-site and an ethylene-diamine moiety.

The same protocol allowed for the assembly of “cap” **60b** and **88** to synthesize **94**. This dendron offered an orthogonally protected amine for functionalization, and was isolated in 77% yield.

The  $^1\text{H-NMR}$ -spectra were still nicely resolved. The resonances were assignable by 2D- correlated NMR-spectroscopy, even if a differentiation of similar signals was sometimes not possible. The interpretation of the  $^{13}\text{C-NMR}$  spectra was more difficult, but the obtained resonances confirmed the expected structures. **92** and **94** were further characterized by MALDI-TOF MS and analytical GPC.

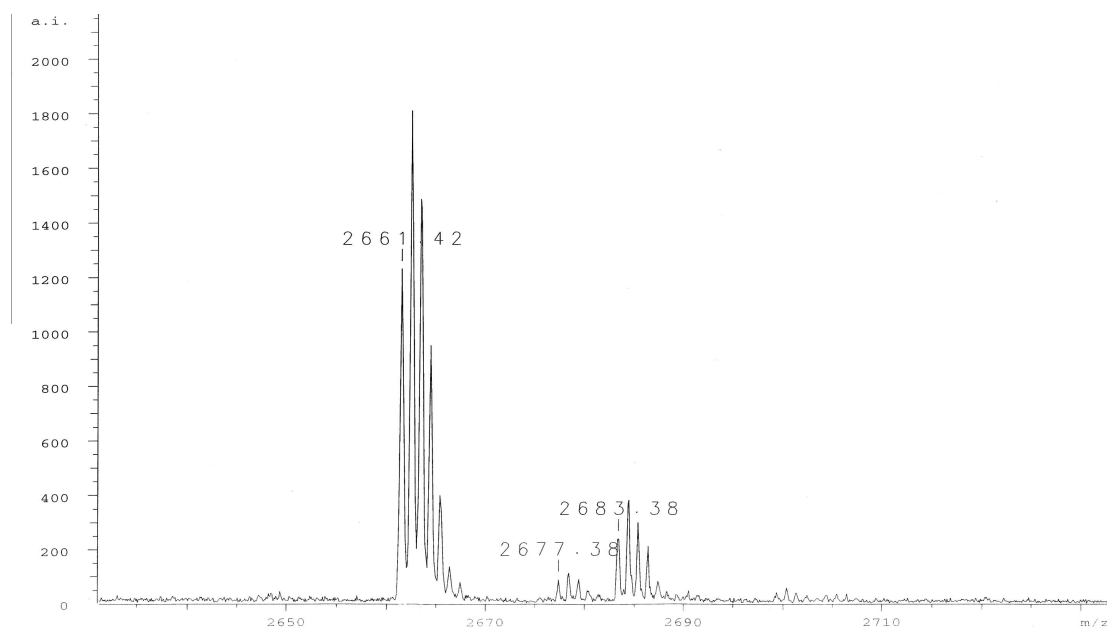


Fig. 34. MALDI-TOF mass spectrum (reflective mode) of **93**.

The ethyl esters of **92** and **94** were selectively addressed with the standard saponification protocol and gave **93** and **95**, respectively. The purity of these acids is representatively illustrated in the GPC-chromatogram of **95**.

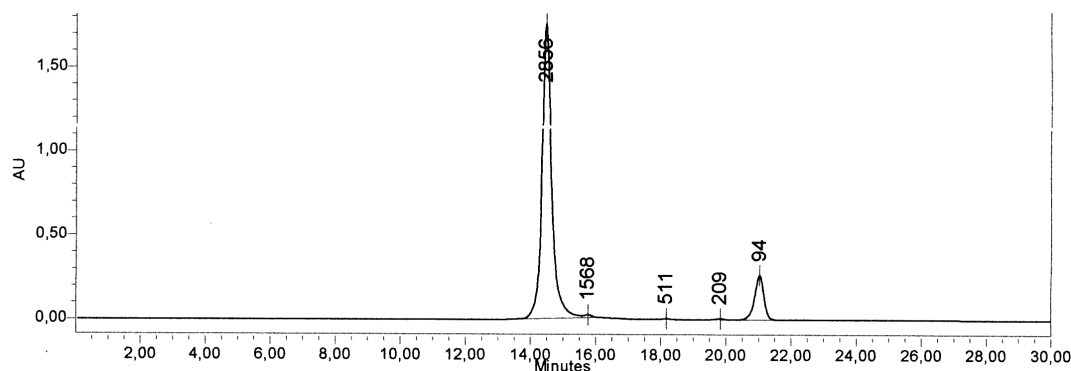
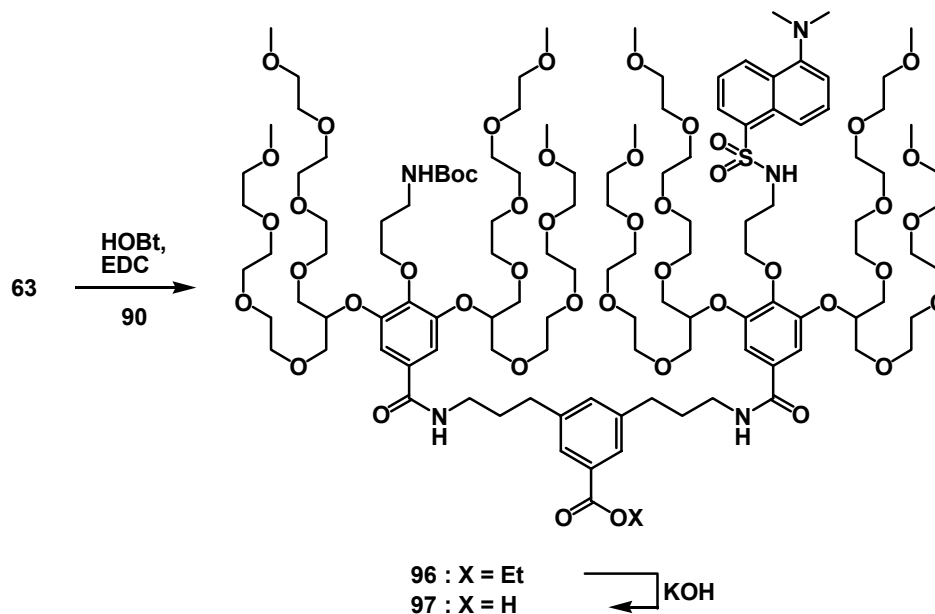


Fig. 35. GPC-chromatogram of **95** (indicating 99% purity; ref. at 21 minutes: toluene).

Another orthogonally equipped, *bis*-“capped” dendron was accessible via the functionalization of **90**. **63** was reacted with **90** and gave dendron **96** in almost quantitative yield (95%). The ester was again selectively addressable by saponification and provided **97**.



Scheme 50. Synthesis of a “capped” G1-dendron with a protected binding-site and a fluorescence tag.

Each of these three dendrons carried 24 ethylene glycol-repeating units and two contrasting motifs. Their benzoic acids allowed for assembly with a branching unit for the construction of a higher generation dendron or for the reaction with a core molecule to give the corresponding dendrimer. **93**, **95** and **97** were synthesized on a scale of several hundred milligram.

The synthesis of analogous *bis*-“capped” dendrons, which carry a protected malonic acid derivative, was unsuccessful. Therefore, G1-dendrimers with these moieties were prepared in a divergent or mixed approach.

### 4.4.3 Synthesis of “Capped” G1-Dendrimers

The envisaged “capped” G1-dendrimers with contrasting surface motifs (Fig. 36) were accessible by different approaches. The *bis*-functional peripheral pattern of these monodisperse OEGylated dendrimers was intended to carry combinations of bidentate ligands (malonates and ethylene-diamines), a fluorescence tag and a free binding-site for post-functionalization with, e.g. a targeting moiety.

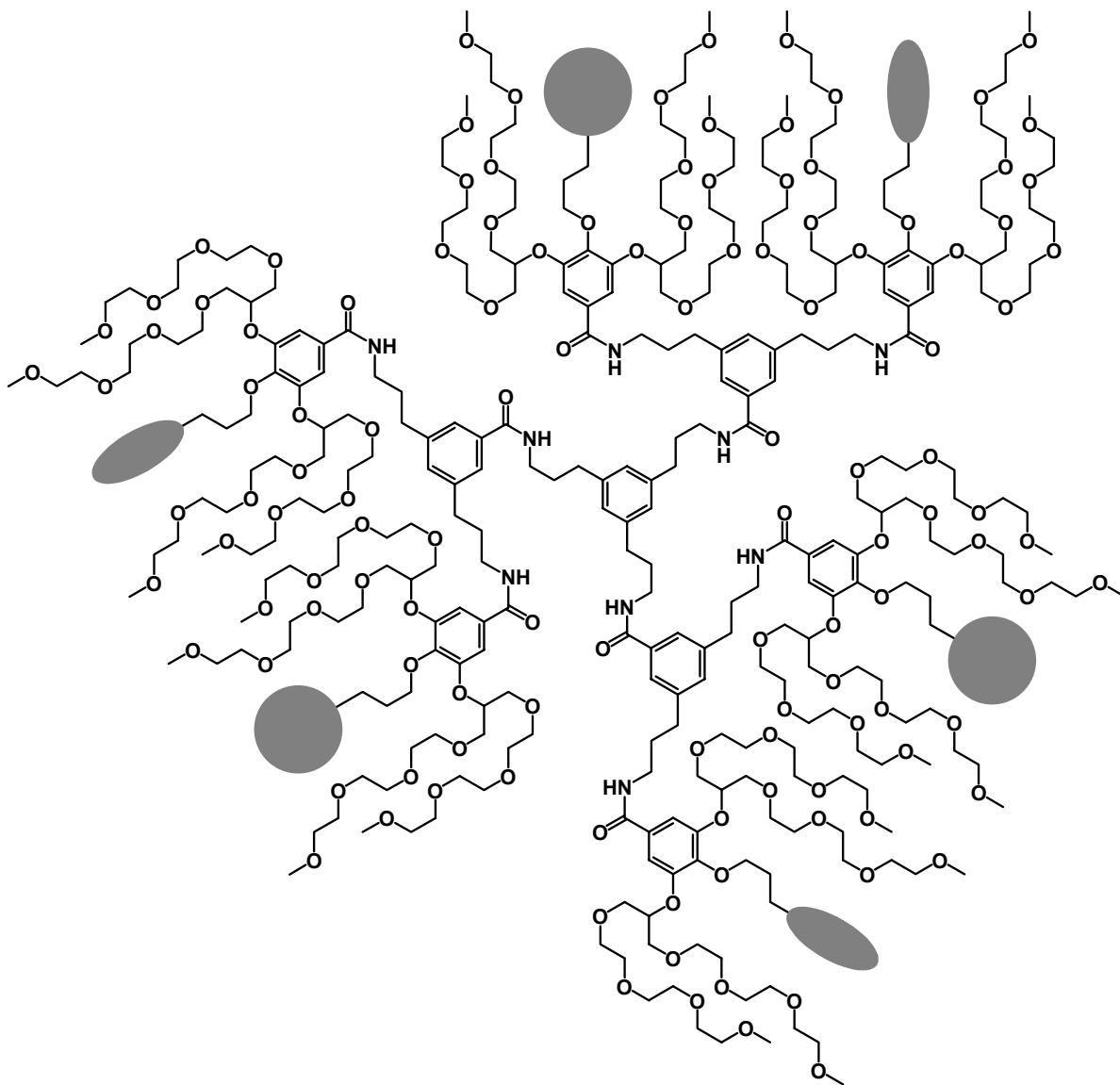


Fig. 36. Structure of the envisaged G1-dendrimers with contrasting surface-motifs.

These dendrimers carried 72 ethylene glycol repeating-units. The number of ethylene glycol repeating units is comparable to that of a linear PEG with a molecular weight of approximately 3100 Da.



The reaction of **93** with **3b** gave dendrimer **98** in excellent 84% yield. This indicated that the coupling efficiency per amide bond formation was higher than 94%. It was possible to purify this dendrimer with column chromatography with very polar solvent mixtures (usually methylene chloride/ methanol mixtures 10:1) and the excess of the dendron was recycled after saponification.

It was possible to assign the majority of the proton resonances with 2D- homo-nuclear correlated NMR-spectroscopy ( $^1\text{H}$ - $^1\text{H}$  COSY). However, it would have taken too much time for the assignment of the carbons by hetero-nuclear correlated methods. The GPC showed a near-monodisperse peak but underestimated the molecular weight. This was not too surprising, since this measurement is calibrated with PS standards. MALDI-TOF measurements in reflective mode were impossible, but the linear mode indicated the molecular weight peak of the sodium salt.

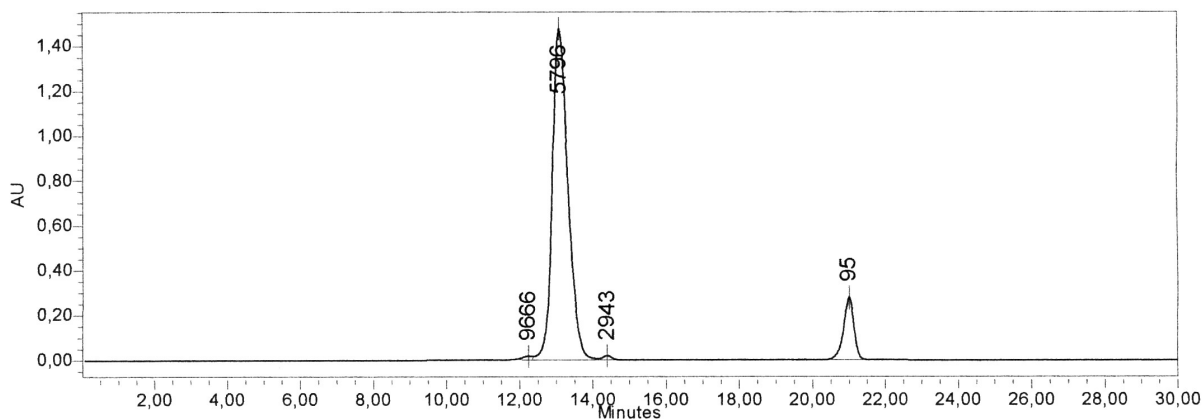


Fig. 37. GPC-chromatogram of **98** (indicating 99% purity; ref. at 21 minutes: toluene).

The deprotected dendrimer **99** was obtained after treatment of **98** with a large excess of TFA in methylene chloride. The resonance for the *tert*-butyl group was used as reference for monitoring of the deprotection procedure with  $^1\text{H}$ -NMR. The reaction time for the cleavage of all *N*-Boc groups was very long. The characterization of the deprotected dendrimer **99** was based on spectroscopic and spectrometric data of standard methods.

This dendrimer possessed three deprotected ethylene-diamine moieties with potential for platinum complexation and its fluorescence dansyl-labels should allow for studying cellular uptake. The molecular weight of **99** (7653 Dalton) is very high for such a low generation dendrimer.

Another G1-dendrimer with an ethylene-diamine moiety was synthesized by the reaction of dendron **95** with **3b**. **100** was gained in excellent yields and offered a





The *N*-Boc group is superior to the *N*-Cbz group, because the removal of the *N*-Cbz group by catalytic hydrogenation does not work in the presence of the dansyl group. Both protective groups can be cleaved with an excess of TFA, but the removal of the *N*-Boc group performs much faster and at milder reaction conditions.

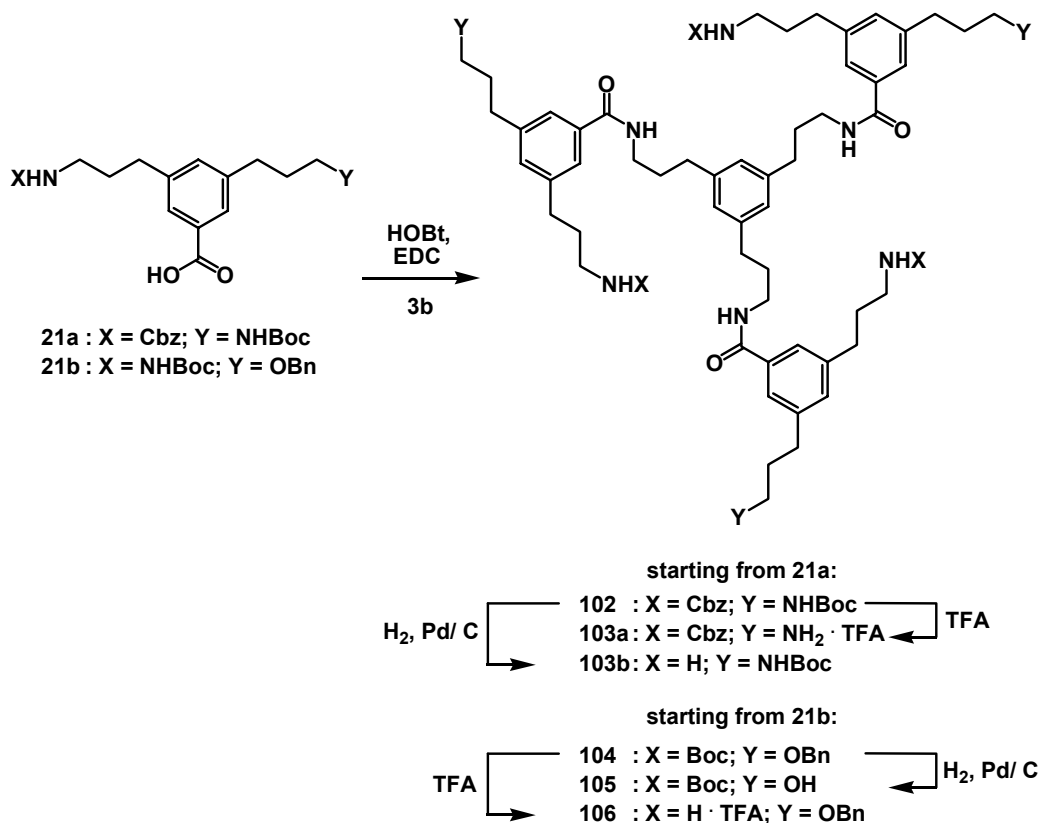
This protected amine in **100** and **101** was intended for a linkage to folic acid. However, the model reactions on the G0-dendrimer indicated that the amide coupling for folic acid is of low preparative value for dendrimers which possess a larger number of peripheral amines.

#### 4.4.3.2 Synthesis of G1-Dendrimers with Contrasting Surface-Motifs via Divergent and Mixed Approach

The convergent synthesis of “capped” dendrons with a malonic acid derivative was limited by the weak orthogonality of the branching unit towards more than one ester. The divergent protocol was supposed to make the intended *bis*-“capped” dendrimers with malonic acid moieties accessible. Divergent syntheses of G1-dendrimers are usually not restricted by sterical stress during the coupling procedure. Since the applied coupling and deprotection protocols worked almost quantitatively for the related convergent synthesis, it was reasonable to try this approach.

The assembly of **21a** with **3b** yielded dendrimer **102**, which was already synthesized by Fuchs. This dendrimer offered orthogonally protected amines for chemically stable surface-functionalization via amide linkages. The deprotection of the *N*-Boc groups of **102** gave the partially deprotected dendrimer **103a**. The free amines were to be covered prior to deprotection of the *N*-Cbz groups. It was neither possible to verify directly that the acidic deprotection conditions did not affect the *N*-Cbz group nor to purify the compound. Comparable reactions on G1-dendrons showed that the acidic deprotection partially affected the *N*-Cbz group. Amido coupling reactions on this dendrimer (divergent synthesis of **107**, p. 88) showed impurities that may have arisen from the lack of orthogonality in the deprotection procedure with TFA. This reduced the preparative value of this strategy.

However, a change in the deprotection strategy allowed for the divergent construction of such dendrimers. The deprotection of the *N*-Cbz groups of **102** by catalytic hydrogenation performed without affecting the *N*-Boc groups and gave **103b**. The deprotected amines were then used for further divergent functionalization.



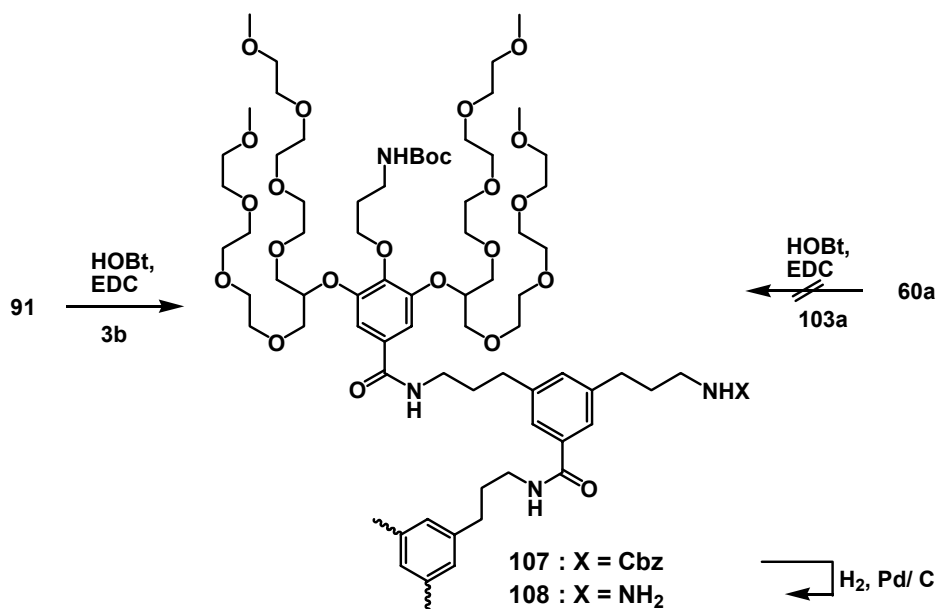
Scheme 54. Synthesis of G1-dendrimers with orthogonally protected synthons.

**104** was obtained from the reaction of **3b** with dendron **21b**. This dendrimer was intended to potentially allow for the divergent surface-functionalization with ester- and amide-linkages. Under physiological conditions an amide-linkage is much more stable than an ester-linkage and would possibly allow for a specific degradation. Both synthons were selectively addressed and quantitatively deprotected. Dendrimer **105** was obtained after catalytic hydrogenation of the benzyl-ether and the *N*-Boc group of **104** was cleaved with TFA and gave **106**.<sup>VIII</sup>

The reaction of “cap” **60a** and **103a** gave **107**, but its purification was tedious. It was not possible to separate the by-products with a higher substitution pattern, with column chromatography. Alternatively, **107** was synthesized in a mixed approach. The assembly of **91** with **3b** made **107** easily accessible after purification with column chromatography. **91** was obtained from **19** (Scheme 47, p. 78) which was also accessible by the deprotection of an *N*-Boc group with TFA in the presence of an *N*-Cbz group (Scheme 21, p. 47). This deprotection protocol also affected the *N*-Cbz

<sup>VIII</sup> I would like to thank Anke Roth who worked on the synthesis of *tris*-orthogonally protected dendrons and the synthesis of the dendrimers **104-106** during her “Forschungspraktikum”.

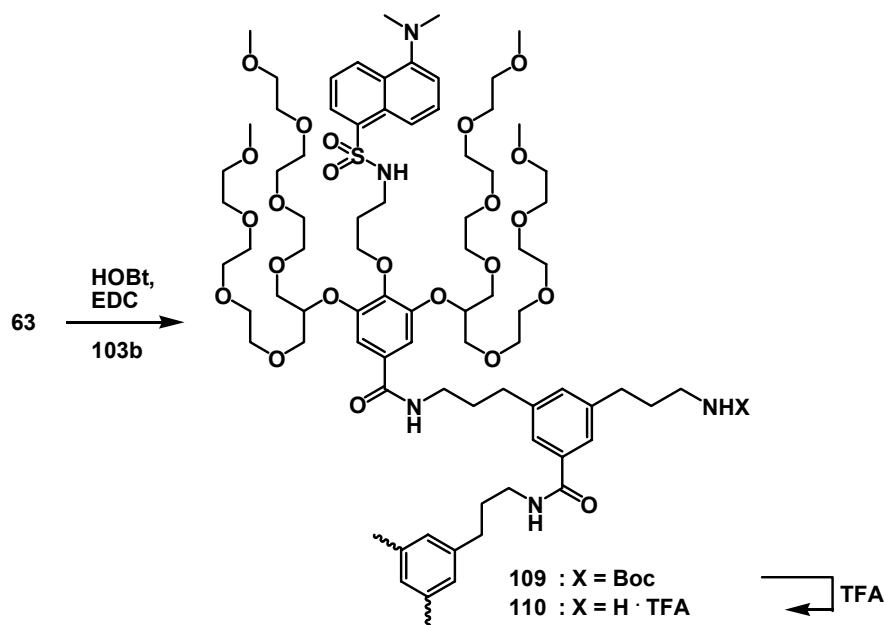
group. These *bis*-deprotected by-product was much more polar and was easily removed by standard column chromatography. The purification of **103a** should, in general, also benefit from this difference in polarity. However, the very high polarity of these *tris*-amines made purification with standard column chromatography impracticable.



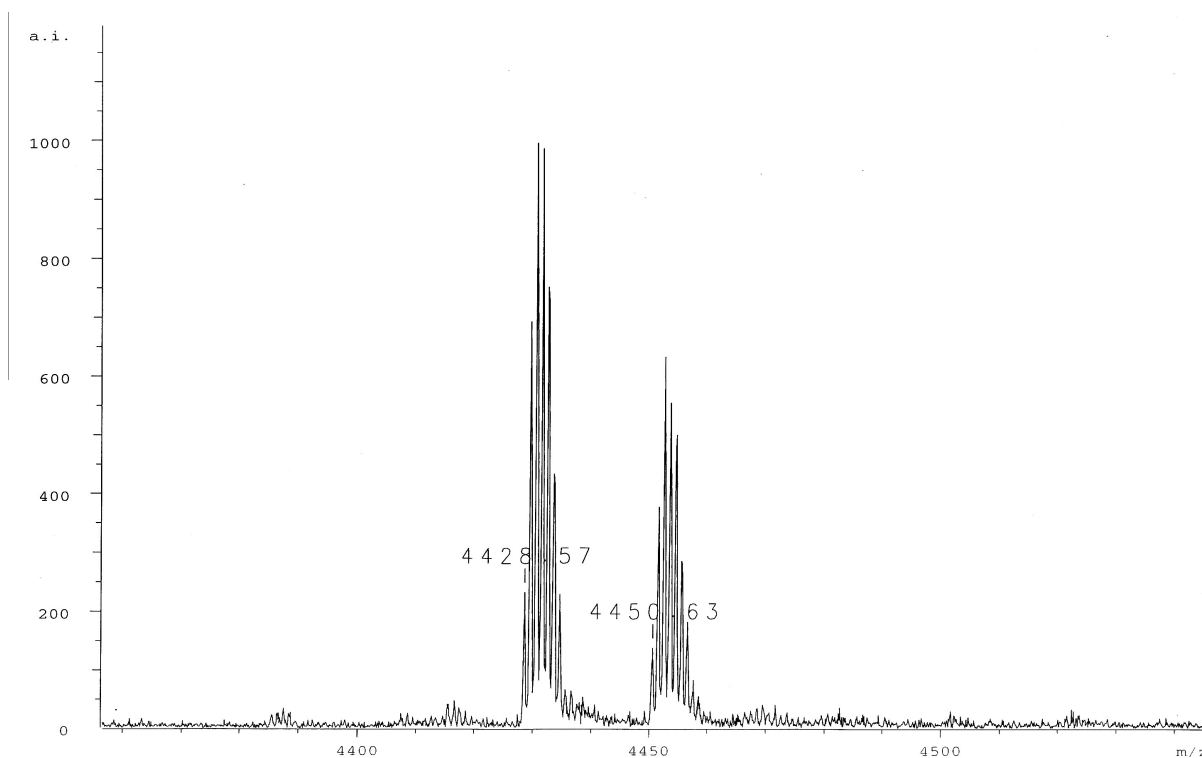
Scheme 55. Divergent and mixed approach towards the synthesis of **107**.

**108** was gained by the catalytic hydrogenation of the *N*-Cbz group of **107**. The free amines enabled further divergent functionalization.

The synthesis of a G1-dendrimer with a malonic acid moiety and a fluorescence tag was also achieved in a divergent protocol. Initially, a fluorescence tag was introduced to the dendrimer. After purification with column chromatography **109** was obtained almost quantitatively from the reaction of **103b** with **63**.

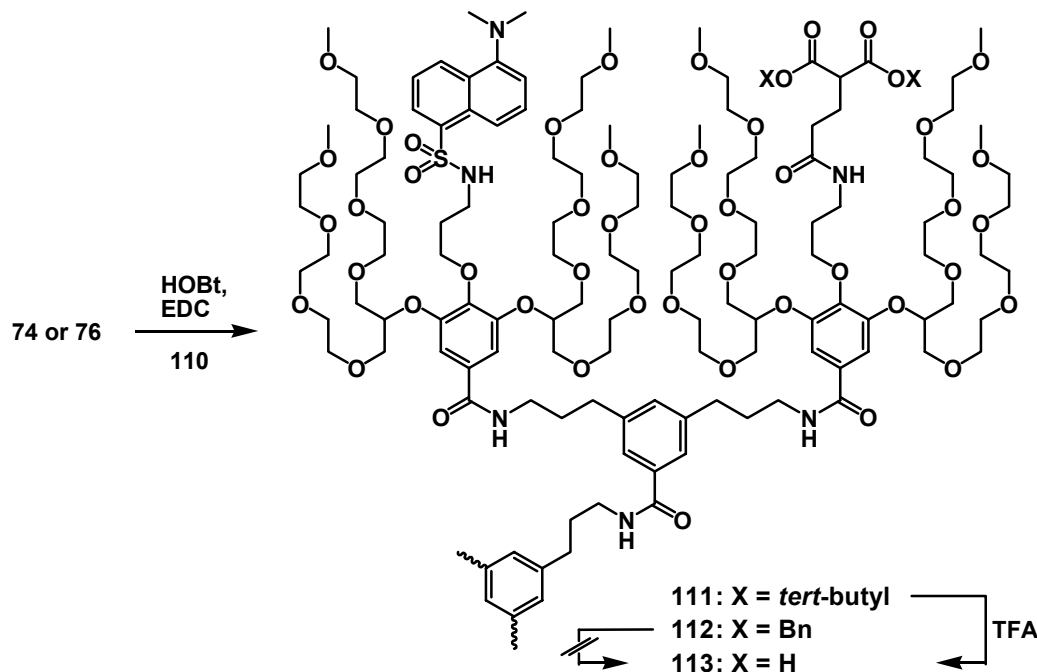
Scheme 56. Divergent synthesis of **109**.

The deprotection of the *N*-Boc groups easily proceeded with an excess of TFA in methylene chloride and gave **110** without further purification.

Fig. 38. MALDI-TOF mass spectrum (reflective mode) of **110**.

Both **74** and **76** were reacted with the *mono*-“capped” **110** and gave the corresponding dendrimer **111** and **112** in good to excellent yields. Initially, the reaction was carried out in methylene chloride to be able to recover the excess of the

“caps” (in accordance with the synthesis of **79** and **80**, chapter 4.4.1). The separation of the dendrimers and **74/ 76** with column chromatography was tedious. Therefore, the excess of active ester was scavenged with methanol to give the corresponding methyl esters.



Scheme 57. Synthesis of a “capped” G1-dendrimer with a fluorescence tag and a malonic acid moiety.

These were much easier to separate from the dendrimer, but it was not possible to reconvert them into **74/ 76**.

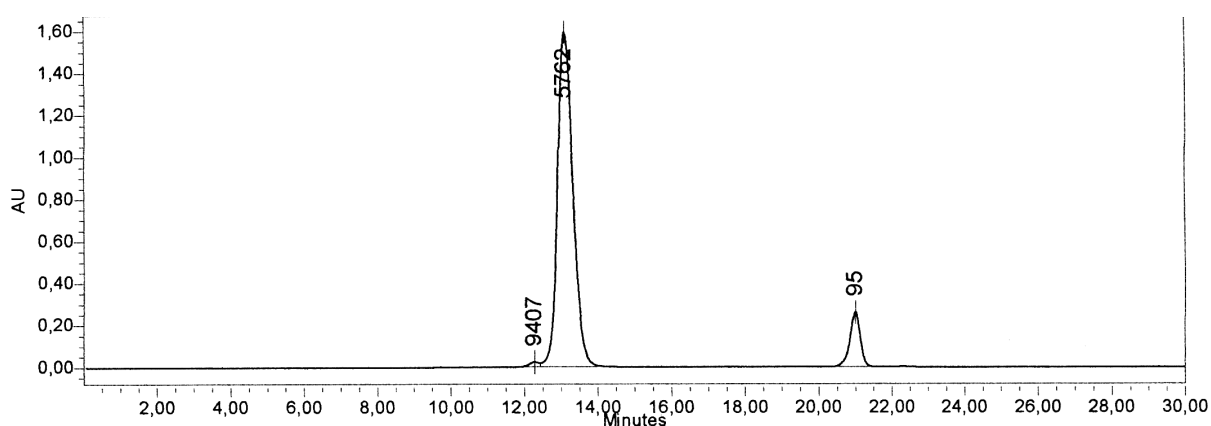


Fig. 39. GPC-chromatogram of **111** (indicating 99% purity; ref. at 21 minutes: toluene).

Dendrimer **113**, which provides free malonic acids with potential for platinum complexation, was obtained via deprotection of **111** with TFA in methylene chloride.

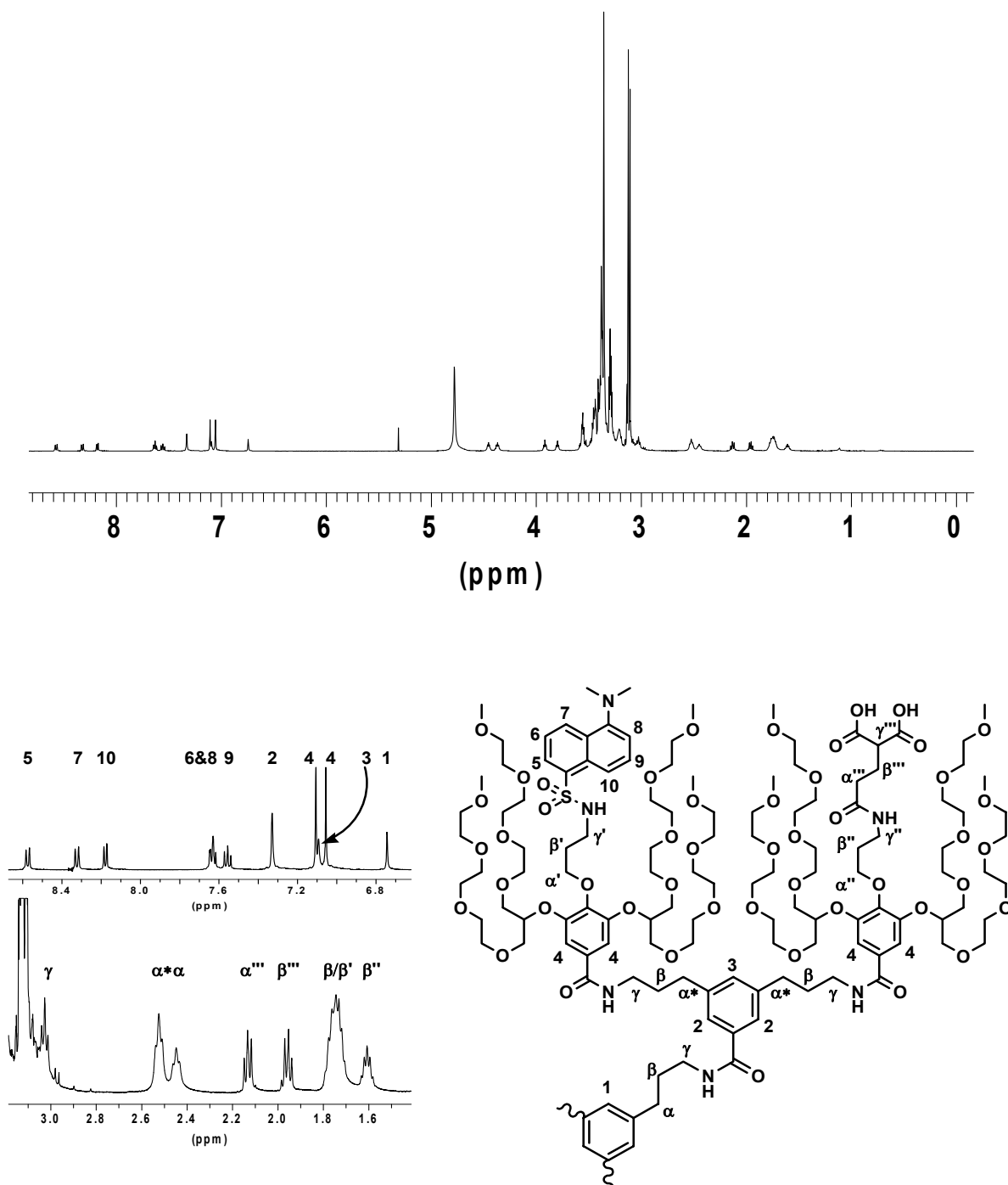


Fig. 40.  $^1\text{H-NMR}$  spectrum (500 MHz,  $d^4$ -methanol) of **113**.

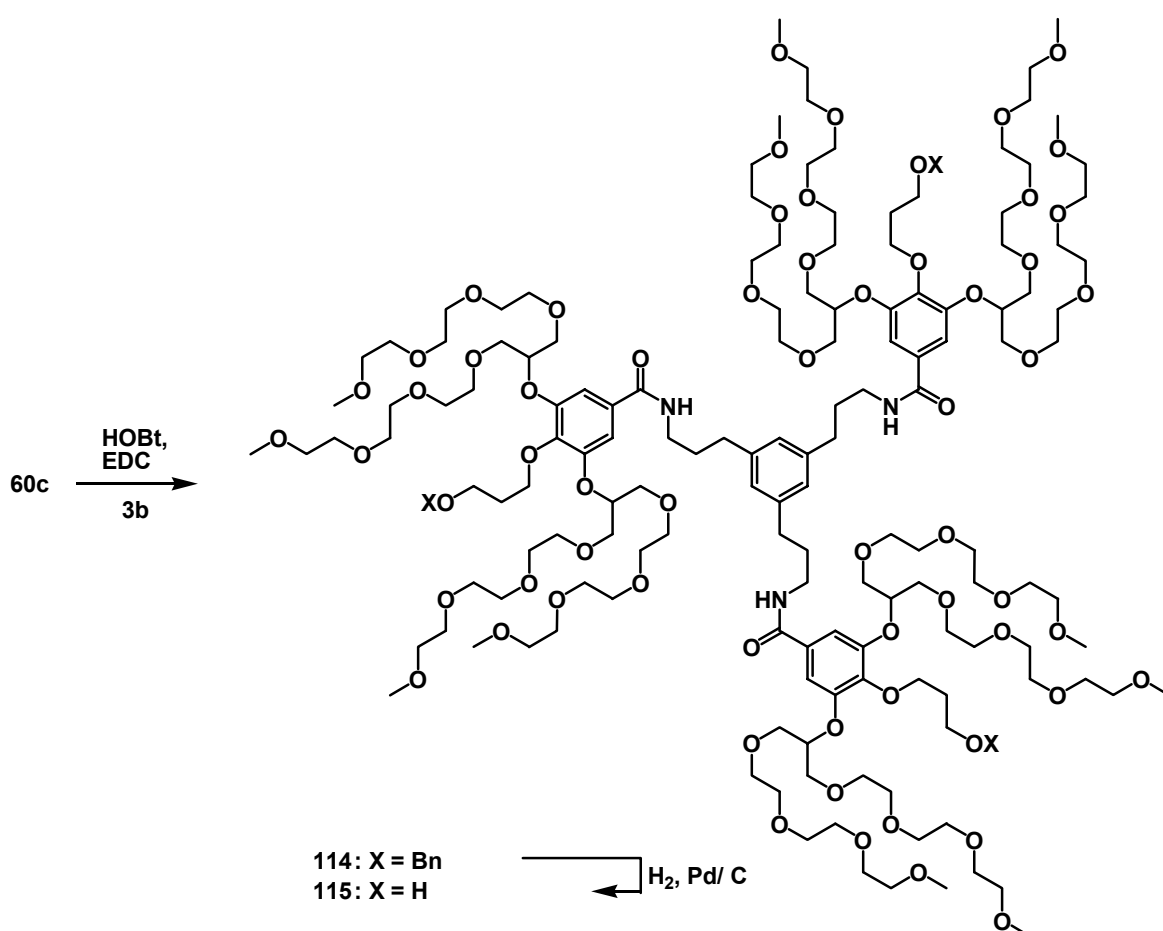
The progress of the cleavage of the *tert*-butyl esters was conveniently monitored with  $^1\text{H-NMR}$  spectroscopy. After the resonance for the *tert*-butyl ester had completely disappeared, the excess of TFA was removed by co-evaporation with methylene chloride and gave the pure dendrimer **113** without further work-up. It was not possible to deprotect the benzyl esters of **112** to gain **113**. The typical deprotection protocol with Pd/ C in a hydrogen atmosphere did not affect the benzyl-esters at all.

Attempts to optimize this reaction by increasing the temperature, the hydrogen pressure, or by using different solvents, did not succeed. A reasonable explanation towards this dilemma is that the sulfur in the dansyl-label may have poisoned the palladium catalyst and, consequently, has prevented the deprotection.

#### 4.4.4 Dendrimers with a pH-Responsive Interface

A site-specific delivery process includes the controlled release of drugs from the conjugate at the desired site of action. A selective liberation of drugs from a carrier can be achieved by the introduction of a labile spacer between carrier and drug.

Among acid-responsive spacers ortho esters have attracted particular attention. Szoka and coworkers synthesized PEG-lipid conjugates that were linked with diortho ester moieties.<sup>184</sup> These were stable for more than 3 hours under physiological conditions (37°C, pH ≈ 7.0) and degraded completely within one hour at pH 5. This very promising spacer-class was reported to be accessible via several approaches.



Scheme 58. Synthesis of G<sub>0</sub>-dendrimers for the assembly with a pH-responsive interface.

Originally, ortho esters were used as protective groups for carbonyl compounds. They were among the few derivatives that were not affected by the attack of strong nucleophiles such as Grignard reagents.<sup>185</sup> Their stability increases as they become



more constrained, and cyclic ortho esters are more readily cleaved by acidic hydrolysis than acetals or ketals.

The strategy for the synthesis of a dendrimer with an acid-labile ortho ester interface was based on the assembly of primary alcohols. These were supposed to be provided by the dendrimer and a building block that bears a 1,3-diol moiety. **115** (Scheme 58) possessed propanol binding-sites and was used to study these esterification reactions.

**112** was obtained from the amido-coupling reaction of the acid **60c** and the core **3b** under standard conditions. It was then converted to **115** by catalytic hydrogenation with Pd/ C as catalyst.

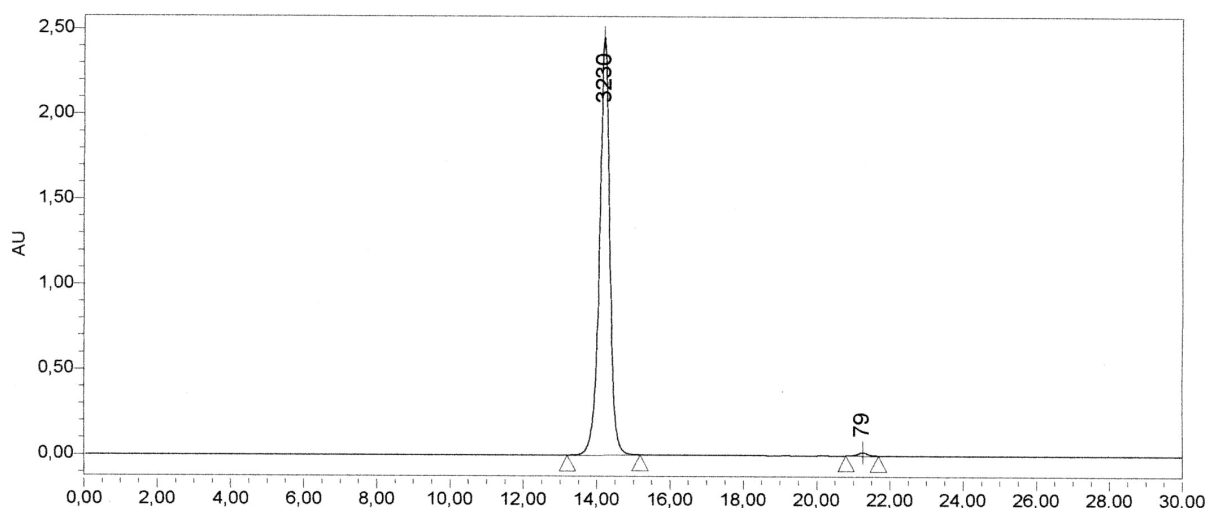
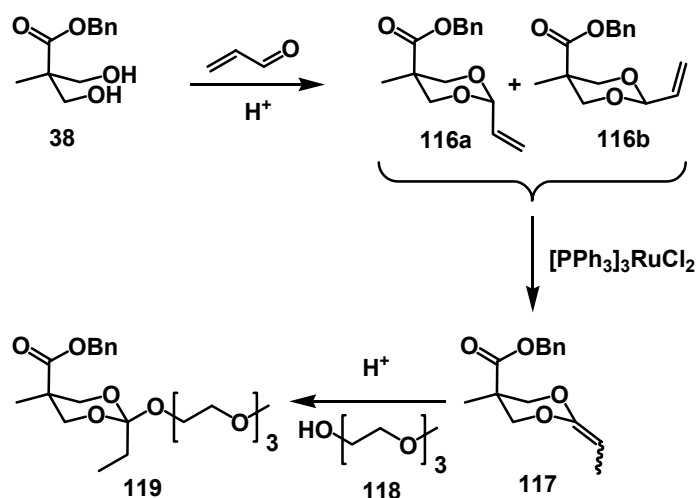


Fig. 41. GPC-chromatogram of **115** (indicating 99% purity; ref. at 21 minutes: toluene).

Two model reactions were considered to be appropriate protocols to learn more about the efficiency of ortho esterifications. The first approach to form an ortho ester was based on the addition of an alcohol to a ketene acetal (Scheme 59). The synthesis of ketene acetals is typically described to be difficult and impracticable. However, Crivello and coworkers published a protocol for the isomerization of vinyl-acetals to give ketene acetals in the presence of a ruthenium catalyst.<sup>186, 187</sup> Their protocol made a large number of ketene acetal monomers accessible. The mechanism for this rearrangement was not discussed in detail. However, the driving force can be assigned to the increased resonance interaction between the double bond and the lone-pair of the ether oxygen. In addition, the transformation of a terminal to an internal double bond increases the thermodynamic stability.

Such vinyl-acetals were obtained from the reaction of **38** with acrolein. A mixture of the two configurational isomers **116a/b**, which were easy to separate with column chromatography, was gained in good yields.



Scheme 59. Model reaction for the synthesis of an ortho ester via ketene acetal intermediate.

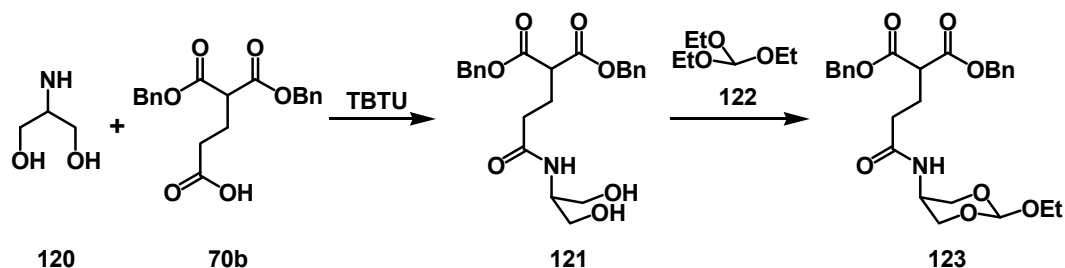
Both compounds were treated separately with [PPh<sub>3</sub>]<sub>3</sub>RuCl<sub>2</sub>, but the conversion to **117** was not as straight forward as described. The rearrangement was monitored by <sup>1</sup>H-NMR spectroscopy and the number of unassignable resonances increased with the reaction time. In a reaction screening, the amount of catalyst, the temperature and the reaction time were varied. A complete isomerization was still not achieved, and it was not possible to suppress the formation of side-products. Since it was impossible to purify the ketene acetal, the raw mixture was scavenged with **118**. The typical carbon resonance for an ortho ester (between  $\delta = 110$  to  $120$  ppm) was not observed from <sup>13</sup>C-NMR. Therefore, it was concluded that **119** was not formed.

The second approach towards ortho esters was based on a transesterification reaction. This protocol used catalytic amounts of concentrated sulfuric acid to obtain alkoxy-dioxolanes from the reaction of a diol with commercially available **122**.<sup>IX</sup>

**120** (serinol) was reacted with the malonic acid derivative **70b** under standard amide coupling conditions and gave **121** in good yields (Scheme 60). The best results for

<sup>IX</sup> I am very grateful to Carsten Winterboer who worked on the synthesis of acid-responsive interfaces in his "Forschungspraktikum" and supported this part of my research.

these couplings were obtained with TBTU as active ester reagent. The yields decreased dramatically with other active ester reagents (HOBt/EDC or HSu/DCC).



Scheme 60. Model reaction for the synthesis of an ortho ester by employing a transesterification procedure.

**121** was a suitable model compound to study the transesterification, because it possessed a protected bidentate ligand and a 1,3-diol. It was, however, not possible to control this reaction and to isolate **123**. The high number of by-products, which were detected by TLC and HPLC, clearly indicated that this method had a low preparative value. In another transesterification step, **123** was intended to react with **115** (Scheme 58, p. 93) to link the bidentate ligand via the pH-responsive ortho ester to the macromolecule. The lack of accessibility of **123** invalidated this strategy.

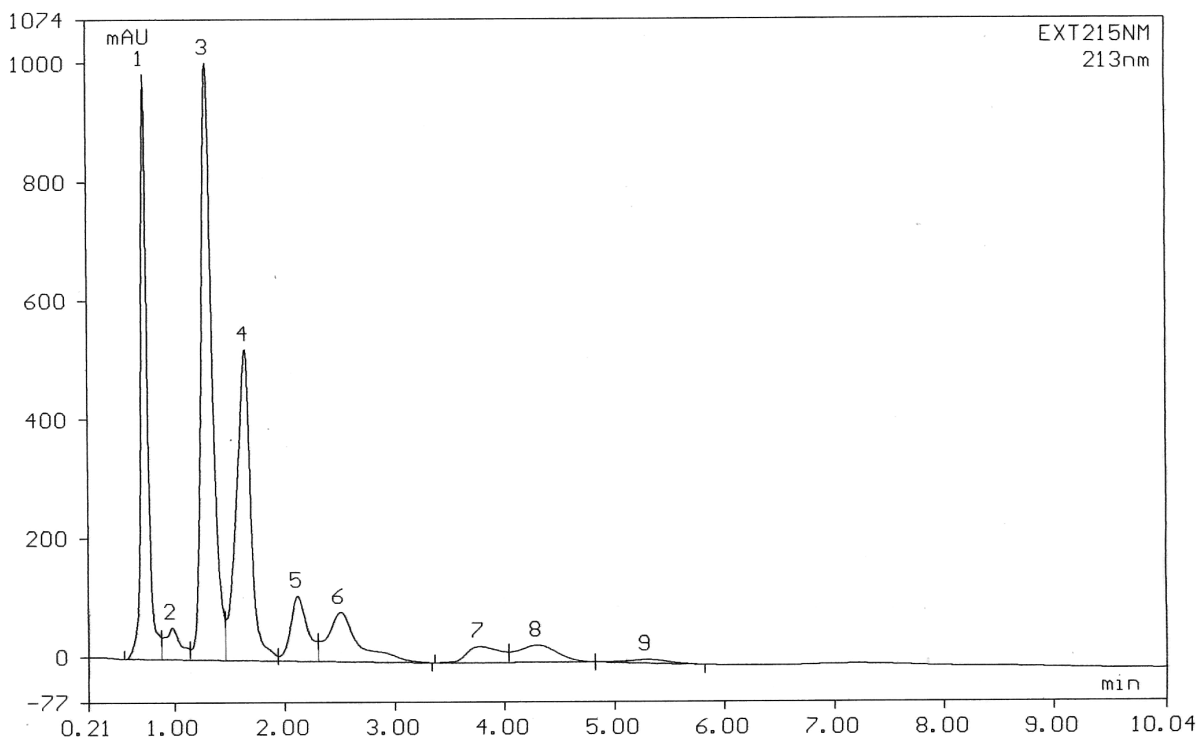


Fig. 42. RP-HPLC-chromatogram of **123**.

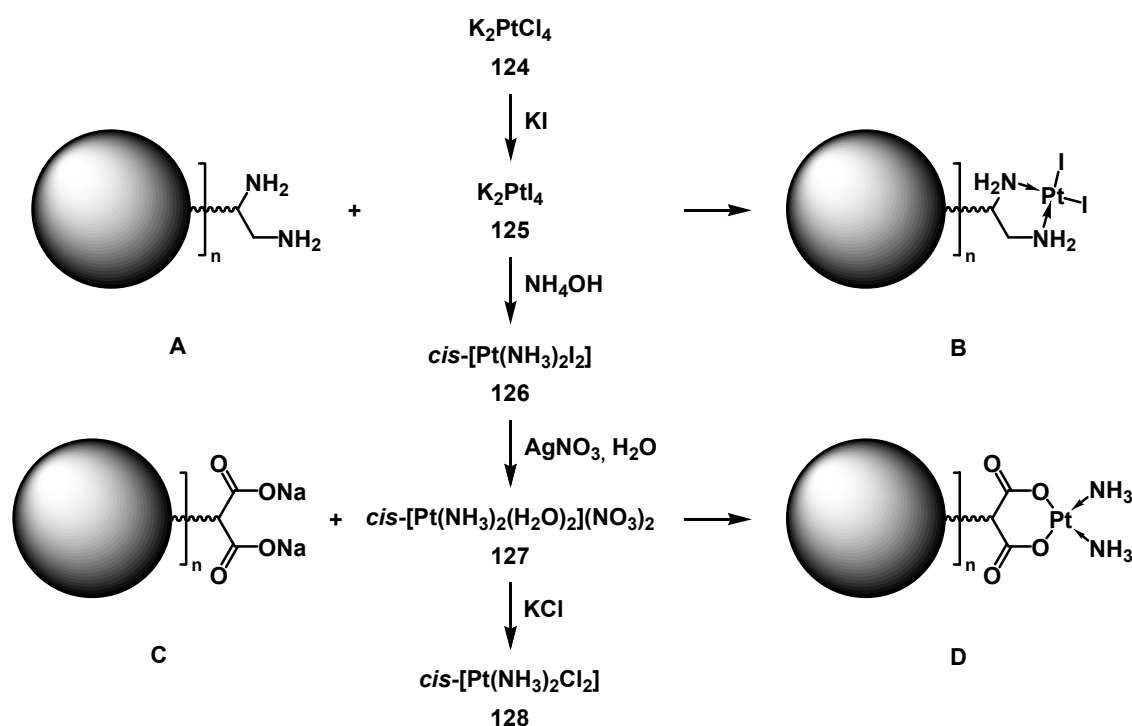
The objective to design pH-responsive interfaces based on ortho esters was unsuccessful. However, the initial idea to integrate a systematic drug release junction

was approached by the synthesis of dendrimers **81** (Scheme 42, p. 69) and **113** (Scheme 57, p. 90) with free malonic acids for platinum complexation. These bidentate ligands have the potential to chelate  $\text{Pt}^{2+}$  and still possess release mechanisms for the metal ion by hydrolysis.

#### 4.4.5 Dendrimer-Platinum Conjugates

The herein reported accessibility of dendrimers with free binding-sites offered the opportunity to study their ability to form complexes with platinum. Bidentate ligands (diamino propionic acid- or malonic acid-moieties) have great potential for platinum complexation, because their chelating binding-structure can force the metal-ion into *cis*-geometry.

The synthesis of such platinum complexes required the preparation of suitable precursors. Dhara reported an optimized protocol for the synthesis of *cis*-[Pt(NH<sub>3</sub>)<sub>2</sub>Cl<sub>2</sub>] by initial formation of **126**.<sup>188</sup> This procedure uses the *trans*-effect of ligands in square-planar platinum-complexes<sup>X</sup>.



Scheme 61. Synthesis of platinum precursor for the assembly with bidentate ligands.

At first, **124** was converted to its iodo-analogue **125**. Iodide is a much stronger  $\sigma$ -base than chloride and even more than ammonia. Therefore, **125** can better direct

<sup>X</sup> *Trans*-effect: This effect occurs in square-planar complexes. It describes the influence of ligands X on the acceleration of the substitution of their *trans*-ligands. The effect increases for ligands X, which are good  $\sigma$ -donors or  $\pi$ -acceptors. The acceleration is associated to the increasing overlap-integrals of ligand and Pt and can be correlated to the nucleophilicity of the entrance-group as well as to the stability of the leaving-group.



indicated that the first fraction contained the dendrimer. Since platinum complexes with *cis*-configuration show UV-absorption at 200-210 nm, the shoulder at 204 nm can be understood as an indication for such a complex. However, some aromatic compounds have comparable absorption behavior in polar solvents as well. Therefore, the assignment of this absorption is very speculative.

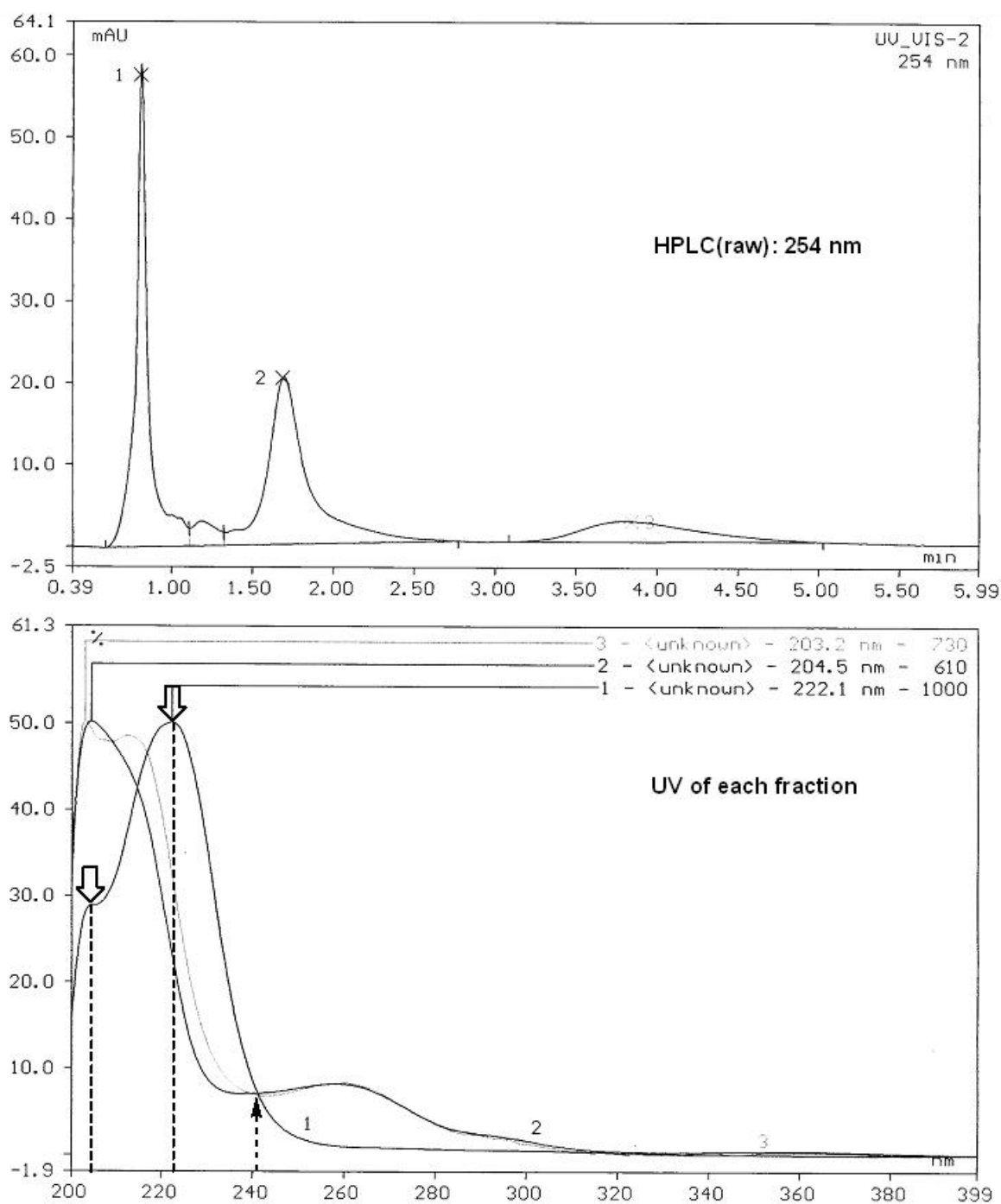


Fig. 43. HPLC-chromatogram of raw dendrimer-platinite and UV-spectrum of each fraction.

The determination of the purity of the first fraction was done by comparing the analytical HPLC-chromatograms at different wave-lengths. With detection at 230 nm, the purity of the sample increased from 82% for the raw mixture to 95% after separation with RP-HPLC (Fig. 44). It was clearly indicated that the relative concentration of the sample increased. The absolute values are rather doubtful, because the UV-absorptions differ very much at this wave-length.

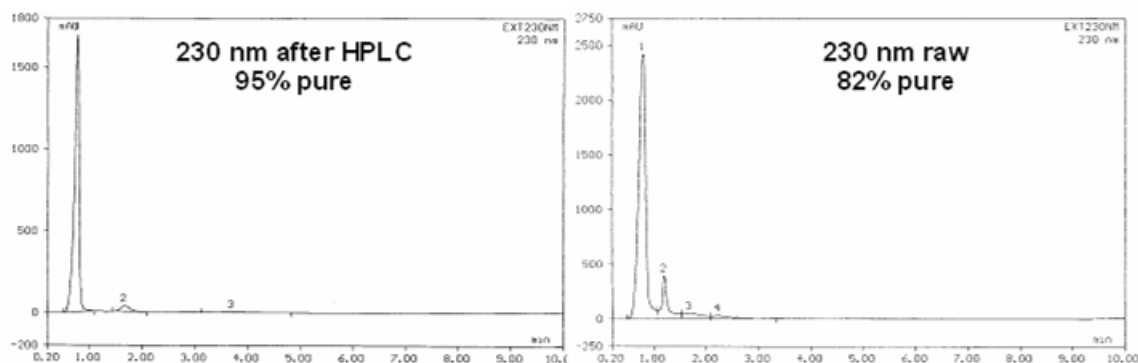


Fig. 44. Analytical HPLC-chromatogram of dendrimer-platinate at 230 nm.

The detection at 239 nm supported this interpretation. The relative purity increased from 69% for the raw mixture to 91% for the purified fraction. Peak number two, with a retention time of 1.20 minutes, disappeared almost completely in both chromatograms.

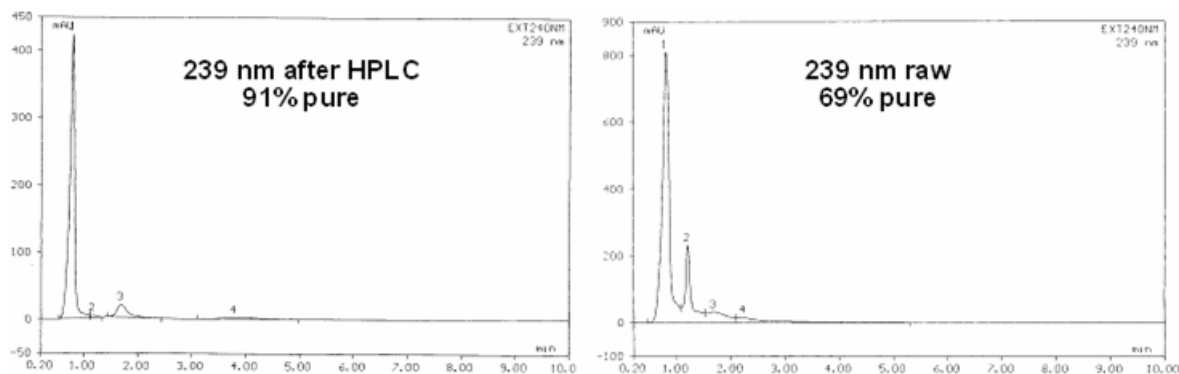


Fig. 45. Analytical HPLC-chromatogram of dendrimer-platinate at 239 nm.

Further purification with preparative GPC was not possible, because the solubility of the sample in THF was too low. Another possibility for a molecular-weight-discriminating purification would be dialysis or ultra-filtration. Both techniques were not applied yet, but their potential for such separations will, hopefully, be investigated in the near future.



The concentrated fraction was further characterized by NMR-spectroscopy. The comparison of the NMR-spectra of unplatinated **78** and **129** showed, that the proton-resonances for the ligand moiety shifted completely to lower field (Fig. 46), whereas the carbon resonances shifted to higher field. This was an indication for a successful platination. The assembly of amines with platinum demands for  $\sigma$ -donation of the amine's lone-pair to platinum. The positivated nitrogens electronically equilibrate this donation by an enhanced polarization of their  $\sigma$ -bond with the adjacent methylenes and transfer their polarization. This deficiency of electron-density should cause a shift to lower field for the proton resonances and a shift to higher field for the carbon resonances of the methylene groups.

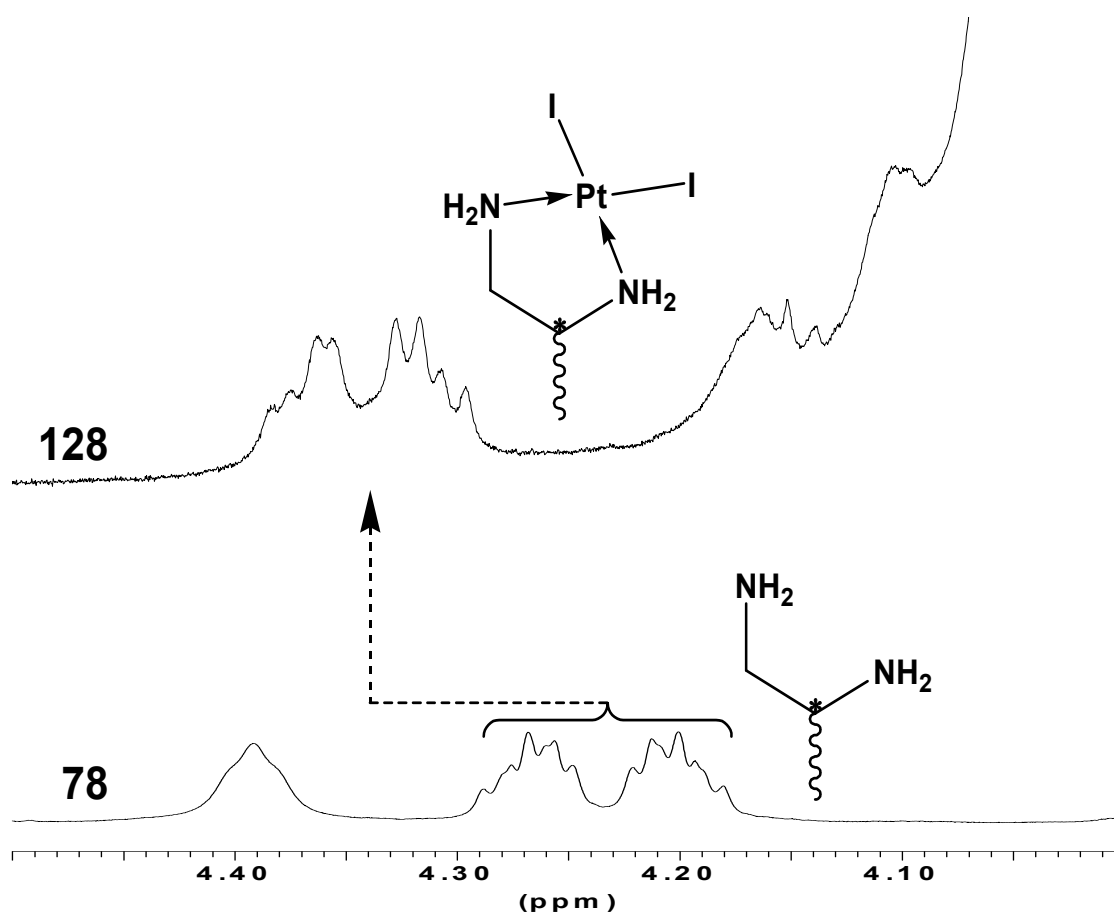
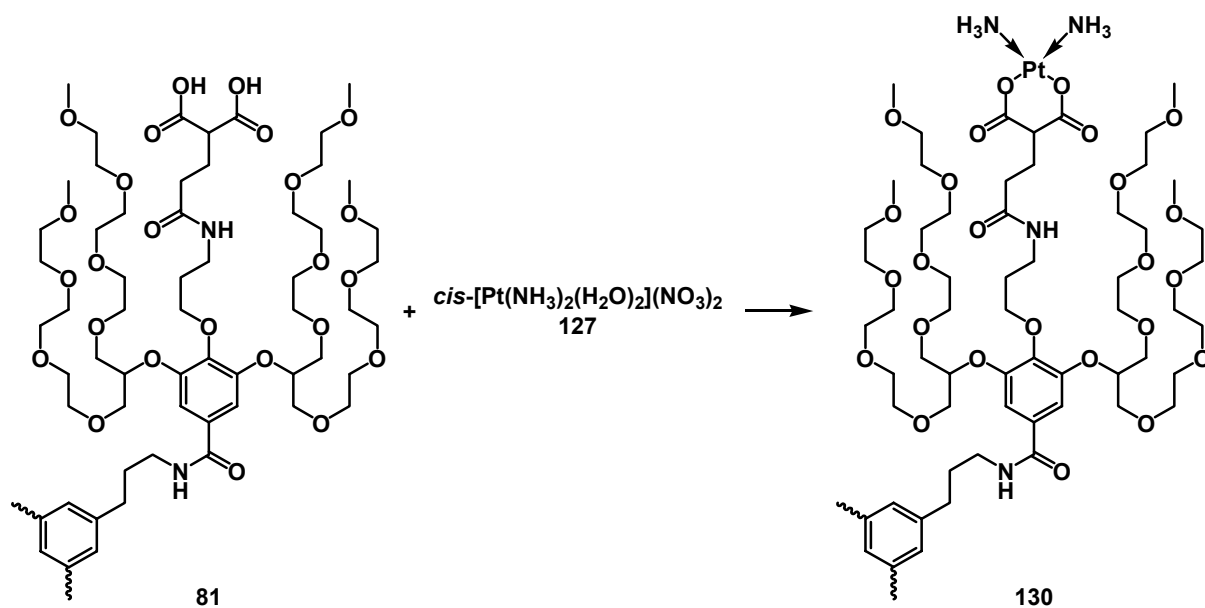


Fig. 46. Comparison of proton resonances for the ligand in compounds **78** and **129** by their <sup>1</sup>H-NMR spectra (500 MHz, d<sup>4</sup>-methanol).

The tendentious agreement of the observed resonances with the predicted values can be regarded as a confirmation for the formation of a platinated dendrimer.



Scheme 63. Synthesis of a dendrimer-platinum conjugate via malonic acid ligands.

Another platinated dendrimer **130** was accessible by the reaction of dendrimer **81** with the precursor **127**. The characterization and purification was again tedious. A structural evidence for a platinum complex with  $^{195}\text{Pt}$ -NMR spectroscopy was not obtained.<sup>XII</sup>

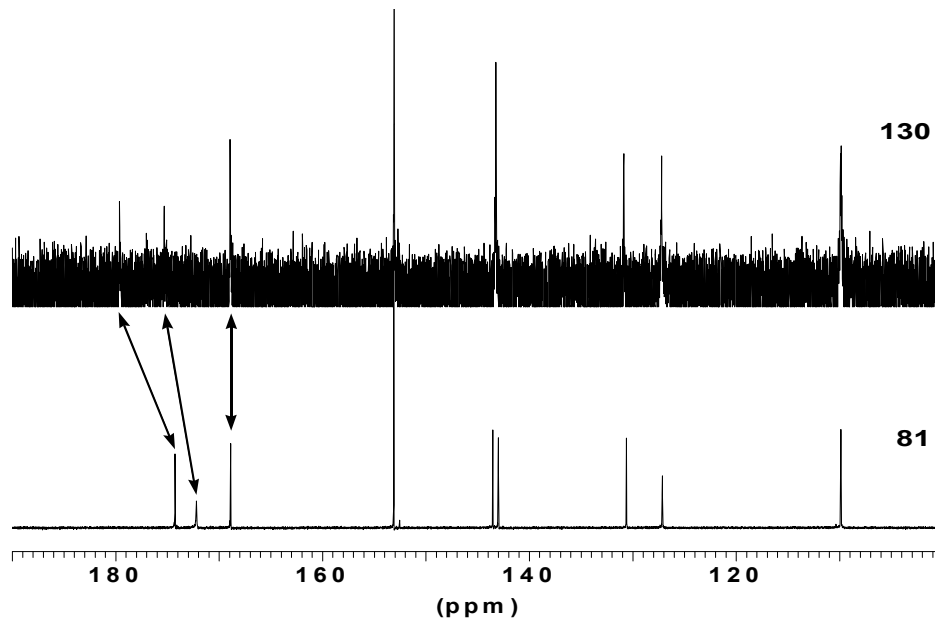


Fig. 47. Comparison of carbon resonances for the ligand in compounds **81** and **130** by their  $^{13}\text{C}$ -NMR spectra (125 MHz,  $\text{d}^4$ -methanol).

<sup>XII</sup> I am very grateful to Dr. Lentz, Institut für Anorganische Chemie, FU Berlin for measuring  $^{195}\text{Pt}$ -NMR.

The synthesized amount was too small to get a nicely resolved spectrum within a reasonable acquisition time. The proton-resonances of the malonate-ligand shifted to higher field and the carbonyl-resonance of the malonate shifted to lower field (Fig. 49). These findings were again in accordance with the calculated predictions. However, it was not possible to obtain a mass spectrum with MALDI-TOF mass spectrometry. The solubility of **130** in THF was much better than that of **129**, but it was still too low for a separation with preparative GPC.

## 4.5 Toxicity of Dendrimers

All dendrimers were examined in MCF-7 cell culture at concentrations of 1-20  $\mu\text{M}$  over a period of 9 days.<sup>XIII</sup> The conditions are described in detail in the experimental section.

The cytotoxicity essay on structurally analogous poly(amidoamin)s<sup>XIV</sup> indicated that the internal structure of these dendrimers, in particular the phenyl branching units, did not play a crucial role. The peripheral motifs of a dendrimer were much more important for its toxicity.

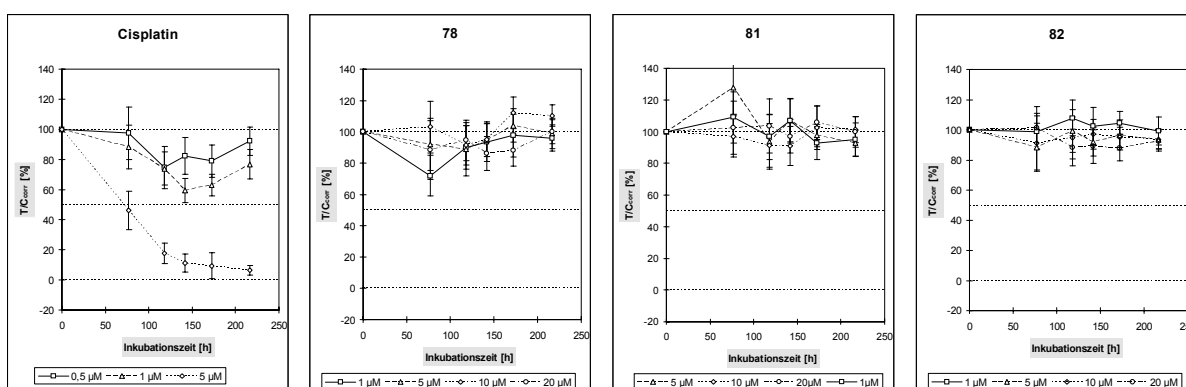


Fig. 48. *In vitro* cytotoxicity of cisplatin and the G0-dendrimers **78**, **81**, **82**.

In accordance with the observations of Duncan and Roberts, representatives with a polycationic surface were found to be cytotoxic. This toxicity was correlated to the number of positive charges and the concentration of the dendrimer in cell culture media. Surprisingly, cationic dendrimers, which were decorated with a bidentate diamino propionic acid, were nontoxic.

The dendrimers synthesized in the present work had an enhanced solubility in water without utilizing polycationic structures; they employed branched, monodisperse ethylene glycol chains. All structures were very well soluble in a broad variety of solvents, including water and DMF. They neither aggregated nor precipitated during the measurements. An approach towards a first structure/ toxicity correlations was examined by using dendrimers of different generations and with different peripheral

<sup>XIII</sup> The cytotoxicity was determined by Timo Kapp, who is a member of the cooperating group of Prof. R. Gust, Institut für Pharmazie, Freie Universität Berlin, Berlin, Germany.

<sup>XIV</sup> These dendrimers were prepared in a parallel dissertation by Sabine Fuchs.

substitution patterns. The assay for very toxic cisplatin is given as a reference for the observed cytotoxic screenings (Fig. 48, p.105).

Two G0-dendrimers with deprotected bidentate ligands for platinum complexation were tested. Dendrimer **78** carried diamino propionic acids which resembles an ethylene-diamine moiety. Dendrimer **81** was equipped with malonic acid derivatives, which represented an *O/O*-chelating moiety. Both compounds did not show any cytotoxicity at any concentration tested. These tests confirmed the results of Fuchs and showed that both bidentate ligands are suitable binding-motifs. The toxicity of the non-complexed dendrimers is very important, because these structures will have a certain circulation time in between drug release and renal elimination. The toxicity-data for the dansylated G0-dendrimer **82** showed a comparable result. No antiproliferative effect was observed. All these dendrimers had molecular weights of approximately 3000-3500 Da, and for none of them even a tendency of toxicity was observed.

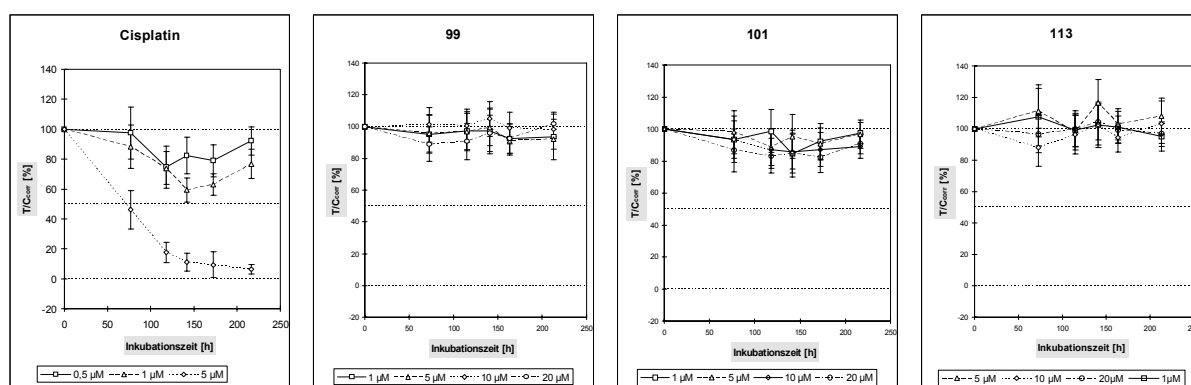


Fig. 49. *In vitro* cytotoxicity of cisplatin and the G1-dendrimers **99**, **101**, **113**.

Examples for the toxicity of a larger G1-dendrimer were gained by the screening of dendrimer **99**, **101** and **113**. These *bis*-“capped” dendrimers had a molecular weight of approximately 7500 Dalton and did not show toxicity at any concentration tested.

These toxicity results were very promising. None of the structural features seemed to have a negative impact on the biocompatibility of the potential drug delivery devices. However, the conclusion that these compounds are nontoxic is not yet fully proved. Since no effect on the exponential growth of the cell-line was detected, it can also be possible that there was no interaction between the dendrimers and the cells. In consequence, the absence of antiproliferative effects would not have been an indication for biocompatibility but for an incompatibility of the dendrimer and the cells

towards cellular uptake. The dendrimers with fluorescence dansyl labels are suitably equipped to study cellular uptake and intracellular distribution of the dendrimers by confocal microscopy. The very necessary next step is to prove that these compounds are nontoxic by showing that they are internalized by the same cells.